GENETIC DISSECTION OF THERAPEUTIC INTERVENTION TARGETS IN TRIPLE NEGATIVE BREAST CANCER

Kimberly E Maxfield

A dissertation submitted to the faculty of the University of North Carolina at Chapel Hill in partial fulfillment of the requirements for the degree of Doctorate of Philosophy in the Department of Pharmacology, School of Medicine.

Chapel Hill
2015

Approved by:

Angelique Whitehurst

Gary Johnson

John Sondek

Howard Mcleod

Albert Baldwin

Charles Perou

ABSTRACT

KIMBERLY E MAXFIELD: Genetic Dissection of Therapeutic Intervention Targets in Triple Negative Breast Cancer
(Under the direction of Angelique Whitehurst)

Triple negative breast cancer (TNBC) is the most aggressive and metastatic type of breast cancer, accounting for 20% of all breast cancer diagnoses. Currently, there are no TNBC-specific targeted therapies in the clinic and therefore, broad-spectrum cytotoxic chemotherapeutic regimens remain the standard of care. Due to high rates of innate drug resistance, many TNBC patients do not respond to these regimens and, therefore, have no other therapeutic options. Our group employed a pan-genomic loss of function screen to systematically dissect the molecular architecture that functionally supports TNBC to uncover new therapeutic entry points. We further applied a paclitaxel-based synthetic lethal approach to increase our discovery space to also identify those molecular components that modulate chemoresponsiveness. To encompass the heterogeneity found within the TNBC patient population, we screened four triple negative tumor-derived breast cancer cell lines that represent the spectrum of TNBC oncogenic aberrations and chemoresponse profiles. We also accounted for the two molecular subtypes, claudin-low and basal-like that comprise the majority of TNBC cases. These screens revealed a number of core modulators of tumor cell viability and paclitaxel-induced cellular stress that have not been previously appreciated for supporting TNBC biology at the cell autonomous level. In particular, this strategy implicated the signaling supported by the cytokine receptor, CXCR3, and its ligand, CXCL9, to promote mitotic fidelity and tumor

cell survival in the basal-like TNBC molecular subtype. In addition, we uncovered a requirement for the AMPK family member, SIK2, as a key nutrient sensor that may inhibit excessive autophagy. Inhibition of SIK2 enhanced autophagic flux and a loss of cell viability in a variety of TNBC genetic backgrounds. Finally, we discovered that cancer testes antigen transcription factor, ZNF165, directly repressed expression of negative TGFβ regulators thereby specifying a pro-tumorigenic TGFβ gene expression profile. Given that the expression of ZNF165 is otherwise restricted to the male testes, ZNF165 may represent a mechanism by which tumors engage anomaly-expressed proteins to promote survival. Taken together, our screening approach uncovered novel TNBC tumor cell vulnerabilities that identified cellular processes that could lead to new therapeutic approaches.

ACKNOWLEDGEMENTS

First and foremost, I would like to thank my mentor, Dr. Angelique Whitehurst, for her mentorship over the last five years. She spent countless hours teaching and training me and providing an environment that constantly pushed me to become scientist and person I am today. Secondly, I would like to thank my committee for their time and guidance. I'd also like to thank the UNC Pharmacology Department for fostering both scientific and personal growth. In particular, I'd like to thank Dr. Gary Johnson who provided consistent support, particularly as our lab relocated.

Next, I would like thank my labmates, both at UNC and UT Southwestern, for their scientific input and camaraderie that was critical for moving my project forward. In particular, I'd like to thank Dr. Rebecca Sinnott DeVaux and Josh Wooten. As the graduate student a year ahead of me, Becky provided valuable guidance as I moved through graduate school. She stayed late with me for student seminars and took many of my calls while writing this document. Working with Josh Wooten was also particular pleasure. I met Josh my first year of graduate school and watched him grow into an inquisitive scientist and return to graduate school himself.

Outside of lab, I would like to thank my family. Their unwavering support was critical for my success and perseverance throughout graduate school. A special thanks also goes to Ernesto Perez, Tamara Taggart and Ganesh Kabamur. I am very fortunate to have met three extraordinary friends over the past few years that have offered their unconditional support along the way.

TABLE OF CONTENTS

LIST OF TABLES

LIST OF FIGURES

LIST OF ABBREVIATIONS AND SYMBOLS

AKT	Protein Kinase B
AMP	Adenosine Monophosphate
AMPK	AMP Activated Kinase
ATCC	American Type Culture Collection
ATG5, 12, 13	Autophagy Protein 5, 12, 13
BRCA1	Breast Cancer 1, Early Onset
BSA	Bovine Serum Albumin
cAMP	Cyclic AMP
CCND1	Cyclin D1
CD49f	Integrin α6
ChIP-Seq	Chromatin Immunoprecipitation followed by NGS
cKIT	V-Kit Hardy-Zuckerman 4 Feline Sarcoma Viral Oncogene Homolog
CQ	Chloroquine
CRISPR	Clustered Regularly Interspaced Short Palindromic Repeat
CTA	Cancer Testis Antigen
CTCL	Cutaneous T-cell Lymphoma
CTG	Cell Titer Glo
CTL	Cytotoxic T-Lymphocytes
CTRL	Control
CXCL9	Cytokine CXC Motif Ligand 9
CXCR3	CXC Motif Receptor 3

DAPI	4’, 6 diamidino-2-phenylindole
DMD	Duchenne Muscular Dystrophy
EGFR	Epithelial Growth Factor Receptor
EMT	Epithelial to Mesenchymal Transition
EpCAM	Epithelial Cell Adhesion Maker
ER	Estrogen Receptor
ERE	Estrogen Response Element
EtOH	Ethanol
FACS	Fluorescent Activated Cell Sorting
FBS	Fetal Bovine Serum
FDA	Food and Drug Administration
FIP2000	Focal Adhesion Kinase Family Interacting Protein of 200 kDa
GABARAPL	GABA(A) Receptor Associated Protein Like 1
GFP	Green Fluorescent Protein
GLUT4	Glucose Transporter Type 4
GREAT	Genomic Regions Enrichment Annotation Tool
HBSS	Hank’s Balanced Salt Solution
HDAC	Histone Deacetylase
HER2	HER2/ ERBB2 Growth Receptor
HSP90	Heat Shock Protein 90
IGF-1	Insulin Growth Factor -1
IRS-1	Insulin Receptor Substrate -1
JAK	Janus Kinase

kDa	Kilodaltons
LKB1	STK11 – Serine/Threonine Kinase 11
MAD2	Mitotic Arrest Deficient 2
MHC	Major Histocompatibility Complex
mTOR	Mechanistic Target of Rapamycin
NCI	National Cancer Institute
ncRNA	Non-coding RNA
NGS	Next Generation Sequencing
NOTCH	NOTCH1
NSCLC	Non-Small Cell Lung Cancer
p35	CDK5R1 – Cyclin-Dependent Kinase 5, regulatory subunit 1
PARP1	Poly (ADP-Ribose) Polymerase 1
PBTA	Phosphate-Buffered Saline with Tween 20 and BSA
pCR	Pathologic Complete Response
PDGFRβ	Platelet-Derived Growth Factor Receptor Beta
PI3K	Phosphatidylinositol-4,5-Bisphosphate 3-Kinase
PKA	Protein Kinase A
PR	Progesterone Receptor
PTEN	Phosphatase and Tensin Homolog
qPCR	Quantitative Polymerase Chain Reaction
RAPTOR	Regulatory Associated Protein of mTOR Complex 1
RICTOR	Raptor Independent Companion of mTOR Complex 2
RNAi	RNA Interference

s.d.	Standard Deviation
S.E.M	Standard Error Mean
SBE	SMAD Binding Element
SIK1	Salt Inducible Kinase 1
SIK2	Salt-Inducible Kinase 2
SIK3	Salt Inducible Kinase 3
siRNA	small interfering RNA
SNAI1	SNAIL1
SRC	SRC Proto-Oncogene, Non-Receptor Tyrosine Kinase
STAT	Signal Transducer and Activator of Transcription
TBST	Tris-Buffered Saline with Tween 20
TGFβ	Transforming Growth Factor Beta
TIC	Tumor Initiating Cells
TNBC	Triple Negative Breast Cancer
ULK1	UNC-51 Like Autophagy Activating Kinase 1
VEGF	Vascular Endothelial Growth Factor
VEGFR	Vascular Endothelial Growth Factor Receptor
WCL	Whole Cell Lysate
WISP1	WNT1-Inducible Signaling Pathway Protein 1
ZNF165	Zinc Finger 165

CHAPTER I: Introduction

The Global Burden of Breast Cancer

Currently, breast cancer is one of the most common forms of cancer affecting women (1). Following the development of targeted therapies and improved mammography technologies and guidelines in the 1980s and 1990s, the breast cancer mortality rate dropped 40 % from 1990 to 2006. However, the incidence of breast cancer is increasing globally in both developed and developing nations. The lifetime risk of breast cancer is currently 1 in 8 and breast cancer remains the primary cause of death in women (2, 3).

Breast Cancer Heterogeneity

Most breast tumors arise from abnormal growth of the epithelial cells that form the milk-producing gland at the apex of the milk duct (lobular carcinoma) or that line the duct itself (ductal carcinoma). As a whole, breast tumors are a very heterogeneous group of tumors at the level of morphological and biological features, gene expression profiles, patient outcomes and therapeutic responses (4, 5). These differences can be classified based on both histopathologic and molecular features. This section discusses breast cancer heterogeneity and the current classification systems along with their defining characteristics.

Pathologic Classification of Breast Cancer – Through pathologic evaluation, a

few key receptors have been identified to define several distinct breast cancer subtypes. The next three paragraphs will discuss estrogen receptor (ER) positive breast cancer, HER2 amplified breast cancer and triple negative breast cancer (TNBC).

Estrogen Receptor Positive (ER+) Breast Cancer - Two thirds of diagnosed breast tumors are classified as hormone receptor positive based on expression of the growth-promoting estrogen and/or progesterone receptors (ER and PR, respectively). Of premenopausal women, ER+ breast cancer comprises 60 % of diagnosed breast tumors. For post-menopausal women, this percentage jumps to 75 % (6, 7). The estrogen and progesterone receptors are nuclear hormone receptors that remodel chromatin and drive pro-proliferative gene networks. Upon estradiol binding, the estrogen receptor translocates to the nucleus, binds to its estrogen response elements (ERE) and drives the transcription of pro-proliferative genes such as IGF-1, CCND1 and IRS-1 (8, 9). Most estradiol is locally synthetized and, therefore, tumors can engage an estradiol autocrine loop to promote cell autonomous tumor cell proliferation (10-12). It has been known for over a century that hormone ablation (removal of hormone producing tissues) had anti-cancer effects in ovarian, breast and pituitary tumors. In the late 1960s, ER expression was discovered as a prognostic marker for hormone ablation therapy in breast cancer. By the mid-1980s, estrogen receptor positive breast tumors were demonstrated to be highly dependent on estrogen receptor signaling and were responsive to inhibition of ER signaling (9, 13). ER+/ progesterone receptor positive (PR+) breast tumors are generally not classified as aggressive tumors. These tumors are typically classified as highly differentiated and slow growing. They are also highly correlated with lower grades, and

recurrence rates. With the Food and Drug Administration (FDA) approval of ER+ specific targeted therapies in 1977 (discussed in the next section), it is now standard clinical practice to evaluate ER+ expression prior to treatment decisions (9, 14, 15).

Human Epidermal Growth Factor Receptor 2 (HER2) Amplified Breast Cancer - Twenty to thirty percent of breast tumors are amplified for the HER2 receptor (16-18). HER2 is a member of the Epidermal Growth Factor Receptor Family (EGFR), which includes HER1, 2, 3, and 4. These receptor tyrosine kinases are upstream of MAPK and PI3K/ AKT signaling and are critical for cell growth, survival and proliferation (19). Following ligand binding, HER receptors can either homodimerize or heterodimerize to drive downstream activation proliferation and survival pathways. There are no HER2 specific ligands and, therefore, HER2 predominately acts as a co-receptor for the other HER2 family members (20, 21). On the surface of a HER2 amplified breast tumor cell, the number of HER2 receptors on the cell surface can be increase by up to a million fold compared to non-tumorigenic tissue (19, 22). Without the presence of a ligand, excess HER2 receptors induce dimerization to potently drive downstream pro-tumorigenic signaling. The HER2 receptor was first discovered as the transforming component of the avian erythroblastosis tumor virus that was highly homologues to HER1 (or EGFR) (23-26). In 1987, HER2 amplification was then found in breast cancer and quickly correlated with large, advanced grade, rapidly dividing tumors and poor prognosis (22, 27). Consistent with this, HER2 amplification can be observed in early stage disease, such as, neoplastic ductal carcinoma in situ (27-29). Prior to the development of HER2 targeted therapy (discussed in the next section), HER2 amplified tumors had the second worst

chemotherapeutic response and patient prognosis after triple negative breast cancer (16-18).

Triple Negative Breast Cancer (TNBC) - The remaining 15-20 % of breast tumors are classified in the histopathologic subtype called triple negative breast cancer (TNBC). This subtype is defined by a lack of expression of the estrogen receptor, progesterone receptor and is not HER2 amplified. TNBC tumors are very aggressive, progress quickly to metastasis, and over-represented in younger women minorities (30). Little is known about the etiology of TNBC. Systematic genomic evaluation of large TNBC patient cohorts reveals that no known common molecular aberrations collectively define TNBC. Loss of function mutations in the tumor suppressor, TP53, is the only tested oncogenic aberration with a mutational frequency higher than 10% (31). Without a targetable oncogenic aberration, the development of TNBC targeted therapies is challenging.

Molecular Classification of Breast Cancer – With the advent of gene expression technologies, the heterogeneity of breast cancer was further investigated using cDNA microarrays. This approach resulted in stratification of breast cancer into six distinct molecular subtypes called luminal A, luminal B, HER2-enriched, normal-like, basal-like and claudin-low (32). Each of these subtypes has a unique gene expression profile that translates into distinct patient prognosis and chemotherapeutic responses, suggesting that breast cancer heterogeneity is founded in fundamental differences in the underlying tumor architecture (33, 34). There is also significant overlap between the molecular subtypes and the histopathologic subtypes, suggesting that the expression of hormone and

growth receptors is an important determinate of the overall tumorigenic gene expression signature. The next paragraphs describe the molecular subtypes and how they relate to the histopathologic subtypes.

Luminal Subtypes - There are two luminal subtypes, luminal A and luminal B. Both are characterized by expression of keratins, integrin β4 and laminin (32, 33). When considered together, the luminal subtypes are highly correlated ER and PR positive breast tumors without HER2 amplification (32, 33, 35, 36). Consistent with ER+/PR+ tumors, luminal tumors are more differentiated and less proliferative than the HER2-enriched, or basal-like and claudin-low subtypes (32, 33). The main difference between luminal A and luminal B subtypes is a proliferation signature found in the luminal B subtype. Luminal tumors have very low pCR rates to cytotoxic chemotherapeutics. However, luminal tumors are usually low grade and not aggressive and given that there are currently available targeted therapies (discussed below), patient prognosis for luminal breast tumors are the best among all the breast cancer (37-40).

HER2-Enriched Subtype - HER2 amplified tumors are accompanied by a unique expression profile and, therefore, comprise their own HER2-enriched subtype (32). These tumors exhibit a proliferative gene signature and are low in the luminal, basal-like and claudin-low gene markers. Notably, about 50 % of the HER2 enriched subtype contains ER+ and non-HER2 amplified tumors, suggesting there may be another mutation event driving the same expression profile seen with HER2 amplification (32, 33, 35, 36).

Normal-Like Subtype - The normal-like subtype encompasses normal breast tissue from reduction mammoplasty and a small number of tumor samples. These samples typically have high levels of stromal and immune infiltrates, generating controversy over whether this subtype is an artifact of the contaminating normal stromal and immune cells (32, 35).

Claudin-Low and Basal-Like Subtypes - The two remaining molecular subtypes, basal-like and claudin-low, are predominately, but not exclusively, categorized as TNBC, encompassing 75 % - 80 % of all TNBC cases. However, these subtypes have dramatically different morphologies, expression profiles and chemoresponsiveness (32, 36). Basal-like tumor cells are epithelial in morphology with concurrent expression of epithelial markers like E-cadherin, Cytokeratin and EpCAM. The basal-like name originates from the expression of the cytokeratins 5, 6 and 17, characteristic of the basal layer found in the skin (33, 35, 41). In contrast, the claudin-low subtype is more mesenchymal with a fibroblast-like morphology and characterized by lack of expression of epithelial markers. The name 'claudin-low' originates from the lack of the adherens junction protein, claudin. These tumors also exhibit features of tumor initiating cells (TICs), which is driven by enhanced Transforming Growth Factor Beta (TGFβ) signaling-induced transcription of ZEB, TWIST1 and SNAI1 (33, 35, 41, 42). Furthermore, claudin-low tumors are more chemoresistant than basal-like tumors and are often enriched in residue disease following treatment with chemotherapy (32, 33, 35, 43).

Therapeutic Approaches in Breast Cancer

The pathological and molecular subtypes discussed above have prognostic and predictive capacities in the clinic that directly inform breast cancer treatment decisions. The following paragraphs outline the standard of care therapeutic approaches in breast cancer.

Current Therapeutic Approaches in ER+ Breast Cancer – Selective estrogen receptor modulators (SERMS) are one of the first targeted therapies in the field of oncology. The primary mechanism of action of first generation SERMS is direct binding to the estrogen receptor, antagonizing the downstream pro-proliferative estrogen receptor-induced transcription (2, 8). Tamoxifen is the founding member of SERMS and was first identified during attempts to make contraceptives in the early 1960s (44, 45). After failing as an anti-fertility treatment, tamoxifen was demonstrated to improve response and overall survival rates in ER+ breast cancer patients and was approved by the FDA in 1977 (13, 46). Currently, tamoxifen is the first line treatment for ER+ breast cancer and treatment is typically maintained for 5 years (47). Following its implementation in the clinic, tamoxifen has drastically improved ER positive breast cancer patient prognosis with close to 80 % five year survival rates (37-40). Tamoxifen is also used as a preventative measure in high-risk patients without increasing the risk of osteoporosis (48). However, depending on the tissue, tamoxifen can have either anti-estradiol effects or pro-estradiol effects. Therefore, there are significant toxicities associated with tamoxifen treatment, particularly in post-menopausal women. These include an increased risk of endometrial cancer, vaginal bleeding and discharge and blot

clots (49, 50). Furthermore, estradiol can have non-genomic effects and has been shown to activate oncogenic signaling cascades such as RAS/RAF/ MAPK. Therefore, inhibition of the estrogen receptor may not attenuate all the pro-tumorigenic effects of estradiol (51). Given these limitations, aromatase inhibitors are being explored as alternatives to SERMs. Aromatase is the key enzyme in the steroid synthesis pathway that converts testosterone to estradiol, and pharmacological inhibition directly prevents estradiol synthesis (2, 8). Thus far, three aromatase inhibitors have been developed; anastrazole, letrozole, and exemestane. The most promising inhibitor is letrozole, which reduces the risk of recurrence by 31 % and disease free survival by 18 % when compared to tamoxifen-treated patients with significantly less side effects (52-55). Currently, aromatase inhibitors are FDA-approved for breast cancer prevention and clinical trails are underway to further explore a role in breast cancer treatment (48) (Clinicaltrials.gov, NCT00530868 and NCT00382070)

Current Therapeutic Approaches in HER2 Amplified Breast Cancer – A successful targeted therapeutic approach has been developed for HER2-amplified classification of breast cancer. Trastuzumab is a humanized monoclonal antibody that binds directly to the extracellular domain of HER2 and attenuates tumor progression by triggering receptor internalization and subsequent degradation (56). As an antibody, trastuzumab also engages the immune system and recruits natural killer cells to bind to CD16 surface receptor to trigger antibody-dependent cellular cytotoxicity (ADCC) (57, 58). Furthermore, trastuzumab binding interferes with receptor dimerization and attenuates downstream MAPK and PI3K/ AKT signaling to prevent cell proliferation (59-

61). Trastuzumab was first discovered at Genentech in the early 1990s as having growth inhibition capabilities on breast cancer tumor-derived cell lines that exhibited HER2 amplification (62, 63). Two seminal studies in 2001 and 2002 revealed that trastuzumab treatment almost doubled initial response rates and survival time over standard chemotherapy in HER2 amplified breast cancer (17, 64). Trastuzumab is now the first line therapeutic for HER2 amplified breast cancer patients. Given that traztuzumab functions both directly and indirectly, traztuzumab is also used in combination with other chemotherapeutic agents, such as paclitaxel, in non-HER2 amplified tumors, although, the success of these regimens remains unclear. HER2 expression is now routinely evaluated in the clinic prior to treatment decisions (16, 18, 65).

Current Therapeutic Approaches in TNBC – By definition, TNBC lacks expression of both the estrogen receptor, progesterone receptor and further it is without HER2 amplification. These characteristics make TNBC patients ineligible for tamoxifen-based and trastuzumab-based therapies. Given that there is no known unifying targetable oncogenic aberration found in TNBC, the current standard of care remains cytotoxic chemotherapeutic agents where the anti-mitotic, paclitaxel, is a critical component (66, 67). In the 1960s, paclitaxel was originally discovered from an National Cancer Institute (NCI)-sponsored screening initiative to identify natural products with anti-cancer effects (68). Decades later in the early 1990s, paclitaxel was found to have potent anti-cancer properties in ovarian cancer (69). Given this success, paclitaxel was quickly tested and incorporated into the standard of care for non-small cell lung cancer (NSCLC) and breast cancer by the mid-1990s (70-72). Paclitaxel functions by directly binding to β-tubulin,

thus inhibiting the microtubule dynamicity required for proper mitotic spindle alignment during mitosis (73). Inhibition of proper spindle alignment engages the spindle assembly checkpoint and prevents mitotic progression. Paclitaxel's mechanism of cell death relies on the cell's ability to initiate apoptosis following a prolonged mitotic arrest (74). Currently, in TNBC, paclitaxel is part of chemotherapeutic regimens that include platinum-based or topoisomerase inhibitor DNA damaging agents as part of a combination therapy (30). Fortunately, many TNBC patients initially respond to paclitaxel-based therapies, with pathological complete response (pCR) rates reported to range from 26 - 45 %, making them the highest response rates among all the breast cancer subtypes (75). However, the majority of chemonaïve TNBC tumors retain residual disease and exhibit high rates of relapse within the first three years of treatment. Without additional treatment options these patients present with poor clinical prognosis (33, 75). Unfortunately, due to the vast heterogeneity of TNBC breast tumors, the cellular mechanisms underlying the innate paclitaxel resistance remain poorly understood.

Paclitaxel Treatment in the Molecular Subtypes of TNBC – The molecular subtypes have provided some insight into the basis of TNBC paclitaxel response heterogeneity. The two molecular subtypes that comprise the majority of TNBC, basal-like and claudin-low, have drastically different pCR rates to paclitaxel-based therapies. Basal-like tumors are highly responsive to first line paclitaxel/ anthracycline-based chemotherapy with pCR rates of 73 % (76). Claudin-low tumors are more chemoresistant with strikingly lower pCR rates (35 %) following treatment with the same chemotherapeutic regimens as basal-like tumors (33). This suggests that within TNBC,

there are fundamental differences in the cellular architecture that are responsible for determining paclitaxel-responsiveness. Currently, there are ongoing clinical trials evaluating the efficacy of paclitaxel/ platinum based therapies in combination with additional chemotherapeutics, such as cyclophosphamide. Furthermore, these trials are exploring different dosing regimens to uncover more effective therapeutic strategies while limiting drug concentration (66, 67, 77) (Clinicaltrials.gov - NCT02299999). However, improvement of paclitaxel response rates requires an increased understanding of the cellular determinates of paclitaxel responsiveness, leading to the design of more informed combination therapies. The TNBC molecular subtypes may provide a platform to start exploring fundamental differences in paclitaxel responsiveness.

Current Investigation into Targeted Therapies for TNBC

TNBC is the most aggressive form of breast cancer and the standard of care has significant limitations. As a result, TNBC has the worst prognosis among the breast cancer subtypes. Investigating new therapeutic strategies for TNBC is currently a priority in the breast cancer field. The following paragraphs describe the current state of targeted therapy research in TNBC.

PARP Inhibitors - There is one targeted therapeutic approach currently under investigation that will benefit TNBC patients. This approach leverages loss of function mutations in the gene, BRCA1, found almost exclusively within the basal-like molecular subtype of TNBC (66). BRCA1 mutant tumors account for 5-10 % of all breast tumors and about 25 % of TNBC tumors, and are associated with aggressive disease and poor

patient prognosis (78, 79). BRCA1 is a member of the homologous-recombination double-stranded DNA repair pathway and BRCA1 mutant tumors are exquisitely sensitive to therapeutic inhibition of PARP1 (79). PARP1 is a key component of a second DNA-damage repair pathway, Base Excision Repair (79, 80) and, therefore, inhibition of PARP1 creates a synthetic lethal interaction with loss of BRCA1 to attenuate the tumor cell's ability to buffer oncogene-induced replicative stress. Initial clinical trials reported an overall response rate of 41 % with the PARP1 inhibitor, Olaparib, compared to 22 % with chemotherapy in BRCA1 mutant breast cancer (81). Currently, Olaparib and the new generation PARP1 inhibitor, Veliparib, are in clinical trials in combination with paclitaxel and carboplatin with BRCA1 mutation status as a biomarker for clinical trial enrollment (Clinicaltrials.gov, NCT00516724 and NCT01078662) (82).

EGFR Inhibitors - A high proportion of TNBC tumors are EGFR (or HER1) amplified, with some studies reporting amplification frequencies as high as 50 % (83). This has particular relevance in the breast cancer field given that 43 % - 89 % of NSCLC have EGFR amplifications and EGFR-amplified NSCLC patients clinically respond to inhibition of EGFR using Erlotinib and Gefitinib (84, 85). Furthermore, as also seen in NSCLC, EGFR amplification is a negative prognostic predicator in TNBC (86). However, the initial clinic trials have not mirrored the clinical responses seen in NSCLC, showing modest improvements in progression free survival from 1.5 months to 3.7 months (87). Therefore, the predictive capacity of EGFR amplification to EGFR inhibitors in TNBC remains under investigation (66, 67). Current clinical trials are using EGFR monoclonal antibody, cetuximab, or EGFR inhibitors in combination with

paclitaxel and carboplatin (Clinicaltrials.gov, NCT00232505 and NCT00463788).

VEGF and VEGFR Inhibitors - Given that TNBC tumors are often characterized as rapidly proliferating, VEGF inhibitors and paclitaxel are being explored as a new combination therapy. Inhibition of VEGF prevents formation of new vasculature within the tumor mass, thus preventing tumor progression (88). Hypoxia or other oncogenic signaling modules, such as TGFβ, can induce VEGF secretion. Once secreted, VEGF binds to its tyrosine kinase receptor to induce pro-angiogenic cellular processes such as cell proliferation, cell motility and prostaglandin production (89). Currently, there are two methods of VEGF signaling inhibition under evaluation. First, there are VEGF inhibitors that bind directly to the VEGF ligand. Second, there are VEGF Receptor (VEGFR) inhibitors that bind to the cell surface receptor (66, 67, 88). Clinical trials with the VEGF monoclonal antibody, bevacizumab, have shown conflicting results causing the FDA to withdraw its approval in TNBC (66, 67, 90). Clinical trials with tyrosine kinase inhibitors targeting VEGFR, such as sorenib and sunitinib, in combination with paclitaxel, are also underway (Clinicaltrails.gov NCT00622466 and NCT00825734). Initial studies using sorafenib were promising but due to high rates of toxicity, the feasibility of implementing sorenib into TNBC therapies remains unclear (91). Sunitinib clinical trials have showed little or no efficacy, but the enrollment criteria for these trials was only limited to non-amplified HER2 tumors. Therefore, the patient population was a mix of TNBC and ER/PR+ tumors (92, 93).

mTOR and PI3K Inhibitors - mTOR inhibitors are also being explored in TNBC

therapeutics. mTOR is a signaling node for many essential cellular processes like cell proliferation, translation and autophagy. mTOR activity is directly downstream of PI3K and AKT signaling (94). Next to TP53, gain of function mutations in PI3K is the second most frequent oncogenic aberration in TNBC, at mutations rates close to 10 % (31, 95). The mTOR inhibitor, everolimus, has exhibited clinical promise in relapsed trastuzumab-resistant breast cancer by increasing progression free survival by 34 % (96). However, everolimus is associated with severe side effects like hyperglycemia. Initial clinical trials evaluating everolimus as a monotherapy in PTEN mutant TNBC showed no clinical benefit (97). Currently, combination therapies between everolimus and the PI3K inhibitors, GDC-0941 and BKM120, are being evaluated with paclitaxel in metastatic breast cancer (Clinicaltrials.gov - NCT00915603, NCT00930930)

Additional Inhibitors - There are a handful of additional targets that have showed promise in pre-clinical models and are now transitioning into clinical trials. The SRC, c-Kit and PDGFRβ inhibitor, dasatinib, in combination with paclitaxel, was successful in pre-clinical models and shown an increase, albeit modest, in the initial response rate and progression free survival in TNBC patients in phase I clinical trials (98, 99). Inhibition of the interleukin 6 inflammatory pathway, JAK/STAT, using the inhibitor ruxolitinib, showed potent inhibition of the stem-like breast cancer cells in vitro and in vivo mouse models (100). Lastly, inhibitors targeting the chaperone protein HSP90 (PU-H71 and ganetespib), have also shown anti-cancer effects in in vitro and mouse studies and are now entering clinical trails (101, 102) (ClinicalTrials.gov - NCT02474173, NCT01677455).

Providing Therapeutic Alternatives for TNBC Patients

The development of effective targeted therapies has altered the therapeutic landscape of breast cancer. The development of tamoxifen-based and trastuzumab-based therapies allows for effective treatment for ER+ and HER2 amplified breast cancer, which encompasses 80 – 85 % of all breast cancer diagnosis. If resistance to these first line therapeutics occur, chemotherapeutic regimens are used as a second line treatment. Given that there are no targeted therapies exist for TNBC, the current standard of care remains paclitaxel-based chemotherapeutic regimens. These regimens are effective but exhibit significant clinical limitation due to 50 % - 80 % innate paclitaxel resistance. Developing targeted therapies for TNBC is problematic without a clear understanding of the pathology and etiology of the disease or the cellular mechanisms determining drug response. As described above, many TNBC targeted therapies currently under investigated are based on clinical expression correlations or application of therapeutic strategies successful in other tumor types. Other than the PARP inhibitor, Olaparib, these approaches have thus far only yielded modest improvements over paclitaxel-based therapies in a small numbers of TNBC patients. A deeper understanding of the functional requirements for TNBC viability and chemotherapeutic response is needed to make more informed and precise treatment decisions and provide effective therapeutic alternatives.

Summary of Dissertation

The goal of this work is to perform a systematic and unbiased analysis of the TNBC functional landscape to identify cell autonomous tumor cell vulnerabilities that may translate into new TNBC therapeutic strategies. To do this, I employed a pan-

genomic loss of function screening approach that leads to a compendium of modulators of TNBC viability and chemotherapeutic response not previously implicated in TNBC tumor cell biology. To identify novel therapeutically tractable and tumor cell selective dependencies, I design and execute a secondary retest 'pipeline' to nominate 3 novel TNBC vulnerabilities, CXCR3, SIK2 and ZNF165, for mechanistic elaboration (Chapter II). Through follow-up studies, I find that CXCR3 cytokine signaling supports TNBC viability in a cell autonomous manner through maintenance of a high fidelity mitosis. This effect may be biased to the basal-like subtype, which nominates a new combination therapy between the CXCR3 inhibitor, AMG487 and paclitaxel using the basal-like subtype as a biomarker for sensitivity (Chapter III). I next uncover that SIK2 acts as an autophagic break to promote the pro-tumorigenic effects of autophagy. I hypothesize that autophagy-dependent tumors may be particularly sensitive to inhibition of SIK2 and, therefore, SIK2 may be a viable therapeutic target in autophagy-dependent metastatic disease (Chapter IV). I further reveal that ZNF165 is a driver of oncogenic TGFβ signaling and TNBC survival and could serve as a biomarker for responsiveness to TGFβ inhibition (Chapter V). Taken together, this work leverages a functional genomics approach to uncovered new cellular mechanisms supporting TNBC biology that could inform future treatment strategies. This work also highlights the strength of pan-genomic screening approaches to reveal new vulnerabilities that lead to the elaboration of new therapeutically actionable concepts (Chapter VI).

CHAPTER II: Employing Loss of Function RNAi Screens to Uncover Cell Autonomous Mechanisms Supporting Triple Negative Breast Cancer

Introduction

RNA Interference (RNAi) is an effective tool for the analysis of gene function. RNAi was first discovered in plants when non-coding RNA (ncRNA) molecules were identified as interfering with gene expression. These ncRNA molecules targeted specific mRNA for degradation prior to translation using base complementarity (103-105). In subsequent studies, RNAi mechanisms were found to be present across all phyla and critical for many developmental programs and removal of foreign DNA following viral infection (106). RNAi was first used as an experimental tool to manipulate gene expression in *Caenorhabitis elegans* in 1998 (107). Since then, RNAi techniques have been successfully adapted for loss of function studies across many model systems including *Drosophila melanogaster*, *Caenorhabitis elegans, Homo sapiens*, and *Mus musculus* (108). With the advent of commercially available RNAi genome libraries, RNAi has been successfully employed in large-scale functional genomic screening efforts and played an essential role uncovering novel modulators of host/ pathogen interactions, cell and organelle morphology, axon guidance and motility, cell cycle, mitosis and tumorigenesis (108-113). Given this success, there are now publically available databases

cataloguing RNAi screens performed in *Homo sapiens*, *Caenorhabitis elegans* and *Drosophila melanogaster* to provide a resource and hypothesis-generating tool for the scientific community (114-116).

High throughput functional RNAi screens have played a critical role in our current understanding of tumor cell biology and chemotherapeutic response. The first RNAi screen dissecting chemotherapeutic response was performed in 2005 and used treatment of a sublethal dose of three chemotherapeutic agents (paclitaxel, cisplatin and etoposide) to identify kinases and phosphatases that when lost, sensitize tumor cells to an otherwise innocuous chemotherapeutic insult. This approach uncovered the pseudophosphatase, MK-STYX, as a modulator of chemotherapeutic response in HeLa cells (117, 118). MK-STYX was later verified to support cytochrome c release for activation of apoptosis (119). This study lay the groundwork for many subsequent chemosensitizer RNAi screens that have provided mechanistic insight into chemotherapeutic drug response for cisplatin, paclitaxel, etoposide, tratuzimab, tamoxifen, gemcitabine, and fluorouracil (120-125). For example, a chemosensitizer screen using the anti-mitotic paclitaxel in NSCLC identified a novel yet critical connection between the RNA polyadenylation machinery and maintenance of a bipolar mitotic spindle (126).

These screens have also led to new therapeutic strategies in the clinic. For example, the genome excision repair protein, HR23B, sensitizes cutaneous T-cell lymphoma (CTCL) cells to histone deacetylase (HDAC) inhibitors through proteasome

deregulation. Consequently, HR23B expression is being explored as a biomarker for sensitivity to HDAC inhibitors in CTCL patients (127, 128).

The intersection of multiple RNAi screens can be further leveraged to reveal selective tumor cell dependencies. Luo and Ellegde et al. performed a siRNA screen in both RAS-mutant and RAS-wildtype colorectal cancer cells to identify genes that specifically support mutant RAS-driven tumor cell viability. This approach uncovered an increased sensitivity to mitotic perturbation in RAS-mutant colorectal cancer cells, revealing that these RAS-mutant cells were more sensitive to treatment with anti-mitotics (129). Taken together, over the past 10 years, RNAi screens have emerged as a powerful technique to uncover new regulators of chemotherapeutic response and new biological concepts that can lead to novel therapeutic intervention strategies.

Given the lack of therapeutic options for TNBC patients, our goal is to begin to identify tumor cell dependencies that may be therapeutically actionable. Here, we design and execute an unbiased pan-genomic loss of function siRNA screen to uncover novel TNBC tumor cell vulnerabilities. We used four tumor-derived cell lines to model the TNBC patient population and employed the chemosensitizer screening strategy to uncover genes that either directly support TNBC viability or modulate chemotherapeutic response to the first line TNBC chemotherapeutic, paclitaxel. This approach revealed many known and unknown modulators of TNBC tumor cell biology and paclitaxel responsiveness. Through a retest pipeline to prioritize penetrant, tumor-selective and therapeutically tractable screen hits, we nominated 3 genes; CXCR3, SIK2 and ZNF165,

for further study as a new TNBC vulnerabilities.

Results

Modeling Triple Negative Breast Cancer for RNAi Screening – TNBC is defined by a lack of hormone and growth receptor expression. Therefore, it is composed of a diverse set of breast tumors that encompasses many different oncogenic aberrations, molecular subtypes and chemoresponse profiles (30). To model this heterogeneous patient population in our screening platform, we employed tumor-derived cell lines, which retain many of their clinically relevant features (41). Furthermore, these cell lines are easily cultured in the laboratory, display growth rates that achieve multiple population doublings during the screen time frame, and can reproducibly achieve greater than 90% siRNA transfection efficiency (Table 1). These attributes make these tumor-derived cell lines ideal TNBC models for high throughput siRNA screening. We initially evaluated 15 TNBC tumor-derived cell lines for the above parameters and selected four cell lines that encompassed the breadth of TNBC heterogeneity and were conducive to efficient high throughput screening (Figure 1A).

TNBC Screen Design – The screen platform used here was modeled after one of the first paclitaxel chemosensitizing screen performed in the H1155 lung cancer cell line (122). We obtained the Dharmacon pan-genomic siRNA library arrayed in a 96 well format, with each well containing a pool of 4 siRNAs targeting 1 gene. First, cells were reverse transfected into the 96 well format and then treated with either vehicle or a sublethal dose of paclitaxel forty-eight hours post-plating. Cell viability was evaluated 96

Table 1: Characteristics of Breast Cancer Tumor-Derived Cell Lines in Laboratory

Cell Line	Molecular Subtype	Triple Negative	Mutations	Transfection Efficiency	Doubling Time
Hs578T	Claudin-Low	Y	HRAS TP53	90 %	2 days
MDA-MB-231	Claudin-Low	Y	KRAS BRAF TP53	90 %	1.5 days
SUM159	Claudin-Low	Y	HRAS PI3K	94 %	<1day
SUM1315	Claudin-Low	Y	BRCA1	91 %	3-4 days
MDA-MB-436	Claudin-Low	Y	BRCA1 TP53	90 %	2 days
WHIM12	Claudin-Low	Y	PI3KCA deletion	> 99 %	2 days
HCC38	Claudin-Low	Y	TP53	> 99 %	2-3 days
MDA-MB-468	Basal-like	Y	EGFR amp PTEN TP53	99 %	2-3 days
SUM149	Basal-like	Y	BRCA1 TP53	> 99 %	1.5 days
SUM229	Basal-like	Y	KRAS TP53	> 99 %	5-7 days
HCC1937	Basal-like	Y	BRCA1 PTEN	96 %	5-6 days
HCC1143	Basal-Like	Y	TP53	98 %	2-3 days
HCC1954	Basal-like	ER[-] PR[-] HER2[+]	PI3K TP53	98 %	1-2 days
HCC1806	Basal-like	Y	EGFR amp	> 99 %	1-2 days

hours post plating (Figure 1B). This two-pronged approach allows for identification of two types of TNBC tumor cell vulnerabilities. The vehicle-treated arm reveals genes that directly support tumor cell viability (Monogenic Lethal). The paclitaxel-treated arm allows for identification of genes that are not necessarily directly required for tumor cell survival but are required to buffer chemotherapeutic cellular stress (Synthetic Lethal) (Figure 1C). Furthermore, identification of therapeutically tractable genes that are synthetic lethal with paclitaxel may nominate new combination therapies in TNBC. Taken together, our screening platform is designed to uncover TNBC Achilles' heels and nominate new therapeutic strategies.

Evaluation of Screen Validity – Following execution of four pan-genomic screens, we employed a z score metric of $\geq$ -2 to identify screen outliers (130). For monogenic lethals, we applied the z score metric to the vehicle-treated viability score (Figure 1C). For synthetic lethal, we applied the z score metric to the ratio of viability score with sublethal dose to paclitaxel to the vehicle treated viability score (Figure 1C). This method revealed 2000 unique siRNAs as screen outliers across both monogenic and synthetic lethal arms. As expected, the top monogenic lethals identified are known supporters of cellular housekeeping functions that all eukaryotic cells require like ubiquitin and proteasomal subunits required for protein homeostasis (Figure 2A). We also identified siRNAs with known functions in tumorigenesis such as RBBP9, which has a role in cell cycle progression and can drive transformation (Figure 2A) (131). Related to paclitaxel-induced cellular stress, our screens uncovered several genes that are known to

A.

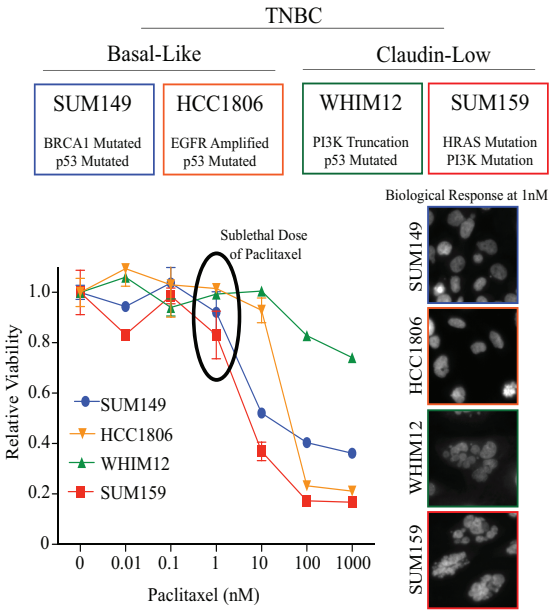
TNBC
Basal-Like
Claudin-Low
SUM149
BRCA1 Mutated
p53 Mutated
HCC1806
EGFR Amplified
p53 Mutated
WHIM12
PI3K Truncation
p53 Mutated
SUM159
HRAS Mutation
PI3K Mutation
Biological Response at 1nM
Sublethal Dose of Paclitaxel
Relative Viability
1.0
0.8
0.6
0.4
0.2
0
SUM149
HCC1806
WHIM12
SUM159
0
0.01
0.1
1
10
100
1000
Paclitaxel (nM)
SUM149
HCC1806
WHIM12
SUM159

B.

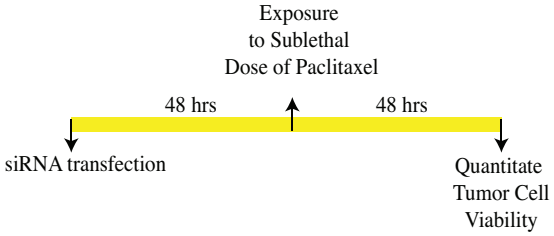
Exposure
to Sublethal
Dose of Paclitaxel
48 hrs
48 hrs
siRNA transfection
Quantitate
Tumor Cell
Viability

C.

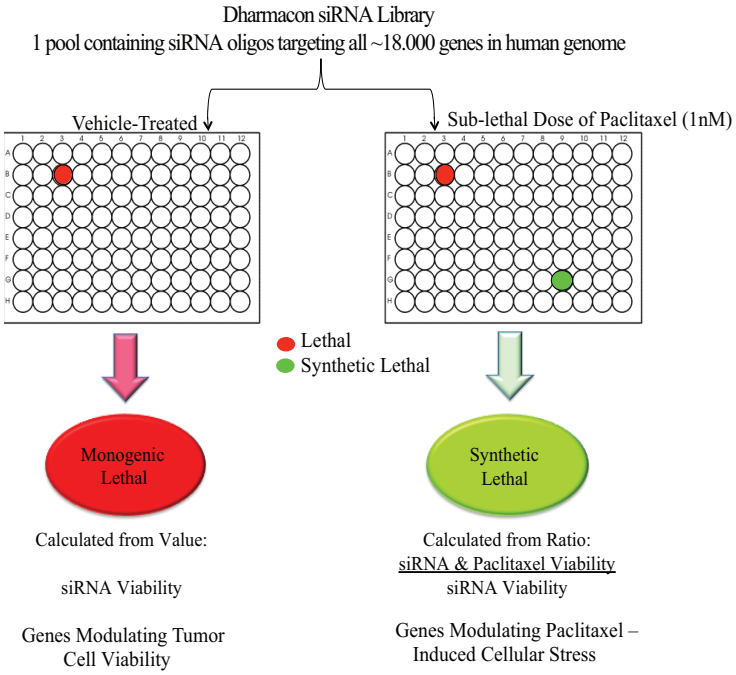
Dharmacon siRNA Library
1 pool containing siRNA oligos targeting all ~18.000 genes in human genome
Vehicle-Treated
Sub-lethal Dose of Paclitaxel (1nM)
Lethal
Synthetic Lethal
Monogenic
Lethal
Synthetic
Lethal
Calculated from Value:
siRNA Viability
Genes Modulating Tumor
Cell Viability
Calculated from Ratio:
siRNA & Paclitaxel Viability
siRNA Viability
Genes Modulating Paclitaxel –
Induced Cellular Stress

Figure 1. Pan-Genomic Loss of Function Screening Strategy to Identify TNBC Molecular Vulnerabilities. A. Characterization of TNBC tumor-derived cells lines used in siRNA screens. Top: Cell line name with indicated oncogenic mutations and molecular subtype. Bottom Left: Paclitaxel dose response curve TNBC screening cell lines. Indicated TNBC cell lines plated in 96 well format and treated 48 hours post plating with indicated paclitaxel doses. CTG assay was performed 96 hours post plating and values represent viability relative to 0 nM paclitaxel (n=3) ± Standard Deviation (s.d). Sublethal paclitaxel dose used for siRNA screen indicated. Bottom Right: Biological response of TNBC cell lines used in screen at sublethal paclitaxel screening dose. Indicated TNBC cell lines were processed as above and incubated with hoeschst stain 96 hours post plating. Representative images displayed. B. Screening time line: TNBC cell lines plated in 96 well format and treated 48 hours post plating with indicated paclitaxel doses. CTG assay was performed 96 hours post plating. C. Pan-genomic siRNA screening strategy to uncover monogenic lethal and synthetic lethal genes in each of the TNBC screening cell lines.

modulate paclitaxel sensitivity in tumor cells, in particular, TACC3 and CASC1 (Figure 2A) (132, 133). Identification of these genes provides validation that we performed a high fidelity screen that is capable of uncovering biology related to TNBC tumor cell survival and chemotherapeutic response. Given that the majority of the screen outliers have not been previously implicated in TNBC tumor cell biology, our screens represent a compendium of putative TNBC vulnerabilities that may lead to a deeper understanding of TNBC biology and identification of new therapeutic entry points.

Identification of Top Priority Candidates for Mechanistic Elaboration - We were interested in identifying novel vulnerabilities in TNBC that are tumor cell selective and could translate into new therapeutic strategies. Given the extensive tumor cell heterogeneity in our screening platform and in the TNBC population, we first identified those siRNAs that are defined as hits in at least two cell lines. This analysis included siRNAs identified as hits either the monogenic lethal or synthetic lethal screening arm. This will increase the discovery space of our screen and increase the likelihood of elaborating a penetrant phenotype. We are interested in new therapeutic entry points and, therefore, narrowed our search to siRNA targeting genes that are considered therapeutically tractable or have a well-defined tumor cell selective expression pattern, which is indicative of a large therapeutic window. We next evaluated loss of these screen hits in the context of normal immortalized breast epithelia to enrich for vulnerabilities that are specific to the transformed state (Figure 2B). This analysis nominated **CXCR3, SIK2 and ZNF165** for mechanistic elaboration to uncover new aspects of TNBC biology that are therapeutically tractable. The following three paragraphs will provide

background on each of these proteins along with rationale for their selection for further mechanistic elaboration.

CXC Motif Receptor 3 (CXCR3) - Our functional genomics approach identified siRNA targeting CXCR3 as a potent supporter of TNBC viability and paclitaxel-induced cellular stress in multiple genetic backgrounds (Figure 3A). Additionally, one of its ligands, CXCL9, was identified as synthetic lethal with paclitaxel in the HCC1806 TNBC tumor-derived cell line (Figure 3A). CXCR3 is the primary cytokine G-protein coupled receptor for members of the CXC ELR-negative cytokine subfamily, which includes CXCL4, 9, 10, and 11 (134, 135). CXCR3 cytokine signaling has been primarily studied for promoting chemotaxis following injury-induced cytokine release in $CD4^+$ Type-1 helper and $CD8^+$ cytotoxic lymphocytes (135-137). CXCR3 also has known functions in angiogenesis and wound repair (138-140). Identification of both CXCR3 and CXCL9 from our screening platform suggests that CXCR3/CXCL9 cytokine signaling supports tumor cell viability and buffers against chemotherapeutic insult in a cell autonomous manner. This is a previously undefined role for cytokine signaling; therefore, mechanistic elaboration of CXCL9/ CXCR3 signaling in TNBC could uncover new mechanisms by which tumor cells can remodel signaling modules to promote the tumorigenic phenotype.

To verify the screen observations were not due to siRNA-off target effects, we evaluated loss of CXCR3 in both the SUM149 and HCC1806 tumor-derived cell lines with two independent siRNA pools and observed reduced TNBC tumor cell viability along with concomitant CXCR3 mRNA depletion (Figure 3B). Repeating this analysis with CXCL9 in HCC1806 cells produced similar results (Figure 3C). Furthermore, small

molecule inhibitors targeting CXCR3 are commercially available and in clinical trials for immune disorders (76) and; therefore, could be repurposed to define new therapeutic strategies in TNBC. Given that our screen identified both the receptor, CXCR3, and its ligand, CXCL9, and CXCR3 is therapeutic tractability, further investigation was focused on the CXCR3/ CXCL9 signaling axis as a vulnerability in TNBC.

SIK2 (Salt Inducible Kinase) - Our pan-genomic siRNA screen identified siRNA targeting SIK2 as both synergizing with the first line chemotherapeutic, paclitaxel in SUM159 cells and supporting tumor cell viability WHIM12 cells (Figure 3D). SIK2 is an AMPK-related kinase containing a targetable canonical ATP binding pocket thus making it an attractive therapeutic target. SIK2 has also recently been implicated with a role in ovarian cancer (141, 142), suggesting SIK2 is an important kinase during tumor evolution. To verify our screen observations were not due to siRNA off-target effects, we evaluated loss of SIK2 in both the SUM159 and WHIM12 tumor-derived cell lines with two independent siRNA pools. We observed reduced TNBC tumor cell viability along with concomitant SIK2 mRNA depletion (Figure 3E). Through a collaboration with Arrien Pharmacueticals, Inc, we obtained a SIK2 selective small molecule inhibitor to facilitate the evaluation of SIK2 as a therapeutic target. Given the therapeutic tractability of SIK2, its recently defined role in ovarian cancer and our access to a novel small molecule inhibitor, we decided to further investigate SIK2 as a vulnerability in TNBC.

A.

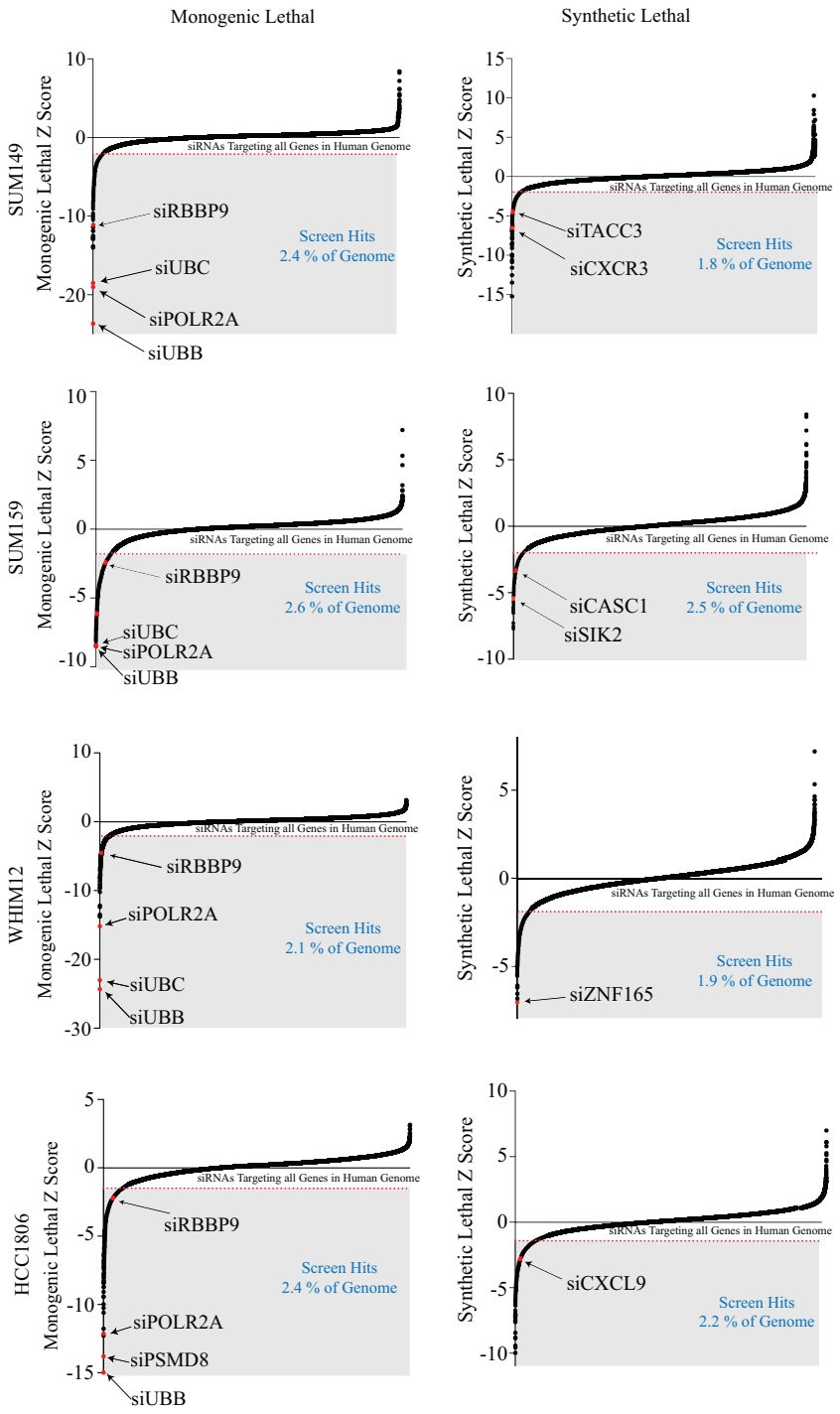
Monogenic Lethal
Synthetic Lethal
SUM149
Monogenic Lethal Z Score
Synthetic Lethal Z Score
siRNAs Targeting all Genes in Human Genome
siRBBP9
siUBC
siPOLR2A
siUBB
Screen Hits
2.4 % of Genome
siTACC3
siCXCR3
Screen Hits
1.8 % of Genome
SUM159
siCASC1
siSIK2
Screen Hits
2.6 % of Genome
Screen Hits
2.5 % of Genome
WHIM12
siZNF165
Screen Hits
2.1 % of Genome
Screen Hits
1.9 % of Genome
HCC1806
siPSMD8
siCXCL9
Screen Hits
2.4 % of Genome
Screen Hits
2.2 % of Genome

B.

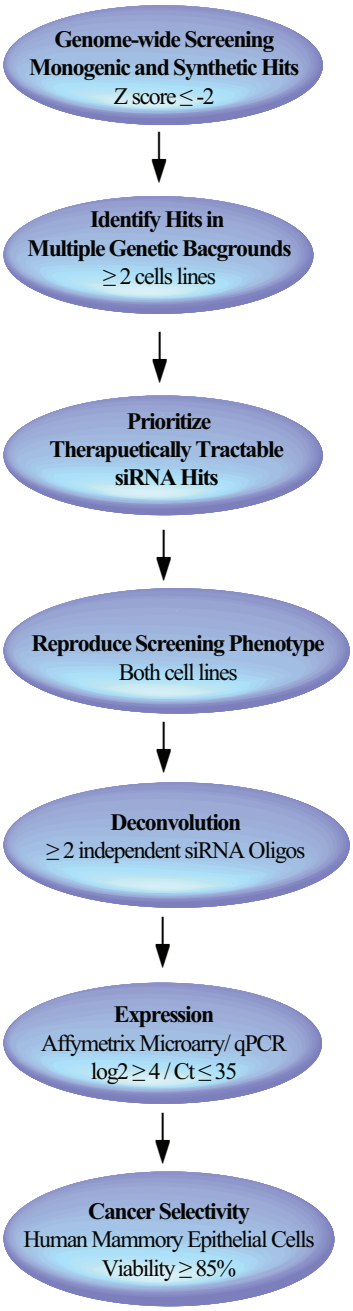
Genome-wide Screening
Monogenic and Synthetic Hits
Z score ≤ -2
Identify Hits in
Multiple Genetic Bacgrounds
≥ 2 cells lines
Prioritize
Therapuetically Tractable
siRNA Hits
Reproduce Screening Phenotype
Both cell lines
Deconvolution
≥ 2 independent siRNA Oligos
Expression
Affymetrix Microarry/ qPCR
log2 ≥ 4 / Ct ≤ 35
Cancer Selectivity
Human Mammory Epithelial Cells
Viability ≥ 85%

Figure 2. Screen Validation and Secondary Screen Retest Pipeline. A. Z score distributions of monogenic and synthetic lethal arms of each of the four pan-genomic screens performed. Screen hits defined with z score ≥ -2. B. Flow-chart of follow-up criteria.

Zinc Finger 165 (ZNF165) - Our functional genomics approach identified siRNA targeting ZNF165 as a supporter of TNBC tumor cell viability in multiple TNBC genetic backgrounds (Figure 3F). Furthermore, ZNF165 was the most potent collaborator with paclitaxel in the chemoresistant WHIM12 TNBC tumor-derived cell line (Figure 1A & 2A). ZNF165 is an unstudied zinc finger domain containing protein and is categorized as a cancer-testis antigen (CTA). Characteristic of CTAs, ZNF165 mRNA expression is testis-restricted but is reactivated in multiple types of cancer including breast, colorectal, bladder, and liver (143, 144). This suggests ZNF165 may be functionally contributing to the tumorigenic platform while exhibiting an extraordinarily wide therapeutic window. To validate our screen findings, we depleted ZNF165 in two TNBC cell lines where it was identified as a hit and observed reduced TNBC tumor cell viability with two independent siRNA pools along with concomitant ZNF165 mRNA depletion (Figure 3G). Traditionally, zinc finger proteins are not considered targetable because they lack an active site binding pocket for which a small molecule inhibitor can be designed. However, zinc finger domains mediate DNA binding and zinc finger proteins are often implicated in transcriptional regulation (145, 146). Given ZNF165's expression profile, functional elaboration of ZNF165's role in TNBC tumor cell biology may reveal tumor-specific signaling modules and downstream targets that could nominate additional TNBC therapeutic entry points.

Discussion

We leveraged a pan-genomic loss of function screening platform to systematically identify therapeutic intervention targets in TNBC. We selected a panel of four TNBC

tumor-derived cell lines that display the distribution of oncogenic aberrations, molecular subtypes and chemoresponsiveness found among TNBC patients. Our two-pronged approach allowed for the identification of genes that directly support TNBC tumor cell viability and genes that are required for buffering chemotherapeutic cellular stress. Here the anti-mitotic, paclitaxel, was used as a chemotherapeutic stressor due to its role as the standard of care chemotherapeutic regime for TNBC patients. Therefore, mechanistic elaboration of genes that synergize with paclitaxel may lead to new combination therapies or stratification strategies identifying sensitive subsets of TNBC patients.

Across all four genetic backgrounds, our screen identified 2000 modulators to TNBC tumor cell viability and paclitaxel-induced cellular stress. These hits included both known and unknown modulators of TNBC tumor cell biology. Known modulators include genes like RBBP9, CASC1 and TACC3 with previously defined roles in tumor cell survival and chemosensitivity (131, 133, 147). This suggests that we performed a high fidelity screen that reveals biology functionally contributing to TNBC tumor cell viability. With this validation, our screen can be viewed as a means to compile TNBC vulnerabilities. Given that we modeled TNBC tumor diversity to encompass the TNBC patient heterogeneity, our screen can be leveraged to address many different questions and generate hypotheses about TNBC tumor cell biology associated with oncogenic aberrations, chemoresponse profiles and/ or molecular subtypes.

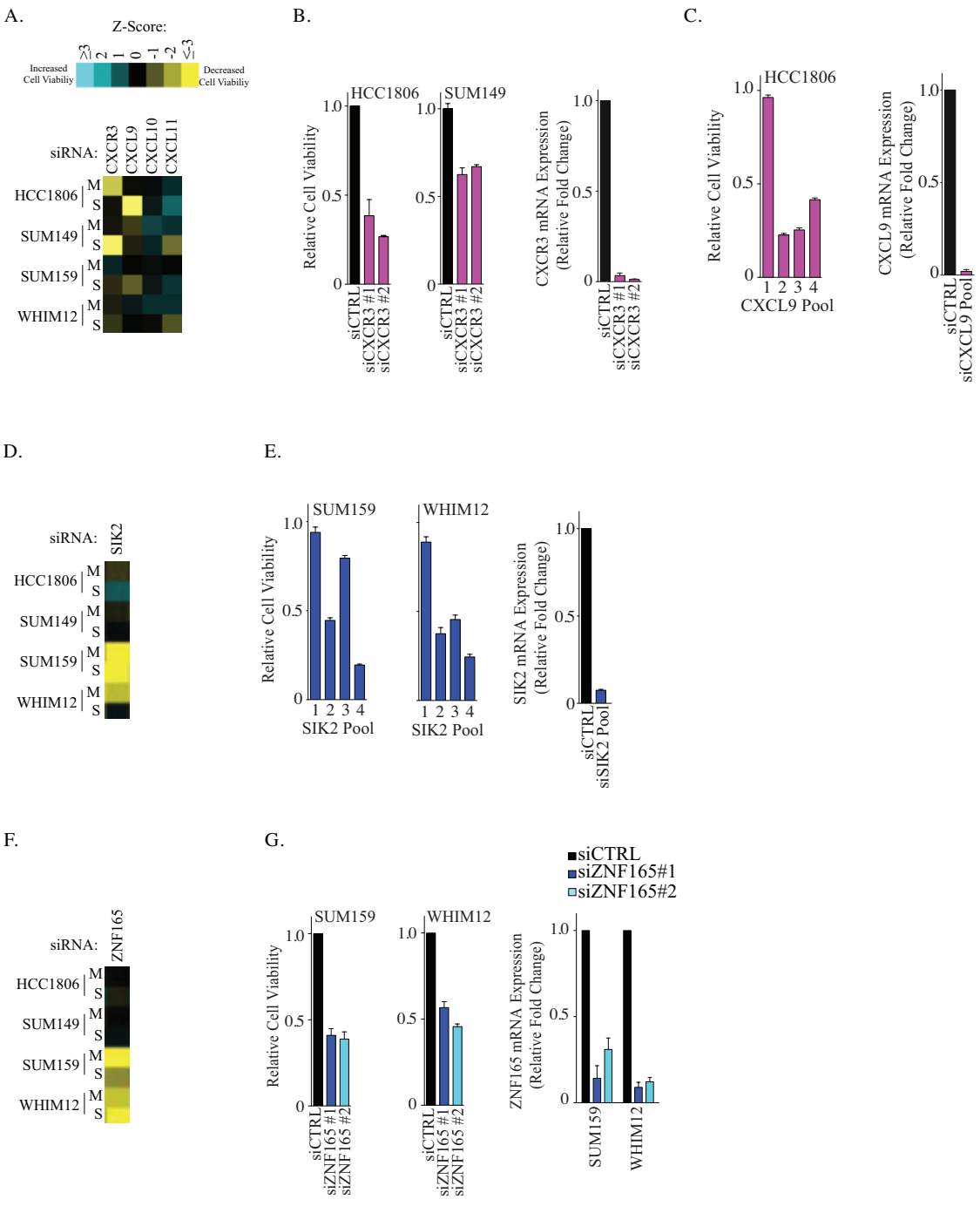
A.
Z-Score:
≥3
2
1
0
-1
-2
≤-3
Increased Cell Viability
Decreased Cell Viability
siRNA:
CXCR3
CXCL9
CXCL10
CXCL11
HCC1806
SUM149
SUM159
WHIM12
M
S
B.
HCC1806
SUM149
Relative Cell Viability
1.0
0.5
0
siCTRL
siCXCR3 #1
siCXCR3 #2
CXCR3 mRNA Expression (Relative Fold Change)
C.
HCC1806
Relative Cell Viability
1 2 3 4
CXCL9 Pool
CXCL9 mRNA Expression (Relative Fold Change)
siCTRL
siCXCL9 Pool
D.
siRNA:
SIK2
E.
SUM159
WHIM12
SIK2 Pool
SIK2 mRNA Expression (Relative Fold Change)
siSIK2 Pool
F.
ZNF165
G.
siCTRL
siZNF165#1
siZNF165#2
ZNF165 mRNA Expression (Relative Fold Change)

Figure 3. Identification of Top Priority Candidates for Mechanistic Elaboration. A. Heat map of screen z scores of CXCR3 and its ligands, CXCL9, 10 and 11. M – monogenic lethal z score. S – synthetic lethal z score. B. Left: Indicated TNBC cell lines were transfected with indicated siRNAs and cell viability was measured 96 hours post transfection (Cell Titer Glo®, CTG). Values represent viability relative to siCTRL (n = 3) ± S.D. Right: Total RNA was isolated from SUM149 cells transfected with either siCTRL or siCXCR3 and quantitative polymerase chain reaction (qPCR) was used to quantitate relative CXCR3 mRNA expression. Bars represent mean (n = 2) ± range. C. Left: Indicated TNBC cell lines were transfected with indicated siRNAs and cell viability was measured 96 hours post transfection (CTG). Values represent viability relative to siCTRL (n=3) ± S.D. Right: Total RNA was isolated from SUM149 cells transfected with either siCTRL or siCXCL9 and qPCR was used to quantitate relative CXCL9 mRNA expression. Bars represent mean (n = 2) ± range. D. Heat map of screen z scores of SIK2. M – monogenic lethal z score. S – synthetic lethal z score. E. Left: Indicated TNBC cell lines were transfected with indicated siRNAs and cell viability was measured 120 hours post transfection (CTG). Values represent viability relative to siCTRL (n = 3) ± S.D. Right: Total RNA was isolated from SUM159 cells transfected with either siCTRL or siSIK2 and qPCR was used to quantitate relative SIK2 mRNA expression. Bars represent mean (n = 2) ± range. F. Heat map of screen z scores of ZNF165. M – monogenic lethal z score. S – synthetic lethal z score. G. Left: Indicated TNBC cell lines were transfected with indicated siRNAs and cell viability was measured 96 hours post transfection (CTG). Values represent viability relative to siCTRL (n = 3) ± S.D. Right: Total RNA was isolated from indicated cell lines transfected with either siCTRL or siZNF165 and qPCR was used to quantitate relative ZNF165 mRNA expression. Bars represent mean (n = 3) ± S.D.

We further employed a secondary screen retest pipeline approach to prioritize TNBC vulnerabilities that are tumor-specific and therapeutically tractable. This strategy led to three candidates – CXCR3, SIK2 and ZNF165 - that were identified as supporting TNBC viability and chemotherapeutic response across multiple genetic backgrounds without affecting normal immortalized mammary epithelia. The remaining chapters will explore the cellular mechanisms behind CXCR3 (Chapter III), SIK2 (Chapter IV) and ZNF165 (Chapter V) supporting TNBC viability. These follow-up studies highlight the strength of RNAi screening approaches to uncover novel biological concepts and nominate new TNBC therapeutic strategies.

Materials and Methods:

Cell lines and reagents - Cell lines were obtained from American Type Culture Collection (ATCC) with the following exceptions: SUM159, SUM149 and HuMEC (gift from Charles Perou, UNC Lineberger Cancer Center), MDA-MB-436, MDA-MB-468, MDA-MB-231, HCC1806 (gift from Gray Pearson, UT Southwestern) and WHIM12 (gift from Matthew Ellis, Baylor College of Medicine). All cell lines were cultured in provider's recommended medium. siRNAs were obtained from GE Healthcare (siGENOME siRNA) or Sigma (Mission® siRNA). CTRL siRNA used was either siRNA targeting FNDC3B, or non-targeting control #5 or #2 (GE Healthcare).

siRNA Transfections - Transfection conditions were optimized using Lipofectamine® RNAiMAX and a lethal siRNA targeting Ubiquitin B (UBB) and a non-targeting control siRNA. Transfection efficiency was calculated as the CTG luminescence values of (1-

siUBB/siCTRL).

siRNA screen and data processing - Pan-genomic siGenome SMART pool siRNA library from GE Healthcare was purchased in 96 well plate format, for a total of 214 master plates. siRNAs were dissolved in 1X siRNA buffer (GE Healthcare) at a final concentration of 5 μM and stored at -80 °C. The library contained 4 independent siRNAs targeting a single gene pooled in a single well. siRNAs were diluted to 250 nM in serum free medium. Thirty microliters of this solution (4.3 pmoles of siRNA) was then aliquoted into empty plates and mixed with 10 mL of a Lipofectamine® RNAiMax (Life Technologies) solution (0.1 μL RNAiMAX in 9.9 μL/well Opti-MEM® (Life Technologies) and incubated for 20 minutes. Cells were harvested in parallel and diluted to target density in 60 μL of growth medium and then dispensed onto the siRNA-lipid mixture and incubated. Forty-eight hours post plating, cells were treated with either 35 ul of media or 35 μL of 3.85X paclitaxel for a final concentration of 1 nM and incubated for an additional 48 hours. Ninety-six hours post plating, cell viability was measured using 15 μL of CellTiter-Glo® (CTG) (Promega) assay system according to manufacturer's protocol. Measurements were made with a Pherastar Plus (BMG) plate reader. Twenty-four master siRNA plates were used per day for a total of 9 plating days for each screen. Raw values were row-median and plate-median normalized by day and a Z score metric was then applied (130). siRNA pools with z-scores < -2 were considered outliers.

Cell Viability Assays - Cells were reverse transfected in 96 well format. Forty-eight hours post plating, cells were fed with 35ul of complete media. Ninety-six hours post

plating, luminescence values were read following addition of 15 µL of Cell Titer-Glo® (CTG) (Promega) on a Pherastar Plus (BMG) plate reader.

Gene expression - Total RNA was isolated using RNA isolation kit (Sigma) and reverse transcribed using the High-Capacity cDNA Reverse Transfection Kit (Life Technologies) according to manufacturer's instructions. An Applied Biosystems Real-Time PCR system and either Solaris™, or TaqMan® Real-Time PCR gene expression assays were used. Gene expression assays were multiplexed with RPL27 or GAPDH as control assays. Relative expression values were calculated using the comparative Ct method.

CHAPTER III: Cytokine CXCR3/ CXCL9 Signaling Axis Supports Mitotic Fidelity and Survival in Basal-Like Triple Negative Breast Cancer[1]

Introduction

Our screening approach identified siRNA targeting CXCR3 as a potent supporter of TNBC viability and paclitaxel-induced cellular stress in multiple genetic backgrounds (Figure 3A&B). Additionally, one of the ligands of CXCR3, CXCL9, was also identified as supporting paclitaxel-induced cellular stress in the HCC1806 TNBC tumor-derived cell line (Figure 3A). Identification of both the receptor and ligand, CXCR3 and CXCL9, from our screening platform suggests that cell autonomous CXCR3/CXCL9 cytokine signaling is supporting tumor cell viability and buffering against chemotherapeutic stress. CXCR3 is a cytokine G-protein coupled receptor. Its ligands include the CXC ELR-negative cytokine subfamily, CXCL4, 9, 10, and 11 (134, 135). CXCR3 cytokine contributes to chemotaxis following injury-induced cytokine release in $CD4^+$ Type-1 helper and $CD8^+$ cytotoxic lymphocytes (135-137); however, CXCR3 has also been implicated in angiogenesis and wound repair (138-140). CXCR3 small molecule inhibitors have been employed to treat immune disorders like psoriasis, and graft vs. host disease (148). CXCR3 signaling was even proposed to be a biomarker for transplant organ rejection (149, 150). However, clinical trials targeting CXCR3 in these contexts

[1] All figures contributed by Kimberly E Maxfield

have failed due to lack of efficacy (76). Mechanistic elaboration of CXCL9/ CXCR3 signaling in the context of TNBC could uncover new mechanisms by which tumor cells can repurpose cytokine signaling to promote the tumorigenic phenotype and may translate into to new therapeutic strategies in TNBC.

Since its initial discovery in 1996, three CXCR3 isoforms have been discovered: CXCR3-A, CXCR3-B and CXCR3-Alt. The two A and B isoforms are due to an alternative-splicing event that leads to an alternative translational start site and excludes the first 50 extracellular N terminal amino acids from CXCR3-A. This region of the receptor is thought to dictate the differences in ligand binding affinity (135, 151). Although both isoforms can bind all CXCR3's ligands, CXCR3-A has a higher affinity for CXCL9, 10, and 11 while CXCL4 preferentially binds CXCR3-B (137, 151).

The CXCR3-A and –B isoforms also have opposing physiological functions. CXCR3-A signaling drives downstream cell proliferation, survival, and motility while CXCR3-B signaling inhibits cell growth, motility and sensitizes cells to apoptotic stimuli (135, 152). CXCR3-A signaling is pertussis toxin sensitive, induces Ca^{2+} release upon ligand stimulation and modulates the actin cytoskeleton in a ROCK-dependent manner, suggesting Gαi coupling (151, 153-155). Intracellular levels of cAMP increase upon CXCR3-B stimulation, which suggests Gαs coupling (151). Stimulation of CXCR3 has also been shown to induce ERK, AKT and SRC phosphorylation events (156), however, given that CXCR3-A and CXCR3-B only differ by a small N terminal deletion in CXCR3-A and therefore cannot be uniquely targeted, the exact regulation of and cellular

consequences resulting from CXCR3 signaling remains poorly understood.

There are also differences in the expression pattern between the CXCR3-A and -B isoforms. The pro-proliferative CXCR3-A is predominately expressed in undifferentiated hematopoietic stem cells and motile immune cells while anti-proliferative CXCR3-B is the primary isoform in differentiated epithelial, endothelial cells and fibroblasts (135). The CXCR3-Alt isoform contains a drastically different C terminal amino acid sequence when compared to both CXCR3-A and B. This translates into only ≤ 5 predicted transmembrane loops and therefore the functionality of this isoform remains to be elucidated (157).

In breast cancer, melanoma and colon cancer, increased expression of CXCR3 and/or its ligands is correlated with more aggressive, metastatic disease and poor patient outcomes (158, 159). Furthermore, CXCL9, 10 and 11 paracrine and autocrine loops have been observed in primary breast cancer samples (160). In breast cancer tumor-derived cell lines, introducing oncogenic gain of function RAS mutations induces CXCL9/10 autocrine loops and silences expression of the anti-proliferative CXCR-B isoform (159). Ligand stimulation of CXCR3 in breast cancer induces Ca^{2+} release and actin cytoskeletal rearrangements leading to increased cellular motility (135, 137, 154), suggesting that CXCR3-A is the predominate isoform expressed on tumor cells. Consistent with a role in promoting cell motility, CXCR3 expression is correlated with increased invasive and metastatic capabilities both in vitro and in vivo (42, 158, 159, 161). Small molecule inhibition of CXCR3 can also attenuate breast carcinoma

metastasis to the lung in a murine model (42), suggesting that tumorigenic expression is critical for acquiring metastatic potential.

Discovery of CXCR3 and CXCL9 in our functional genomics platform uncovers a novel cell autonomous role for CXCR3 and its ligand, CXCL9, in TNBC tumor cell viability and chemosensitivity. Here, we reveal that CXCR3 are required for a high fidelity bipolar spindle during mitosis, loss of which induces a prolonged mitotic arrest and subsequent death. We further show that this vulnerability may be biased to the basal-like subtype. This research uncovers a new cell autonomous role for CXCR3 cytokine signaling in tumorigenesis and nominates CXCR3 as a therapeutic target in combination with the first line chemotherapeutic, paclitaxel, using the basal-like subtype as a biomarker for sensitivity.

Results

CXCR3 Supports Basal-Like Tumor Cell Viability – Identification of CXCR3 in our screen nominates CXCR3/CXCL9 signaling as supporting TNBC viability. To test if CXCR3 is supporting long-term TNBC tumor cell survival, we measured apoptosis using active caspase 3 immunoblot following CXCR3 siRNA depletion and observed that loss of CXCR3 induces active caspase 3. This apoptotic response is correlated with loss of long-term viability as measure by a clonogenic replating assay (Figure 4A). In our screens, CXCR3 was identified as a hit in the two basal-like cell lines. To test if CXCR3 is a basal-like selective vulnerability, we depleted CXCR3 within the isogenic basal-like and claudin-low compartments of the SUM149 cell line. The parental SUM149 cell line

clusters with the basal-like subtype but a small stable subset of SUM149 cells clusters with the claudin-low subtype (33). Using the cell surface markers, EpCAM and CD49f, Fluorescence Activated Cell Sorting (FACS) can be employed to separate the SUM149 parental cell line into its basal-like (EpCAM high and Cd49F low) and claudin-low (EpCAM low and CD49f high) subpopulations. Following FACS analysis, we then measured apoptosis using active caspase 3 immunoblot following CXCR3 siRNA depletion and observed that CXCR3 only supported survival in the basal-like compartment of the SUM149, despite equal protein depletion (Figure 4B). We next tested the effect of CXCR3 on apoptosis across diverse basal-like genetic backgrounds. We observed that CXCR3 protein is detectable in all cell lines regardless of subtype but loss of CXCR3-induced apoptosis was seen in the basal-like cell lines 96 hours post transfection (Figure 4C), suggesting that the basal-like subtype may be more sensitive to CXCR3 depletion. Given CXCR3 protein expression is present regardless of sensitivity, CXCR3 expression may not responsible for the difference in sensitivity. Taken together, these data suggest that CXCR3 cytokine is supporting Basal-Like tumor cell survival.

CXCR3 Supports Basal-Like Mitotic Fidelity - Since our screen identified a collaboration between CXCR3 depletion and the anti-mitotic chemotherapeutic, paclitaxel (Figure 3A), we next asked if loss of CXCR3 modulated tumor cell mitosis. Following depletion of CXCR3, we observed an accumulation of multipolar misaligned mitotic spindles compared to control transfected cells (Figure 5A). We further found that loss of CXCR3 increased the number of cells in mitosis (mitotic index), measured by

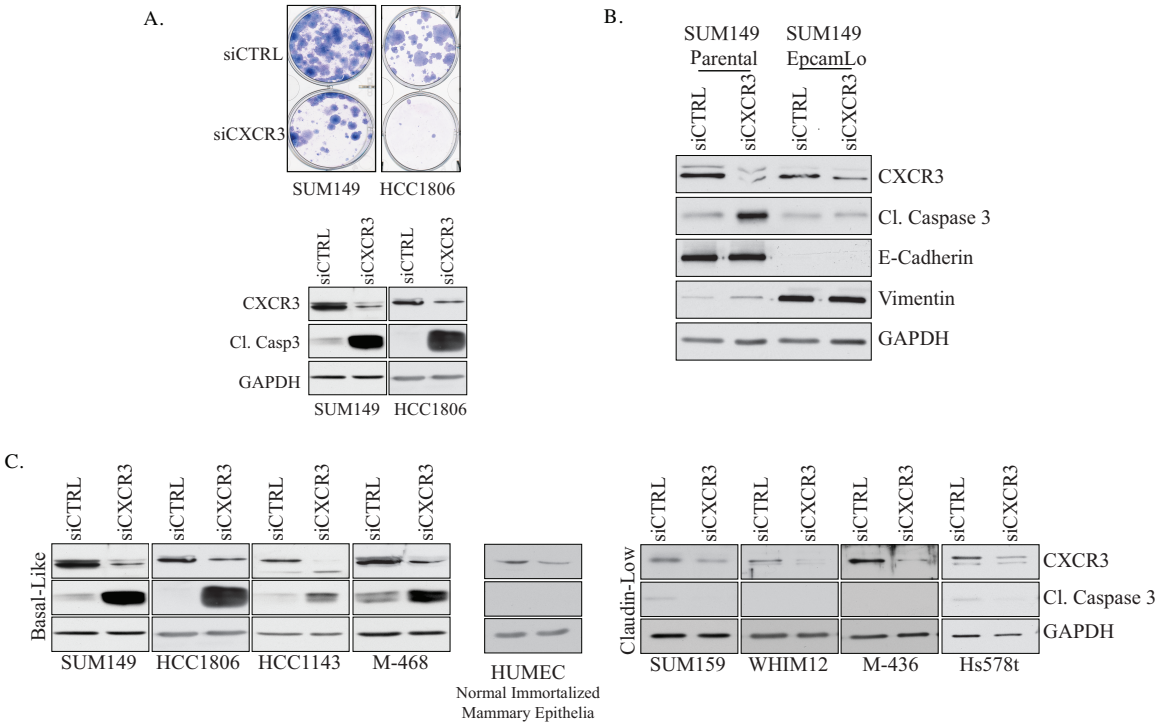

Figure 4. CXCR3 Supports Tumor Cell Viability. A. Top: Indicated TNBC cell lines transfected with indicated siRNAs were re-plated at limiting dilution 96 hours post transfection. Bottom: Indicated TNBC cell lines were transfected with indicated siRNAs and immunobloted with indicated antibodies 96 hours post transfection. B. Whole cell lysates (WCL) of SUM149 cells separated into their claudin-low and basal-like compartments using fluorescence activated cell sorting (FACS) and transfected with indicated siRNAs were immunoblotted with indicated antibodies 96 hours post transfection. C. WCLs from indicated cell lines transfected with indicated siRNAs were immunoblotted with indicated antibodies 96 hours post transfection.

immunofluorescence staining of serine 10 phosphorylation on histone H3B, which is a mitotic-specific phosphorylation event initiated by aurora kinases (162). We observed a mitotic index increase with multiple independent siRNA pools targeting CXCR3. We further observed an accumulation of the mitotic-specific cyclin, Cyclin B1 (163). This suggests the mitotic defects seen following CXCR3 siRNA depletion are not due to siRNA off-target effects (Figure 5B). To further understand siCXCR3-induced mitotic defects, we employed time-lapse video microscopy to observe mitotic progression in real time. We generated SUM149 cells stably expressing GFP (Green Fluorescent Protein)-Histone H2B, to allow for visualization of nuclei. SUM149-GFP-H2B cells were for monitored mitotic transit time and cell fate 48 to 96 hours post siCXCR3 transfection. This analysis revealed that CXCR3 depletion significantly increases mitotic transit time and that an increased mitotic transit time is correlated with mitotic catastrophe, defined as either an aberrant micronucleated mitotic exit or initiation of apoptosis during metaphase (Figure 5C) (164). This is consistent with our group's previous findings that prolonging metaphase increases likelihood of a mitotic catastrophe and thus decreasing tumor cell viability in NSCLC (133). Furthermore, we found that codepletion of CXCR3 and MAD2, an obligate component of the spindle assembly checkpoint (165), rescues the mitotic index increase but also increases the proportion of damaged micronucleated cells (Figure 5D), suggesting that loss of CXCR3 signaling induces mitotic damage, which triggers the spindle assembly checkpoint and prevents mitotic progression. Prolonged engagement of the spindle assembly checkpoint then leads to induction of apoptosis. Lastly, we observed that loss of CXCR3 signaling induces mitotic index increase specifically in the basal-like subtype (Figure 5E). Taken together, these data suggest a

novel cell-autonomous role for CXCR3/ CXCL9 signaling supporting mitotic fidelity that is required for Basal-Like breast cancer cell survival.

Discussion

Our pan-genomic screening TNBC screening approach uncovered a novel cell autonomous role for CXCR3 cytokine signaling supporting tumor cell viability through promoting mitotic spindle alignment. We show that loss of CXCR3 signaling impedes proper spindle alignment, stalling mitotic progression through activation of the spindle assembly checkpoint followed by induction of apoptosis (Figure 6). This is the first report of a cytokine receptor with a cell autonomous role in mitotic spindle alignment. In tumorigenesis, CXCR3 has been primarily studied as a driver of cell motility through actin cytoskeleton rearrangements (137, 155, 166, 167). This has been shown to promote metastasis in multiple tumor types including breast and prostate (42, 152, 153, 158). However, the actin cytoskeleton also plays an important role during mitosis. Actin filaments form a cortex surrounding the periphery of the cell that provides a mechanical link between the plasma membrane and microtubule-based mitotic spindle. This link allows for the tension needed to form a bipolar spindle (168, 169). The formation of the actin cortex is initiated at the onset of mitosis and is facilitated by actin-associated proteins, such as Mitotic Spindle Positioning, G-Protein Signaling Modulator 2, Cofilin 1 and Moesin (76, 162, 165, 170-175). We have preliminary evidence that CXCR3/CXCL9 signaling modulates the actin cytoskeleton in TNBC. Attenuation of CXCL9 signaling induces the loss of actin stress fibers (data not shown). Given this, we

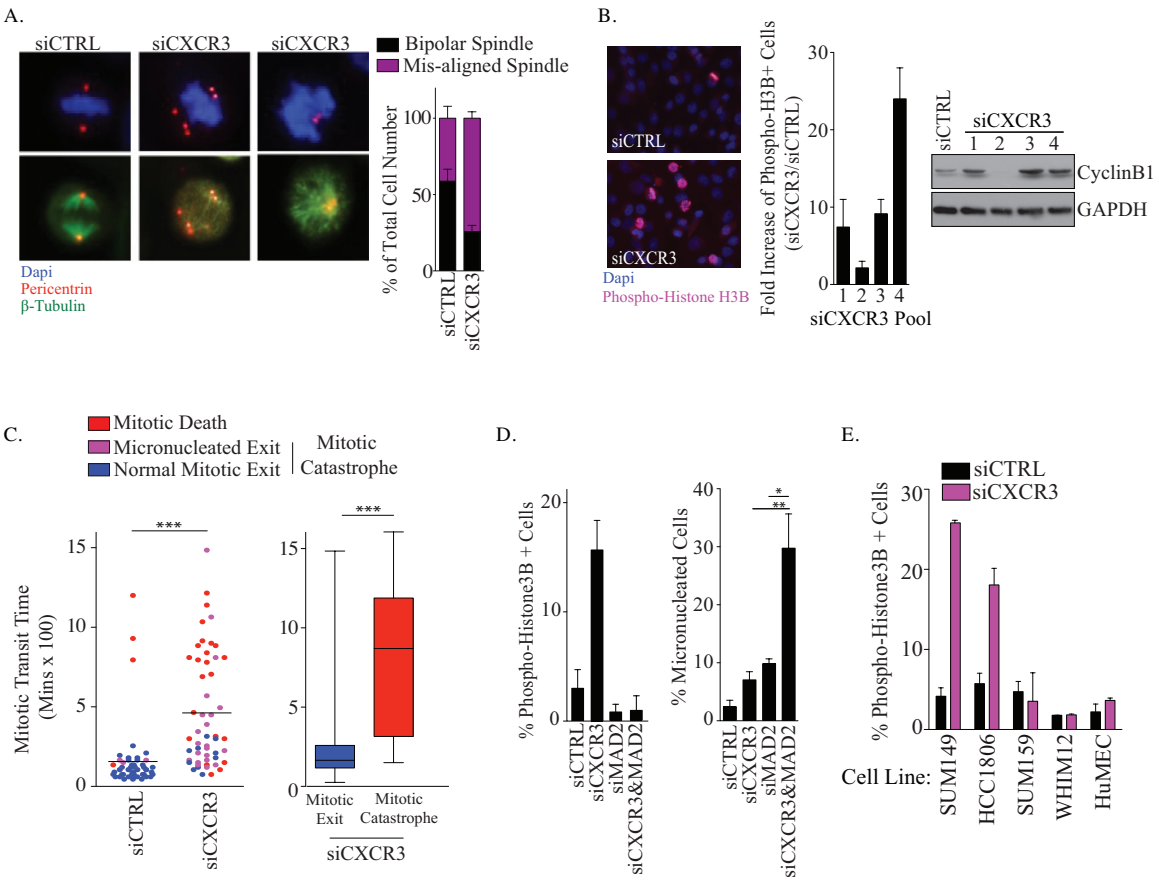
A.
siCTRL
siCXCR3
siCXCR3
Bipolar Spindle
Mis-aligned Spindle
Dapi
Pericentrin
β-Tubulin
% of Total Cell Number
siCTRL
siCXCR3
B.
siCTRL
siCXCR3
Dapi
Phospho-Histone H3B
Fold Increase of Phospho-H3B+ Cells (siCXCR3/siCTRL)
siCXCR3 Pool
siCTRL
siCXCR3
CyclinB1
GAPDH
C.
Mitotic Death
Micronucleated Exit
Normal Mitotic Exit
Mitotic Catastrophe
Mitotic Transit Time (Mins x 100)
siCTRL
siCXCR3
Mitotic Exit
Mitotic Catastrophe
siCXCR3
D.
% Phospho-Histone3B + Cells
% Micronucleated Cells
siCTRL
siCXCR3
siMAD2
siCXCR3&MAD2
E.
siCTRL
siCXCR3
% Phospho-Histone3B + Cells
Cell Line:
SUM149
HCC1806
SUM159
WHIM12
HuMEC

Figure 5. CXCR3 Supports Mitotic Fidelity. A. Left: SUM149 cells transfected with indicated siRNAs for 72 hours were fixed, immunostained with indicated antibodies. Right: SUM149 cells transfected with indicated siRNA were processed as above. Mitotic spindle alignment was quantitated manually for 100 cells per condition. Bars represent mean (n = 2) ± range. B. Left: SUM149 cells transfected with indicated siRNAs for 72 hours were fixed, immunostained with indicated antibodies. Middle: SUM149 cells transfected with indicated siRNA were processed as above. Percent of serine 10 phosphorylated Histone 3B positive cells were quantitated manually for 100 cells per condition. Bars represent mean (n = 4) ± S.D. Right. WCLs from SUM149 cells transfected with indicated siRNAs were immunoblotted with indicated antibodies 72 hours post transfection C. Left: SUM149 cells expressing GFP-Histone H2B were transfected with indicated siRNAs. At 48 hours post-transfection, cells were imaged by live time-lapse microscopy from 48-96 hours post-transfection. Manual single-cell lineage tracing was performed to identify mitotic transit time and mitotic exit phenotype for a total of 100 cells per condition over two independent transfections. Right: Representation of mitotic transit time of cells described above grouped by mitotic exit. P values represents unpaired Student's t test. D. Left: SUM149 cells transfected with indicated siRNAs for 72 hours were fixed, immunostained with indicated antibodies. Percent serine 10 phosphorylated Histone 3B positive cells were quantitated manually for 100 cells per condition. Bars represent percent serine 10 phosphorylated Histone 3B positive cells (n = 3) ± S.D. Right: SUM149 cells processed as above. Micronucleated cells were quantitated manually for 100 cells per condition. Bars represent percent micronucleated cells (n = 3) ± S.D. P values represent unpaired Student's t test. E. Indicated cell lines transfected with indicated siRNAs for 72 hours were fixed, immunostained with indicated antibodies. Serine 10 phosphorylated Histone 3B positive cells were quantitated manually for 100 cells per condition. Bars represent percent serine 10 phosphorylated Histone 3B positive cells (n = 3) ± S.D.

hypothesize that loss of CXCR3 signaling disrupts the actin cortex that provides the tension needed to form a bi-polar mitotic spindle. Loss of this tension then prevents proper mitotic spindle formation thus triggering the spindle assembly checkpoint and subsequent apoptosis. Consistent with this, our original pan-genomic screen also identified the actin-interacting protein and actin-cortex modulator, cofilin (175), as selectively required for tumor cell viability in the same basal-like cell lines that were CXCR3-dependent.

Our results also suggest that CXCR3 may be selectively supporting tumor cell survival and mitotic fidelity in the basal-like molecular subtype. Through cDNA microarray profiling, TNBC can be subdivided into two molecular subtypes; basal-like and claudin-low. These two subtypes have distinct gene expression profiles, morphologies, chemoresponse profiles and patient prognosis in the clinic (33). Furthermore, claudin-low and basal-like tumors also have strikingly differential pCR responses to paclitaxel-based chemotherapeutic regimens. Patients with basal-like tumors are twice as likely to achieve pCR than patients with claudin-low tumors (33), suggesting that basal-like and claudin-low tumors have differential abilities to withstand mitotic stress. Consistent with this, loss of CXCR3 only induced mitotic defects in basal-like cell lines despite equal protein depletion, suggesting there may be fundamental differences with the maintenance of mitotic fidelity between claudin-low and basal-like tumors.

Our original screen identified synthetic lethal relationship between siCXCR3 and siCXCL9-induced mitotic stress and paclitaxel in the SUM149 and HCC1806 basal-like tumor-derived cell lines, respectively. Our findings also uncovered a mitotic role for

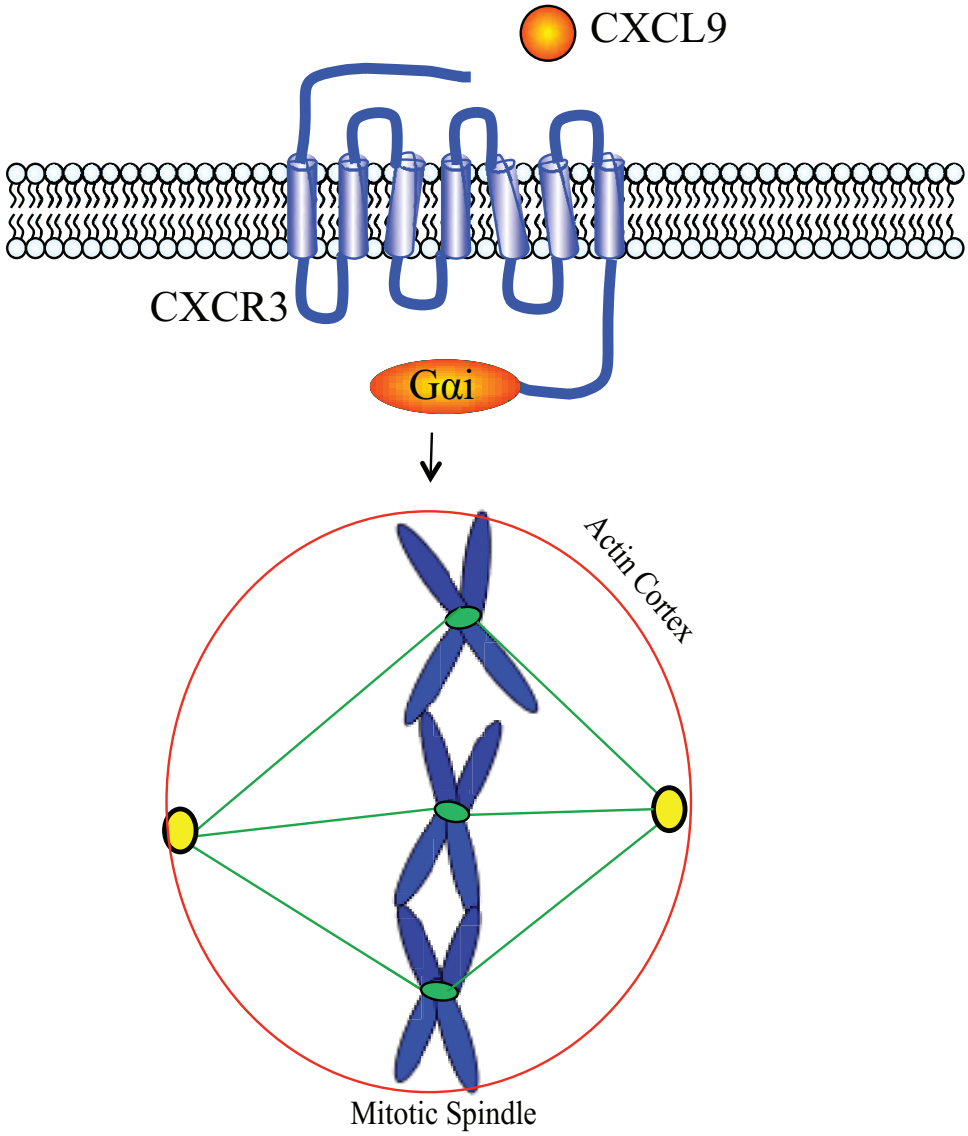

Figure 6. Model of CXCR3/ CXCL9 Signaling Supporting Mitotic Fidelity and Survival. A. CXCL9 binds to CXCR3 and induces ROCK-mediated alterations in the actin cytoskeleton. This disruption alters the actin cortex to prevent proper mitotic spindle alignment.

CXCR3 in basal-like breast cancer, suggesting that inhibition of CXCR3 may synergize anti-mitotic mechanism of paclitaxel. This nominates CXCR3 as a new TNBC therapeutic target. Currently, AMG487 is in clinical trials for immune disorders and, therefore, could be repurposed to form a new paclitaxel combination therapy using basal-like breast cancer as a biomarker for sensitivity.

Materials and Methods:

Cell lines and reagents - Cell lines were obtained from ATCC with the following exceptions: SUM159, SUM149 and HuMEC (gift from Charles Perou, UNC Lineberger Cancer Center), HCC1806 (gift from Gray Pearson, UT Southwestern) and WHIM12 (gift from Matthew Ellis, Baylor College of Medicine). All cell lines were cultured in provider's recommended medium. Antibodies were obtained from Santa Cruz (GAPDH, Rabbit IgG), Abcam (CXCR3, Pericentrin), Sigma (β-tubulin) and Cell Signaling Technologies (Cleaved Caspase-3), Millipore (Serine10 Phospho-Histone 3B). siRNAs were obtained from GE Healthcare (siGENOME siRNA) or Sigma (Mission® siRNA). CTRL siRNA used was non-targeting control (GE Healthcare).

Cell Viability Assays - Cells were reverse transfected in 96 well format. Forty-eight hours post plating, cells were fed with 35ul of complete media. Ninety-six hours post plating, luminescence values were read following addition of 15 μL of Cell Titer-Glo® (CTG) (Promega) on a Pherastar Plus (BMG) plate reader.

Generation of stable cell lines - SUM149 stable cell lines were generated through

retroviral-mediated transduction of pCLNCX-GFP-H2B (a gift from Gray Pearson, UT-Southwestern) and VSV-G. Following infection stable populations were selected using appropriate antibiotics.

Colony formation assay - Cells were reverse transfected with 10 pmoles of siRNA using RNAiMax® (Life Technologies). Ninety-six post transfection, cells were replated at limiting dilution in 6-well format. Cells were fed twice weekly until controls reached confluency at which point colonies were fixed in 3.7 % formaldehyde and stained with Geimsa (Sigma).

Gene expression - Total RNA was isolated using RNA isolation kit (Sigma) and reverse transcribed using the High-Capacity cDNA Reverse Transfection Kit (Life Technologies) according to manufacturer's instructions. An Applied Biosystems Real-Time PCR system and either Solaris™, or TaqMan® Real-Time PCR gene expression assays were used. Gene expression assays were multiplexed with RPL27 or GAPDH as control assays. Relative expression values were calculated using the comparative Ct method.

Immunoblotting - Whole cell lysates were prepared in 2x Laemmli sample buffer and resolved using SDS-PAGE. Gels were transferred to Immobilon® PVDF (Millipore) or nitrocellulose (Bio-rad) membranes, blocked in tris-buffered saline containing 0.1 % Tween20 (TBST) and either 5 % non-fat dry milk or bovine serum albumin (BSA), or Odyssey® blocking buffer and incubated with indicated primary antibodies for 1 hour or overnight. After washes in TBST, appropriate HRP-coupled secondary antibodies

(Jackson Immunoresearch) were used for chemiluminescence.

Immunofluorescence - Cells plated on glass coverslips were fixed with 3.7 % formaldehyde and permeabilized with 0.05% Triton X-100 for ten minutes. Cells were blocked and washed in 1 % BSA, 0.1 % Tween-20 in 1X PBS (PBTA). Cells were incubated with primary antibodies for 1 hour followed by three washes in PBTA. Coverslips were then incubated with Alexa Fluor®-conjugated secondary antibodies (Invitrogen) for 30 minutes followed by 3 washes in PBTA and a wash in H_2O. Prolong® Gold Antifade reagent with DAPI (Life Technologies) was used to mount slips on glass slides and images were acquired on either a Zeiss Axioimager upright microscope (Zeiss) with a CCD camera.

Fluorescence Activated Cell Sorting – SUM149 cells were trypsinized and filtered using 40μM cell strainers. Cells were then spun at 450g for 5 minutes followed by resuspension in Hanks's Balanced Salt Solution (HBSS) with 2% FBS. Cells were then incubated with EpCAM-FITC and CD49f-PE-Cy5 antibodies for 30 minutes at 4°C. Cells were then washed 2X with HBSS with 2 % FBS and were immediately sorted by FITC and Cy5 using Beckman Coulter CyAn ADP using Summit 4.3. Populations enriched for EpCAM high/ Cd49F low and EpCAM low/ Cd49F high were collected and immediately replated in normal growth media. All experiments were set up within 48 hours of FACS sorting.

High-Content Imaging - SUM149 cells stably expressing GFP-histone 2B were reverse

transfected with the indicated siRNAs in 96 well format. Forty-eight hours post-transfection, the cells were imaged on a BD Pathway 855 bio-imager using a 20X high-NA objective. Images were taken every 15 minutes for the next 48 hours and an image sequence was generated using Image J.

CHAPTER IV: AMPK Family Member, SIK2, Restricts Autophagy to Support Tumor Cell Viability in Triple Negative Breast Cancer[2]

Introduction

In our pan-genomic siRNA screen to identify new therapeutic entry points in TNBC, siRNAs targeting Salt Inducible Kinase 2 (SIK2) were identified as synergizing with the first line chemotherapeutic, paclitaxel in SUM159 cells and as required for tumor cell viability WHIM12 cells (Figure 3D&E). SIK2 is one of three SIK family members in the AMPK family of related kinases (176, 177). SIK1 and SIK2 are very closely related with their main difference at the level of tissue expression. SIK1 is primarily expressed in the adrenal glands where it modulates adrenocorticotropic hormone release. SIK2 is highly expressed in adipocytes, hepatocytes and pancreatic β cells and plays a role in modulating gluconeogenesis (178). SIK3 is expressed ubiquitously but has an extensive C terminal elongation, making it less homologous than SIK1 and 2. While overall SIK3's role is also less understood, along with SIK2, it has been implicated in energy homeostasis (178, 179).

Despite only having a few bona fida substrates identified, SIK2 is known as an inhibitor of de novo cellular energy production under ample cellular nutrient conditions (178). One of SIK2's direct substrates, CRTC2, is a transcription factor that translocates

[2] All figures contributed by Kimberly E Maxfield

into the nucleus under low energy conditions to drive transcription of gluconeogenesis genes. In the presence of insulin, SIK2 phosphorylates CRTC2 targeting it for proteasomal degradation and preventing its downstream pro-gluconeogenesis transcription (180, 181). Additional SIK2 direct substrates include Class IIa HDAC and p35. SIK2 phosphorylation of HDAC promotes HDAC nuclear translocation to further prevent expression of energy promoting genes like insulin transporter, GLUT4 (182, 183). SIK2's phosphorylation of p35 leads to p35 degradation and promotion of insulin secretion (184). Little is known about the regulation of SIK2 kinase activity but as a member of the AMPK-related family, SIK kinases can be activated by the tumor suppressor, LKB1, in vitro (177). In vivo, SIK2 kinase activity is inhibited by cAMP/ PKA through phosphorylation of its serine 358 residue (185). Taken together, SIK2 is emerging as an important energy sensing kinase and identification in our screen nominates SIK2 as a functionally supporting TNBC.

Consistent with a role in energy homeostasis, SIK2 has recently been implicated in autophagy. Autophagy is an evolutionarily conserved cell survival pathway resulting in lysosomal degradation of cytoplasmic components to increase nutrient and energy availability under low nutrient conditions. Autophagy initiation is primarily under control of two kinases; AMPK activates autophagy and mTOR inhibits autophagy. When AMPK senses low nutrient conditions, it induces autophagy through an inhibitory phosphorylation event on Raptor/ mTOR and an activating phosphorylation event on ULK1 (186). Furthermore, AMPK-induced phosphorylation of Raptor will inactivate the mTOR complex and release mTOR-mediated inhibition of autophagy (187-189). AMPK-

induced phosphorylation of ULK1 will then initiate the autophagosome initiation complex by forming an ULK1-mATG13-FIP200 complex to drive downstream autophagosome formation (189, 190). mTOR's inhibitory phosphorylation event on ULK1 is mediated by upstream insulin receptor signaling through AKT to prevent autophagy initiation (191-193). AKT can also directly inhibit autophagy with an inhibitory phosphorylation event on Beclin 1, abrogating all autophagosome formation (194). SIK2 was introduced as altering autophagy from a study that revealed overexpression of SIK2 increased the number of autophagic vesicles in HEK293T cells. However, the exact nature of SIK2's role was not elucidated (174). Furthermore, large-scale proteomic studies identified autophagosome-associated protein GABARAPL as a putative interactor with SIK2 (195), suggesting SIK2's energy sensing role may include modulation of autophagy.

SIK2 has recently been implicated in tumorigenesis but it was identified in a cellular context seemingly unrelated to its energy-sensing capabilities. SIK2 was identified as an outlier in a loss of function siRNA screen to uncover mechanisms of tumorigenic polyploidy in ovarian cancer. This study further implicated SIK2 in centrosome splitting during mitosis and was found to synergize with the first line chemotherapeutic, paclitaxel (141). This work led to the development of a SIK family inhibitor, which is in preclinical development in ovarian cancer. Now that a tumorigenic role for SIK2 is starting to gain traction, additional preliminary studies are evaluating roles for SIK2 in tumor types like glioma and prostate cancer (196, 197).

Here, our pan-genomic screening approach identified SIK2 as a vulnerability in multiple TNBC genetic backgrounds. Despite seeing collaboration with paclitaxel, we did not observe any centrosomal defects following SIK2 depletion. Upon evaluation of SIK2 in autophagy, we show that SIK2 acts as an autophagic break in TNBC cell lines and releasing this break causes a loss of TNBC tumor cell viability. We further show that SIK2 supports AKT survival signaling, which is a known inhibitor of autophagy. This work identifies SIK2 as novel TNBC vulnerability by acting as an autophagic brake that may allow tumor cells to benefit from the tumor-promoting aspects of autophagy. SIK2 was recently implicated in supporting ovarian cancer and this work promoted development of SIK family small molecule inhibitors for the evaluation of SIK2 as a therapeutic evaluation (141). Through a collaboration with Arrien Pharmaceuticals, Inc, we obtained one of these inhibitors, ARN3236, and demonstrated that treatment drove excessive autophagic flux in TNBC, further nominating SIK2 as a new TNBC therapeutic entry point.

Results

SIK2 Supports TNBC Viability – Following validation of SIK2 as a screen hit, (Figure 3D&E), we next evaluated the penetrance of the SIK2 dependency in a large panel of TNBC tumor-derived cell lines and found a range of SIK2 dependencies (Figure 7A). This suggests that SIK2 is a selective vulnerability among TNBC tumors. Of note, the HCC1806 cell line retested as siSIK2 sensitive whereas in the HCC1806 pan-genomic screen was not identified as a hit, suggesting SIK2 was a false negative in the screen (Figure 3D&7A). In siSIK2 sensitive lines, we also saw loss of long term viability

following siRNA depletion of SIK2 in a clonogenic replating assay, further suggesting SIK2 is required for long-term TNBC survival (Figure 7B). However, we did not observe induction of active caspase 3 following SIK2 siRNA depletion, suggesting the loss of viability following SIK2 depletion is not due to induction of apoptosis (Figure 7C). We next examined SIK2-sensitive cell lines for centrosomal defects following SIK2 depletion since SIK2 has been recently implicated in centrosome splitting in ovarian cancer (141). However, we also did not observe any centrosomal defects following siRNA depletion of SIK2 in our TNBC tumor-derived cell lines (Figure 7D). These data suggest that SIK2 is a selective vulnerability in TNBC through a centrosome-independent mechanism.

SIK2 Acts as an Autophagic Break – To further examine SIK2 in TNBC, we next evaluated a role for SIK2 in autophagy. SIK2 acetylation was recently implicated in autophagic progression (174) and large-scale proteomic studies identified the autophagy-associated protein, GABARAPL2 (152, 153), as a putative binding partner of SIK2 (195). Furthermore, identification of an apoptosis-independent autophagic death was recently implicated as an important survival pathway in multiple myeloma (173). Following siRNA depletion of SIK2, we observed loss of both LC3-I, and the autophagosome-associated LC3-II (Figure 8A), suggesting loss of SIK2 alters the number of autophagic vesicles within the cell. Upon protein synthesis, LC3 is immediately cleaved to become LC3-I, followed by phosphatidylethanolamine-modification to become LC3-II. This lipidation leads to autophagosome incorporation upon initiation of autophagy (198). Therefore, LC3 protein levels are often used as a quantitative measure of autophagic vesicles within a cell (198). To determine if the loss of LC3-II protein was due to

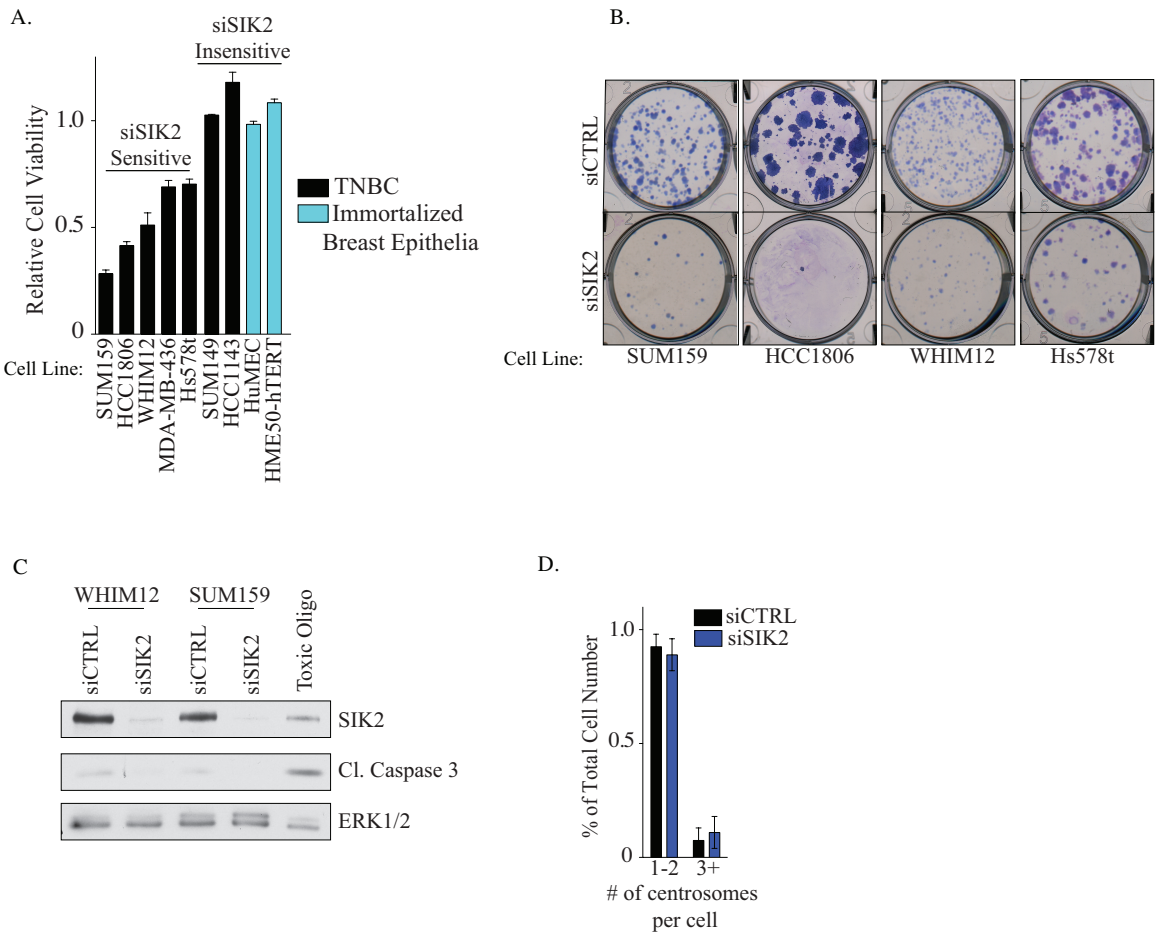

Figure 7. SIK2 Supports TNBC Tumor Cell Viability. A. Indicated TNBC cell lines were transfected with indicated siRNAs and cell viability was quantitated 120 hours post transfection (CTG). Values represent viability relative to siCTRL (n = 3) ± S.D. B. Indicated TNBC cell lines transfected with indicated siRNAs were re-plated at limiting dilution 120 hours post transfection. C. WCLs from of indicated cell lines transfected with indicated siRNAs were immunoblotted with indicated antibodies 120 hours post transfection. D. SUM159 cells transfected with indicated siRNAs were fixed, immunostained with indicated antibody targeting pericentrin for centrosome visualization. Number of centrosomes per cell was quantitated manually for 100 cells per condition. Bars represent percent of total cell number (n = 2) ± range.

inhibition of autophagy or increase in autophagic flux, we depleted SIK2 with two independent siRNA pools in SUM159 cells stably expressing GFP-LC3-II, which will allow for visualization of autophagic vesicles. Following a pharmacologic block of autophagasome/lysosome fusion using chloroquine (199), we observed excessive accumulation of GFP-LC3 positive puncta in chloroquine treated cells depleted of SIK when compared to siCTRL chloroquine treated cells, suggesting loss of SIK2 drives autophagic flux (Figure 8B). To evaluate this observation on the population level, we employed FACS analysis in the GFP-LC3-II stably expressing U2OS osteosarcoma cell line, which exhibits increased basal autophagy facilitating reproducible GFP detection during FACS. We first confirmed the same GFP-LC3-II accumulation following siSIK2 at the single cell level seen in the TNBC SUM159 GFP-LC3-II line (Figure 8C - Top). Following FACS analysis in U2OS-GFP-LC3 cells, we observed greater total GFP fluorescence in the siSIK2 chloroquine treated cells compared to siCTRL chloroquine treated cells indicative of an accumulation of GFP-LC3-II positive autophagosomes, which is consistent with loss of SIK2 driving autophagic flux (Figure 8C - Bottom). Furthermore, we found that loss of SIK2 leads to increased serine 555 phosphorylation on ULK1, which is AMPK autophagy-promoting phosphorylation site (Figure 8D) (200), indicating that loss of SIK2 enhances autophagy-promoting cellular signaling. We also obtained a selective SIK2 inhibitor from Arrien Pharmaceuticals and recapitulated the accumulation of GFP-LC3-II puncta following SIK2 inhibition in conjunction with chloroquine treatment (Figure 8E). This suggests that SIK2 is pharmacologically targetable in TNBC and siSIK2-induced increase in autophagic flux is not due to siRNA off-target effects. Taken together, these data suggest SIK2 functions as an autophagic

break in TNBC.

SIK2 Supports TNBC Viability by Attenuating Autophagy Initiation - An increase in the autophagy-activating phosphorylation site of ULK1 following siSIK2 also suggests that SIK2 modulates autophagy upstream of autophagosome initiation. To test this, we codepleted SIK2 with an obligate component of the autophagosome formation machinery, ATG5 (201, 202), in SUM159 GFP-LC3-II cells. We observed that loss of ATG5 rescued siSIK2-induced accumulation of GFP-LC3-II puncta and loss of endogenous LC3-II both at the single cell and population level (Figure 9A). Furthermore, codepletion with ATG5 rescued TNBC viability loss following siSIK2 (Figure 9B), indicating SIK2 supports tumor cell viability through restricting excessive autophagy.

SIK2 Supports AKT Survival Signaling - SIK2 has been previously reported to alter AKT signaling in ovarian cancer (141). AKT alters cell growth and autophagy in response to nutrient status and is a known inhibitor of autophagy (193). To evaluate a role for SIK2 in AKT signaling in TNBC, we depleted SIK2 with two independent siRNA pools in SUM159 cells and observed loss of the RICTOR-activating serine 473 phosphorylation site on AKT (Figure 9C) (203). We further found concomitant loss of the AKT-specific phosphorylation sites on AKT downstream targets, GSK3β and Beclin1 (Figure 9C&D), providing additional evidence that loss of SIK2 is leading to compromised AKT signaling. Beclin 1 serves as the main initiator of autophagosome formation in response to signaling from ULK1 and AKT (204). The AKT-induced serine 295 phosphorylation on Beclin1 is an inhibitory site (Figure 9D) (194), suggesting that SIK2 supports AKT signaling that leads to inhibition of Beclin 1-induced autophagy.

A.

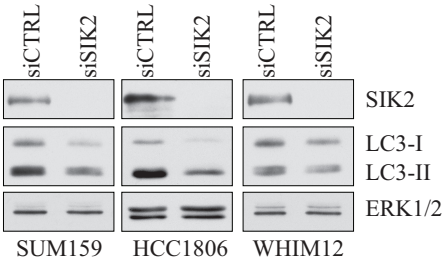
siCTRL
siSIK2
siCTRL
siSIK2
siCTRL
siSIK2
SIK2
LC3-I
LC3-II
ERK1/2
SUM159
HCC1806
WHIM12

B.

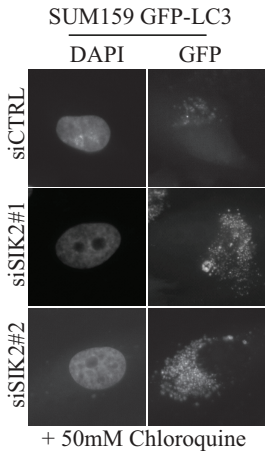
SUM159 GFP-LC3
DAPI
GFP
siCTRL
siSIK2#1
siSIK2#2
+ 50mM Chloroquine

C.

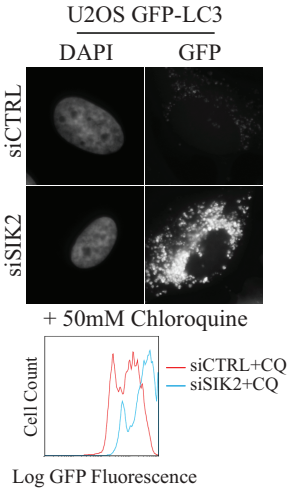
U2OS GFP-LC3
DAPI
GFP
siCTRL
siSIK2
+ 50mM Chloroquine
Cell Count
siCTRL+CQ
siSIK2+CQ
Log GFP Fluorescence

D.

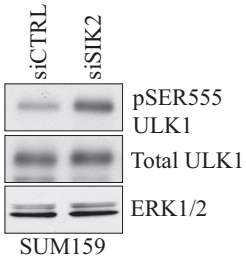
siCTRL
siSIK2
pSER555 ULK1
Total ULK1
ERK1/2
SUM159

E.

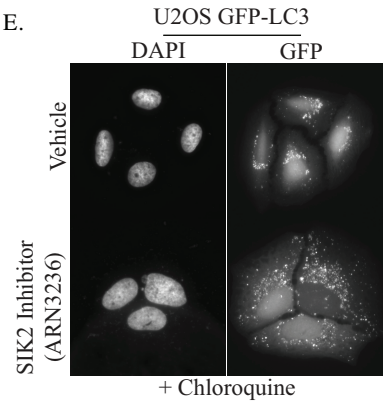
U2OS GFP-LC3
DAPI
GFP
Vehicle
SIK2 Inhibitor (ARN3236)
+ Chloroquine

Figure 8. SIK2 Acts as an Autophagic Break. A. WCLs from indicated cell lines transfected with indicated siRNAs were immunoblotted with indicated antibodies 72 hours post transfection. B. SUM159 cells expressing GFP-LC3 were transfected with indicated siRNAs. Forty-eight hours post-transfection, cells were exposed to 50mM chloroquine for 16 hours. Sixty-four hours post transfection, cells were fixed and mounted. C. Top: U2OS cells expressing GFP-LC3 were transfected with indicated siRNAs. Forty-eight hours post-transfection, cells were exposed to 50mM chloroquine for 16 hours. Sixty-four house post transfection, cells were fixed and mounted. Bottom: U2OS cells expressing GFP-LC3 processed as above were fixed and subject to FACS analysis. CQ: chloroquine. D. WCLs from SUM159 cells transfected with indicated siRNAs were immunoblotted with indicated antibodies 72 hours post transfection. E. U2OS cells expressing GFP-LC3 treated with 1000 nM of SIK2 inhibitor, ARN3236, for 48 hours followed by 16 hours of 50mM chloroquine treatment were fixed and mounted.

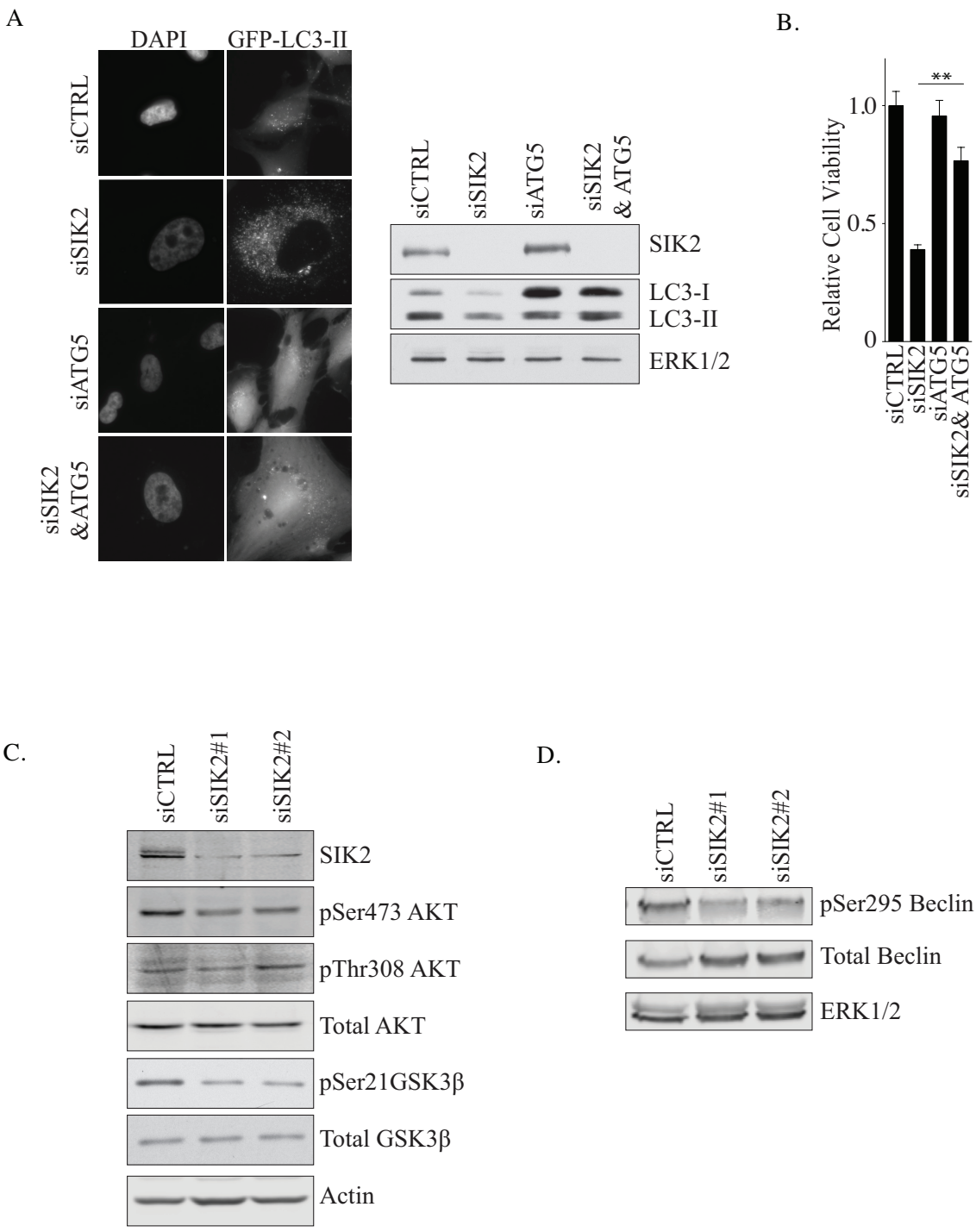
A
DAPI
GFP-LC3-II
siCTRL
siSIK2
siATG5
siSIK2 &ATG5
siCTRL
siSIK2
siATG5
siSIK2 & ATG5
SIK2
LC3-I
LC3-II
ERK1/2
B.
Relative Cell Viability
1.0
0.5
0
**
siCTRL
siSIK2
siATG5
siSIK2& ATG5
C.
siCTRL
siSIK2#1
siSIK2#2
SIK2
pSer473 AKT
pThr308 AKT
Total AKT
pSer21GSK3β
Total GSK3β
Actin
D.
siCTRL
siSIK2#1
siSIK2#2
pSer295 Beclin
Total Beclin
ERK1/2

Figure 9. SIK2 Supports TNBC Viability by Attenuating Autophagy and Survival Signaling. A. Left: SUM159 expressing GFP-LC3 were transfected with indicated siRNAs. Forty-eight hours post-transfection, cells were exposed to 50mM chloroquine for 16 hours. Sixty-four hours post transfection, cells were fixed and mounted. Right: WCLs from SUM159 cells transfected with indicated siRNAs were immunoblotted with indicated antibodies 72 hours post transfection. B. Left: WHIM12 cells were transfected with indicated siRNAs and CTG assay was performed 120 hours post transfection. Values represent viability relative to siCTRL (n = 3) ± S.D. Right: SUM159 cells were transfected with indicated siRNAs were imaged 96 hours post transfection using phase-contrast microscopy. C. WCLs from SUM159 cells transfected with indicated siRNAs were immunoblotted with indicated antibodies 48 hours post transfection. D. WCLs from SUM159 cells transfected with indicated siRNAs were immunoblotted with indicated antibodies 72 hours post transfection.

Taken together, SIK2 acts as an autophagic break possibly through supporting AKT signaling that is required for tumor cell viability in a subset of TNBC tumors.

Discussion

Our pan-genomic siRNA screening approach identified SIK2 as a vulnerability and a collaborator with paclitaxel in WHIM12 and SUM159 tumor-derived cell lines, respectively. We further showed this viability loss was due to excess autophagy. During tumor initiation, autophagy acts as a tumor suppressor by promoting protein turnover and reprieve from metabolic stress. However, autophagy switches to become tumor promoting in late-stage tumors that are under increased metabolic stress due to increased proliferation and/or are poorly vascularized (205). Furthermore in aggressive tumors, autophagy is also thought to be protumorigenic by facilitating anoikis-resistance following ECM detachment during metastatic progression (206, 207). Given this, we hypothesize that SIK2 may become a dependency in late-stage metastatic tumors that require autophagy for survival but need an autophagic break to prevent excessive autophagy from reducing tumor cell viability.

We further found that SIK2 supports the AKT activation. AKT inhibits autophagy directly through inhibitory phosphorylation of Beclin and indirectly through activation of mTORC1(193, 194). SIK2's known substrates all modulate cellular energy production; however, none of the known substrates have been directly implicated in serine 473 phosphorylation of AKT, suggesting that SIK2 may directly phosphorylate AKT or modulate RICTOR kinase activity (Figure 10). This work may nominate new SIK2

substrates and may implicate SIK2 as a novel obligate component of the RICTOR/ AKT/ mTORC1 nutrient signaling pathway.

Furthermore, an anti-cancer synergistic relationship between HDAC inhibitors and mTOR inhibitors has been observed in several tumors types including prostate, head and neck squamous cell carcinoma and B cell leukemia (208, 209). This synergy has revealed significant crosstalk between chromatin acetylation and the AKT/ mTORC2 pathway but the exact nature of this relationship in still under investigation (102, 208, 209). One of SIK2's bona fide targets is HDAC4 that is known to drive expression of genes like the insulin-regulated glucose transporter, GLUT4 (182), suggesting that SIK2 might play a role in this synergistic relationship. Further exploration of SIK2's role in tumorigenic energy signaling may reveal important mechanisms of signaling crosstalk that could inform future TNBC therapeutic strategies.

Lastly, our screen identified a collaboration between SIK2 and the first line antimitotic chemotherapeutic, paclitaxel. However, we did not find mitotic defects following SIK2 depletion, suggesting that in TNBC, SIK2 and paclitaxel do not synergize due to both impinging on the mitotic spindle. Paclitaxel has been reported to modulate autophagic flux in breast and cervical cancer tumor-derived cell lines by altering the cellular metabolic profile (210, 211). Furthermore, recent evidence has suggested that during mitosis following nuclear envelope breakdown, inhibition of autophagy is necessary to protect the mitotic spindle from autophagy-mediated degradation (212). The exact details of this mechanism are still unclear but releasing the inhibition of autophagy

in the context of a mitotic stressor, such as paclitaxel, could lead to a synergistic relationship. We obtained a SIK2 inhibitor of Arrien Pharmaceuticals, Inc, which upon treatment, increased autophagic flux. Taken together, we hypothesize that paclitaxel treatment in conjunction with SIK2 inhibition may collaborate and possibly represent a new combination therapy in TNBC autophagy-dependent tumors.

Materials and Methods

Cell lines and reagents - Cell lines were obtained from ATCC with the following exceptions: SUM159, SUM149 and HuMEC (gift from Charles Perou, UNC Lineberger Cancer Center), HCC1806, MDA-MB-231, MDA-MB-436, MDA-MB-468, (gift from Gray Pearson, UT Southwestern), WHIM12 (gift from Matthew Ellis, Baylor College of Medicine) and U2OS-GFP-LC3 (gift from Micheal White, UT Southwestern). All cell lines were cultured in provider's recommended medium. Antibodies were obtained from Santa Cruz (ERK1/2, Total Beclin), Biolegend (SIK2), Abcam (Pericentrin), Sigma (β-tubulin) and Cell Signaling Technologies (SIK2, Cleaved Caspase-3, LC3B, Total ULK1, Phospho-Serine555 ULK1, Total AKT, Phospho-Serine473 AKT, Total GSK3β, Phospho-Serine 21 GSK3β), Phospho-Solutions (Phospho-Serine295 Beclin 1). siRNAs were obtained from GE Healthcare (siGENOME siRNA) or Sigma (Mission® siRNA). CTRL siRNA used was non-targeting control (GE Healthcare). Chloroquine was purchased from Sigma-Aldrich. The SIK2 inhibitor, ARN3236, was obtained from Arrien Pharmaceuticals, Inc through a Material Transfer agreement.

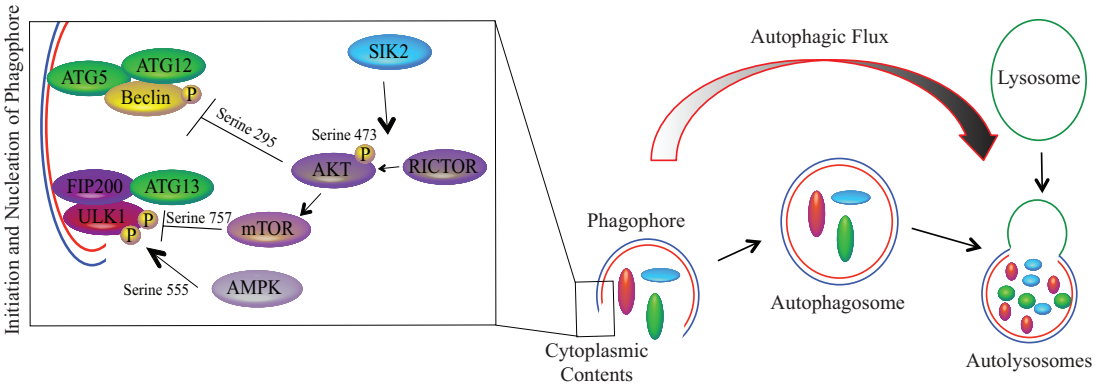

Figure 10. Model of SIK2 Attenuating Autophagy to Promote Tumor Cell Survival. SIK2 supports AKT signaling that in turn activates mTOR. mTOR phosphorylates ULK1 to prevent downstream autophagy. AKT also directly phosphorylates Beclin to inhibit autophagic initiation.

Cell Viability Assays - Cells were reverse transfected in 96 well format. Forty-eight hours post plating, cells were fed with 35ul of complete media. One hundred and twenty hours post plating, luminescence values were read following addition of 15 μL of Cell Titer-Glo® (CTG) (Promega) on a Pherastar Plus (BMG) plate reader.

Generation of stable cell lines - SUM159 stable cell lines were generated through lentiviral-mediated transduction of pCDH-GFP-LC3 (gift from Channing Der, UNC-Chapel Hill Lineberger) delta 8.9 packaging plasmid and VSV-G envelope plasmid. Following infection stable populations were selected using appropriate antibiotics.

Colony formation assay - Cells were reverse transfected with 10 pmoles of siRNA using RNAiMax® (Life Technologies). Ninety-six hours post-transfection, cells were replated at limiting dilution in 6-well format. Cells were fed twice weekly until controls reached confluency at which point colonies were fixed in 3.7 % formaldehyde and stained with Geimsa (Sigma).

Gene expression - Total RNA was isolated using RNA isolation kit (Sigma) and reverse transcribed using the High-Capacity cDNA Reverse Transfection Kit (Life Technologies) according to manufacturer's instructions. An Applied Biosystems Real-Time PCR system and either Solaris™, or TaqMan® Real-Time PCR gene expression assays were used. Gene expression assays were multiplexed with RPL27 as control assays. Relative expression values were calculated using the comparative Ct method.

Immunoblotting - Whole cell lysates were prepared in 2x Laemmli sample buffer and resolved using SDS-PAGE. Gels were transferred to Immobilon® PVDF (Millipore) or nitrocellulose (Bio-rad) membranes, blocked in tris-buffered saline containing 0.1 % Tween20 (TBST) and either 5 % non-fat dry milk or bovine serum albumin (BSA), or Odyssey® blocking buffer and incubated with indicated primary antibodies overnight. After washes in TBST, appropriate HRP-coupled secondary antibodies (Jackson Immunoresearch) were used for chemiluminescence.

Immunofluorescence - Cells plated on glass coverslips were fixed with 3.7 % formaldehyde and permeabilized with 0.05 % Triton X-100 for ten minutes. Cells were blocked and washed in 1 % BSA, 0.1 % Tween-20 in 1X PBS (PBTA). Cells were incubated with primary antibodies for 1 hour followed by three washes in PBTA. Coverslips were then incubated with Alexa Fluor®-conjugated secondary antibodies (Invitrogen) for 30 minutes followed by 3 washes in PBTA and a wash in H_2O. Prolong® Gold Antifade reagent with DAPI (Life Technologies) was used to mount slips on glass slides and images were acquired on either a Zeiss Axioimager upright microscope (Zeiss) with a CCD camera.

Fluorescence Activated Cell Sorting – U2OS GFP-LC3 cells were reverse transfected with 10 pmoles of indicated siRNA using RNAiMax® (Life Technologies). Sixteen hours prior to FACS analysis, cells were treated with either vehicle or 50mM Chloroquine. Seventy-two hours post transfection, cells were trypsinized, 2X washed with PBS and fixed with EtOH cells for 30 minutes at 4C. Cells were then washed 2X

with PBS and sorted by GFP fluorescence using Beckman Coulter CyAn ADP using Summit 4.3 and analyzed using ModFit 4.0 DNA Analysis software. A minimum of 1.0 x 10^4 events were used for analysis.

CHAPTER V: Cancer Testes Antigen, ZNF165, Promotes TGFβ Pathway Activation and Drives Expression of the WISP1 Oncogene[3]

Introduction

Our functional genomics approach identified siRNA targeting Zinc Finger 165 (ZNF165) as a supporter of TNBC tumor cell viability in multiple TNBC genetic backgrounds (Figure 3G). Furthermore, ZNF165 was the most potent synergizer with paclitaxel in the chemoresistant WHIM12 TNBC tumor-derived cell line (Figure 1A and 3F). ZNF165 is a zinc finger domain containing protein and is characterized as a cancer-testis antigen (CTA). Characteristic of CTAs, ZNF165 mRNA expression is testis-restricted but is reactivated in multiple types of cancer including breast, colorectal, bladder, and liver, where upon re-expression, it induces a humoral immune response (143, 144). Zinc finger domains mediate DNA binding and zinc finger proteins are often implicated in transcriptional regulation (145, 146), therefore, ZNF165 is a putative transcription factor. However, no mechanistic data is known about ZNF165's function in spermatogenesis or tumor cells.

[3] Elements of the work referenced in this chapter will be published in Nature Communications. The original citation is as follows:
Kimberly E. Maxfield and Patrick J. Taus, Kathleen Corcoran, Joshua Wooten, Jennifer Macion, Yunyun Zhou, Mark Borromeo, Rahul K. Kollipara, Jingsheng Yan, Yang Xie, Xian-Jin Xie, and Angelique W. Whitehurst. (2015). Comprehensive Functional Characterization of Cancer-Testis Antigens Defines Obligate Participation in Multiple Hallmarks of Cancer. Nature Communications. In press.

Cancer-Testis Antigens (CT-antigens, CTAs) were discovered from efforts to identify tumor antigens by isolating patient-derived cytotoxic T-lymphocytes (CTLs) (213, 214). Since their discovery, greater than 250 genes have been classified as CTAs with testes/cancer-biased expression patterns (215). Anomalous expression of testis proteins in somatic tissue evokes a cellular and/or humoral immune response because the testes are immune privileged due to the development the auto-antigens during spermatogenesis. Therefore, upon re-expression, these proteins are recognized as foreign and presented through the classical Major Histocompatibility Complex pathways (MHC) (216). Many of these proteins were originally considered as targets for immunotherapy (217-219). The CTA, NY-ESO-1, has exhibited efficacy in melanoma and synovial sarcoma patients using vaccination or adoptive T-cell transfer, respectively (220, 221).

Few CTAs have defined roles in either testis or tumor cells. Murine knockout models have been generated for twenty-four CTAs, the majority of which only exhibit gametogenic defects. In normal physiology, CTAs have been shown to contribute to chromosome pairing during meiosis, sperm motility, translational regulation during sperm maturation, chromatin remodeling, and transcriptional regulation (222). In tumorigenesis, CTAs have roles in centrosomal clustering, regulation of microtubule dynamics, p53 silencing and modulation of differentiation signaling (122, 147, 223-225). This suggests that CTAs participate in diverse, malignant behaviors. Further investigation of CTAs, such as ZNF165, could reveal novel aspects of tumor cell biology that could be therapeutically leveraged.

In this chapter, we start to functionally annotate ZNF165 in TNBC tumorigenesis. Given ZNF165 is a putative transcription factor, we employed ChIP-seq analysis to reveal that ZNF165 directly binds to distal regulator regions of and represses expression of the negative regulators of the TGFβ pathway, SMURF2 and SMAD7. This leads to enhanced TGFβ signal transduction and significant modulation of the TGFβ-induced transcriptional network to promote expression of oncogenes. Furthermore, we show that ZNF165 is required for TNBC tumor progression in vivo and exhibits a tumor selective protein expression pattern. Our work reveals how gametogenetic programs can disrupt on normal signaling modules to promote tumorigenic behaviors.

Results

ZNF165 Selectively Supports TNBC viability and TGFβ Signaling - In an orthogonal dataset evaluating CTA participation in tumorigenic behaviors, ZNF165 was identified as selectively supporting TNBC viability in comparison to other tumor types including sarcoma, prostate, lung, and melanoma (Figure 11A). Furthermore, ZNF165 was also identified as supporting TGFβ-induced transcription in the WHIM12 TNBC tumor-derived cell line, which is the same cell line that requires ZNF165 for its viability (Figure 11B). To confirm this observation is not due to siRNA off-target effects, we evaluated ZNF165 depletion with two independent siRNA pools on the canonical TGFβ target gene, SNAI1, and observed that ZNF165 is required for TGFβ-induced transcription of SNAI1 (Figure 11C). Inhibition of TGFβ is a high value therapeutic intervention target in late stage disease because activation of TGFβ signaling drives epithelial to mesenchyme transition (EMT) that is required for highly metastatic and

aggressive tumors (226). However, TGFβ is an important developmental cytokine that can drive both differentiation and self-renewal depending on the cellular context and has been shown to be tumor suppressive differentiation in early tumorigenesis (226). Therefore, understanding the cellular contexts that differentiate between the tumor-promoting and tumor-suppressive roles of TGFβ is critical for successfully implementation of TGFβ inhibitors in the clinic (227). By leveraging the intersection of our two unbiased screening approaches, we identified that ZNF165 is essential for the TNBC viability while supporting TGFβ signaling in these cells.

ZNF165 is a Putative Transcription Factor that Directly Represses Expression of TGFβ Negative Regulators - ZNF165 is an uncharacterized member of the SCAN-$(C_2H_2)_n$ sub-family of zinc finger proteins and contains a SCAN heterodimerization domain and five C2H2 motifs, which are classical zinc finger domains that mediate association with DNA (Figure 12A) (143, 228, 229). ZNF165 also localizes to the nucleus in tumor cells and associates with 9 proteins with gene-regulatory activity (Figure 12B&C) (146, 230). Given these indications of transcriptional activity, we performed ChIP-Seq analysis in WHIM12 cells stably expressing ZNF165-V5 to identify putative target genes. This analysis returned 281 ZNF165 binding sites associated with 447 genes. De novo motif enrichment identified 3 motifs that comprised ~90 % of these binding sites (Figure. 12D - Left), confirming that ZNF165 either directly binds or is part of a complex that directly binds DNA. This analysis also nominates these motifs as the direct ZNF165 binding sequences. Genomic Regions Enrichment of Annotation Tool

A.

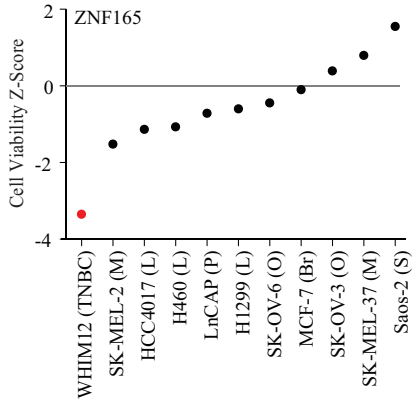
ZNF165
Cell Viability Z-Score
2
0
-2
-4
WHIM12 (TNBC)
SK-MEL-2 (M)
HCC4017 (L)
H460 (L)
LnCAP (P)
H1299 (L)
SK-OV-6 (O)
MCF-7 (Br)
SK-OV-3 (O)
SK-MEL-37 (M)
Saos-2 (S)

B.

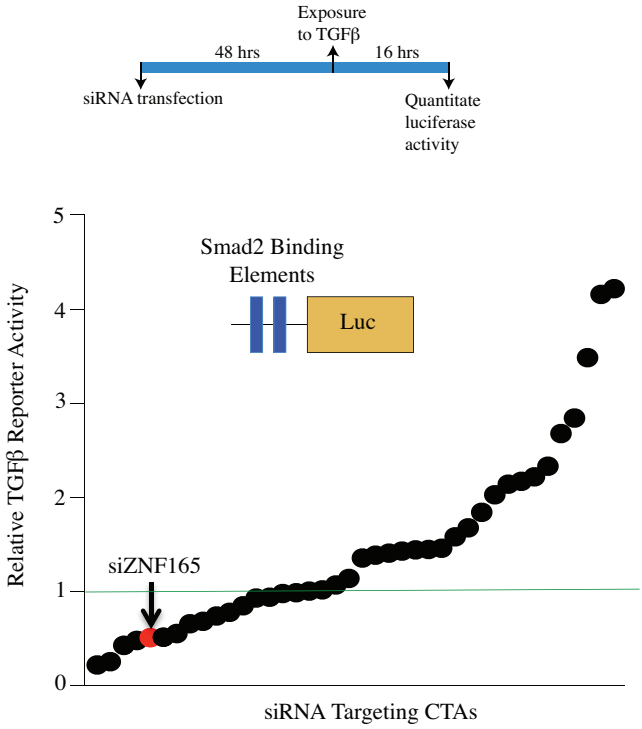
Exposure
to TGFβ
48 hrs
16 hrs
siRNA transfection
Quantitate
luciferase
activity
Smad2 Binding
Elements
Luc
Relative TGFβ Reporter Activity
5
4
3
2
1
0
siZNF165
siRNA Targeting CTAs

C.

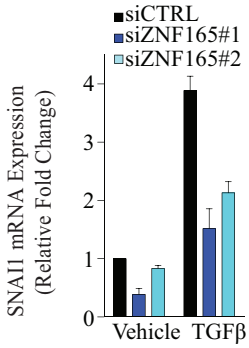
siCTRL
siZNF165#1
siZNF165#2
SNAI1 mRNA Expression
(Relative Fold Change)
4
3
2
1
0
Vehicle
TGFβ

Figure 11. ZNF165 is Selectively Required in TNBC and Supports TGFβ signaling. A. siZNF165 Z-scores in each cell line from the cancer-testis antigen (CTA) cell viability screen (CTG) M: Melanoma, L: Lung Adenocarcinoma, P: Prostate Cancer, Br: Luminal Breast Cancer, O: Ovarian, S: Sarcoma. B. Top: Schematic of time course of the TGFβ-induced SMAD Binding Element (pSBE) luciferase assay from the CTA signaling screen. TGFβ signaling screen was performed prior to siZNF165 induce cell viability defects. Bottom: Raw screening data from WHIM12 pSBE signaling screen displayed as change in fold induction of TGFβ-induced luciferase activity. Arrow indicates ZNF165 as a screen hit in WHIM12. C. Total RNA was isolated from WHIM12 cells transfected with either siCTRL or siZNF165 and exposed to either 3 hours of vehicle or 10 ng/mL TGFβ 48 hours post transfection. qPCR was used to quantitate relative SNAI1 mRNA expression. Bars represent mean (n = 3) ± S.D.

(GREAT) pathway analysis revealed that genes associated with ZNF165-peaks are significantly enriched in the TGFβ signaling pathway (23 genes; $q = 6.96 \times 10^{-3}$) (Fig. 12D - Right). This gene set included SMURF2 and SMAD7, TGFβ target genes that negatively regulate signaling by degrading the canonical TGFβ signal transducer, SMAD2/3 (Figure 12E) (231, 232). We validated these findings by ChIP-qPCR (Figure 12F). To test if these SMURF2 and SMAD7 binding sites have transcriptional consequences, we evaluated SMURF2 and SMAD7 mRNA following ZNF165 stable overexpression and found attenuation SMURF2 and SMAD7 mRNA (Figure 12G). Depletion of ZNF165 led to an accumulation of SMURF2 mRNA upon siRNA depletion in two independent cell lines (Figure 12H). Taken together, our data suggests that ZNF165 directly inhibits SMURF2 and SMAD7 gene expression.

ZNF165 Globally Modulates TGFβ-Induced Transcription – Given that ZNF165 supports TGFβ signaling and directly represses SMURF2 expression, we next investigated ZNF165 in TGFβ signal transduction. An increase in SMURF2 protein would be predicted to lead to a loss of SMAD2 protein. Indeed, we found that depletion of ZNF165 with two independent siRNA pools led to an accumulation of SMURF2 protein and an attenuation of SMAD2 protein (Figure 13A). Conversely, WHIM12-ZNF165-V5 cells exhibited an accumulation of SMAD2/3 protein and transient overexpression of ZNF165 in H1299 cells (a NSCLC-derived cell line chosen for its high level of transfection efficiency not attainable in the TNBC setting) was also sufficient to stabilize SMAD2/3 (Figure 13B). Loss of ZNF165 also led to loss of the active

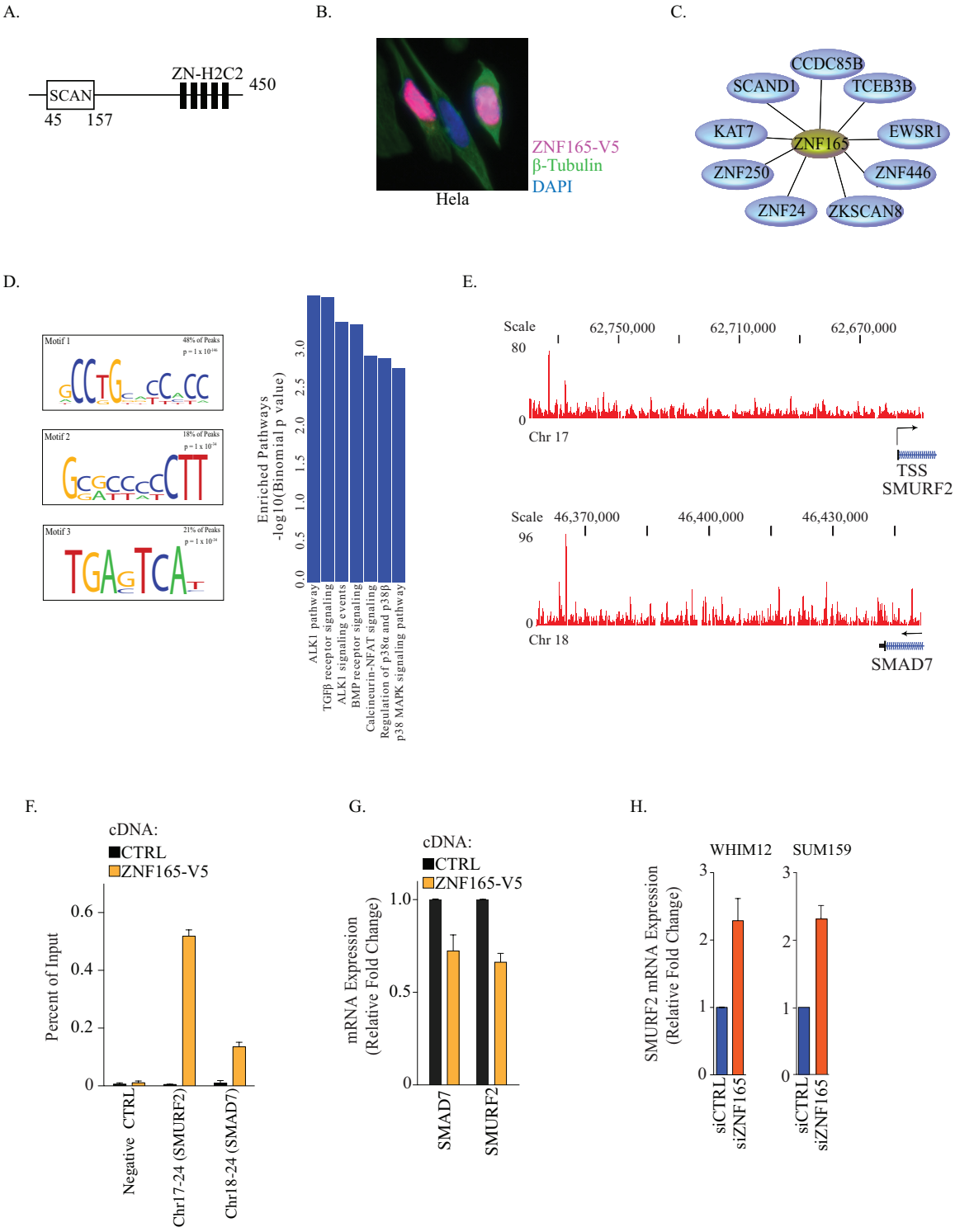
A.
SCAN
ZN-H2C2
450
45
157
B.
ZNF165-V5
β-Tubulin
DAPI
Hela
C.
CCDC85B
SCAND1
TCEB3B
KAT7
ZNF165
EWSR1
ZNF250
ZNF446
ZNF24
ZKSCAN8
D.
Motif 1
48% of Peaks
Motif 2
18% of Peaks
Motif 3
21% of Peaks
Enriched Pathways
-log10(Binomial p value)
ALK1 pathway
TGFβ receptor signaling
ALK1 signaling events
BMP receptor signaling
Calcineurin-NFAT signaling
Regulation of p38α and p38β
p38 MAPK signaling pathway
E.
Scale
62,750,000
62,710,000
62,670,000
Chr 17
TSS
SMURF2
Scale
46,370,000
46,400,000
46,430,000
Chr 18
SMAD7
F.
cDNA:
CTRL
ZNF165-V5
Percent of Input
Negative CTRL
Chr17-24 (SMURF2)
Chr18-24 (SMAD7)
G.
cDNA:
CTRL
ZNF165-V5
mRNA Expression
(Relative Fold Change)
SMAD7
SMURF2
H.
WHIM12
SUM159
SMURF2 mRNA Expression
(Relative Fold Change)
siCTRL
siZNF165
siCTRL
siZNF165

Figure 12. ZNF165 Directly Represses Negative Feedback Regulators of the TGFβ pathway. A. Domain map of ZNF165. SCAN: SCAN oligomerization domain; ZN-H_2C_2: canonical zinc finger motifs. B. Forty-eight hours after transfection with ZNF165-V5, HeLa cells were fixed and immunostained with indicated antibodies. C. Interaction data for ZNF165 based on yeast 2-hybrid proteomic analyses. D. Left: Motifs identified using the HOMER findMotifsGenome module based on the WHIM12-ZNF165-V5 ChIP-Seq. P-values represent hypergeometric distribution analysis. Right: GREAT pathway enrichment from WHIM12-ZNF165-V5 ChIP-Seq. Binomial FDR q-values calculated from Poisson distribution in HOMER findPeaks module using Bonferroni and FDR correction method. E. WHIM12-ZNF165-V5 ChIP-Seq peak located in distal regulatory region of SMURF2 and SMAD7. TSS: Transcription Start Site. F. ChIP-qPCR of WHIM12-ZNF165-V5 cells immunopreciptated with V5 antibody using primers designed to the SMURF2 and SMAD7-associated chromatin regions identified in the WHIM12-ZNF165-V5 Chip-Seq. Bars represent mean of percent of input pulled (n = 2) ± range. G. Total RNA from WHIM12-ZNF165-V5 was isolated and qPCR was used to quantitate relative levels of SMURF2 and SMAD7. Bars represent mean (n = 3) ± Standard Error Mean (S.E.M). H. WHIM12 and SUM159 cells were transfected with indicated siRNAs for 48 hours. qPCR was used to quantitate relative SMURF2 mRNA expression (right). Bars represent mean (minimum of n = 2) ± range.

phosphorylated form of SMAD2 that is required for TGFβ-induced transcription (Figure 13C). To further test this, we evaluated the SMAD2 sub-cellular localization in response to TGFβ stimulation following siRNA depletion of ZNF165 and observed loss of SMAD2 nuclear translocation required for SMAD2-mediated transcription (Figure 13D). Given this, we next wanted to evaluate the effect of ZNF165 on TGFβ transcriptional output. Using a SMAD Binding Element (SBE) reporter system, we observed that exogenous expression of ZNF165 was sufficient to drive TGFβ-induced transcription (Figure 13E). Furthermore, using whole genome expression profiling in SUM159 and WHIM12 cells depleted of ZNF165 and stimulated with TGFβ, we found that 28 % and 25 % of all TGFβ modulated genes were affected by ZNF165 depletion, representing an enrichment with a probability of $P = 1.09 \times 10^{-13}$ and 3.69×10^{-11}, respectively by random chance according to hypergeometric distribution analysis (Figure 13F). This suggests that ZNF165 expression significantly modulates the transcriptional response to TGFβ stimulation in TNBC. In agreement with the ChIP analysis, canonical TGFβ targets that are negative feedback regulators (SMURF2 and SMAD7) were activated upon ZNF165 depletion (Figure 13G) (231-234). ZNF165 was also required for the expression of 30 of the TGFβ-modulated genes, many of which mediate neoplastic processes (WISP1, DPYSL3, USP2, CRAYB, GPR124, FGD4, and RASGRP1) (Figure 13G) (235-246). Taken together, these data suggest that ZNF165 expression is sufficient to enhance TGFβ signal transduction, significantly modulating the TNBC TGFβ transcriptional network to promote expression of oncogenes.

ZNF165 Drives Expression of Putative Oncogene, WISP1 - One of the most dramatically repressed genes that required ZNF165 for TGFβ induction was WISP1, a poorly characterized oncogene that promotes growth and survival in colon cancer (Figure 13G) (239, 247-250). We find that ZNF165 depletion leads to reduced WISP1 protein accumulation while overexpression of ZNF165 is sufficient to stimulate the activity of luciferase fused to the WISP1 promoter and enhance WISP1 mRNA and protein (Figure 14A,B&C). With respect to TGFβ signaling, WISP1 makes an obligate contribution to osteogenic differentiation by supporting BMP-2-induced SMAD 1/5/8 activation (251). Thus, we examined whether WISP1 influenced TGFβ signaling in the TNBC tumorigenic context. We observed that WISP1 is required for TGFβ-induced SMAD2/3 phosphorylation (Figure 14D). Furthermore, overexpression of WISP1 was sufficient to promote activation of a luciferase reporter fused to the SBE (Figure 14E), thereby suggesting that in addition to repressing negative feedback, ZNF165 directly supports feed forward amplification of TGFβ signaling through WISP1 activation. Furthermore, WISP1 is essential for viability in multiple TNBC settings (Figure 14F). Taken together, this analysis indicates that ZNF165 expression directly promotes TGFβ pathway activity by repressing negative feedback and promoting expression of target oncogenes essential for feed forward amplification of TGFβ signaling and TNBC survival.

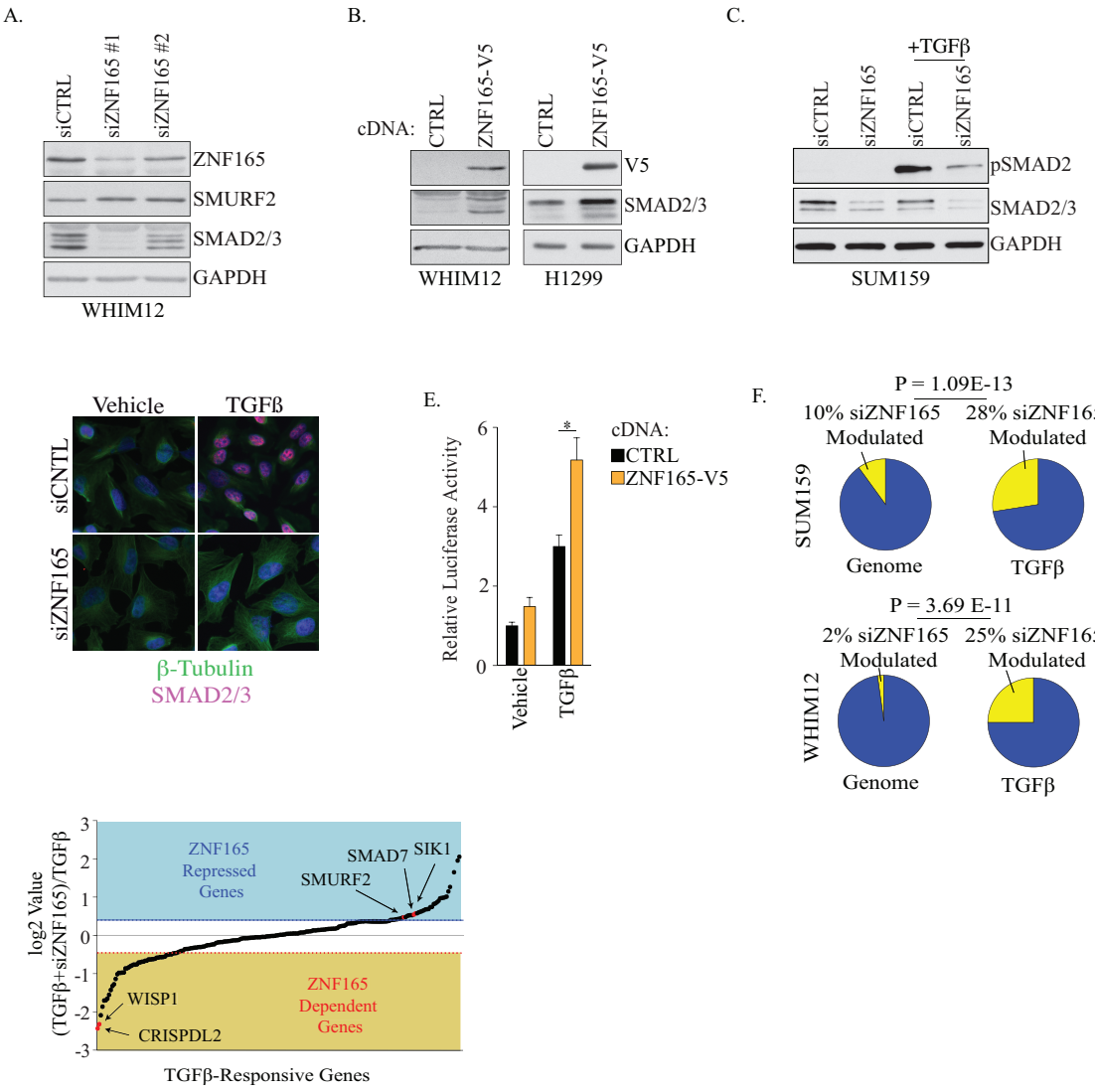
A.
siCTRL
siZNF165 #1
siZNF165 #2
ZNF165
SMURF2
SMAD2/3
GAPDH
WHIM12
B.
cDNA:
CTRL
ZNF165-V5
CTRL
ZNF165-V5
V5
SMAD2/3
GAPDH
WHIM12
H1299
C.
+TGFβ
siCTRL
siZNF165
siCTRL
siZNF165
pSMAD2
SMAD2/3
GAPDH
SUM159
D.
Vehicle
TGFß
siCNTL
siZNF165
β-Tubulin
SMAD2/3
E.
Relative Luciferase Activity
cDNA:
CTRL
ZNF165-V5
Vehicle
TGFβ
F.
P = 1.09E-13
10% siZNF165 Modulated
28% siZNF165 Modulated
SUM159
Genome
TGFβ
P = 3.69 E-11
2% siZNF165 Modulated
25% siZNF165 Modulated
WHIM12
Genome
TGFβ
G.
log2 Value (TGFβ+siZNF165)/TGFβ
ZNF165 Repressed Genes
SMAD7
SIK1
SMURF2
WISP1
CRISPDL2
ZNF165 Dependent Genes
TGFβ-Responsive Genes

Figure 13. ZNF165 Globally Modulates the TGFβ Transcriptional Response. A. WCLs from WHIM12 transfected with indicated siRNAs for 48 hours were immunoblotted with indicated antibodies. B. Left: WCLs from WHIM12-ZNF165-V5 cells were immunoblotted with indicated antibodies 48 hours post transfection. Right: WCLs from H1299 cells transiently transfected with indicated cDNAs were immunoblotted with indicated antibodies. C. WCLs from SUM159 cells transfected with indicated siRNAs and exposed for 30 minutes to either vehicle or 10 ng/mL TGFβ 60 hours post transfection were immunoblotted for indicated antibodies. D. SUM159 cells transfected with indicated siRNAs and exposed for 30 minutes with either vehicle or 10 ng/mL TGFβ 60 hours post transfection were fixed, immunostained with indicated antibodies. E. Indicated cDNAs were co-transfected with the SMAD Binding Element (SBE) luciferase reporter into HEK293T cells. Following 24 hours of 100 ng/mL TGFβ stimulation, luciferase activity was measured. Bars represent mean (n = 11) ± S.E.M. F. For SUM159 cells (top) and WHIM12 cells (bottom), fraction of genes modulated following siZNF165 based on SAM analysis of Affymetrix microarray data (FDR ≤ 10 %) (left pie chart). Fraction of TGFβ-induced genes significantly modulated by siZNF165 (Student's t-test, $p \leq 0.05$). P-value for enrichment calculated by hypergeometric distribution analysis. G. TGFβ-induced genes from the SUM159 Affymetrix microarray (SAM analysis) ranked by siZNF165 effect on TGFβ induction.

ZNF165 Supports TNBC Viability In Vitro and In Vivo - We next elaborated on our initial discovery that ZNF165 was essential for the viability of WHIM12 TNBC cells by assessing this phenotype in a larger cohort of tumor and normal-immortalized cell lines. Here, we found that depletion of ZNF165 reduced viability in TNBC, but not normal immortalized breast epithelia (Figure 15A). Furthermore, depletion of ZNF165 led to activation of caspase-3 and a decrease in long-term growth as observed by clonogenic replating assays (Figure 15B&C), suggesting that ZNF165 is required for long term survival in TNBC. To next examine the role of ZNF165 during tumorigenesis, we assessed the consequences of ZNF165 depletion in a mouse xenograft model. WHIM12 cells stably infected with shZNF165 were injected subcutaneously and tumor growth was monitored for 6 weeks. In comparison to the control shRNA group, tumors from shZNF165 mice were attenuated in growth and exhibited reduced Ki-67 staining (Figure 16E&F). Taken together, these findings suggest that ZNF165 promotes tumorigenesis by activating the TGFβ pathway, which in TNBC, is essential for tumor cell survival in part through activation of the WISP1 oncogene.

As member of the CTA cohort, ZNF165 exhibits a testes-biased mRNA expression pattern (144). To evaluate ZNF165 protein expression in TNBC, we examined ZNF165 protein expression in 10 primary TNBC, 3 normal, and 5 benign-adjacent tissues, including 2 matched pairs of tumor and benign-adjacent tissue. ZNF165 protein expression was detectable in 9 of the 10 tumor tissues tested, with minimal accumulation in benign or normal breast-derived samples (Figure 15F), confirming ZNF165's therapeutically attractive expression profile.

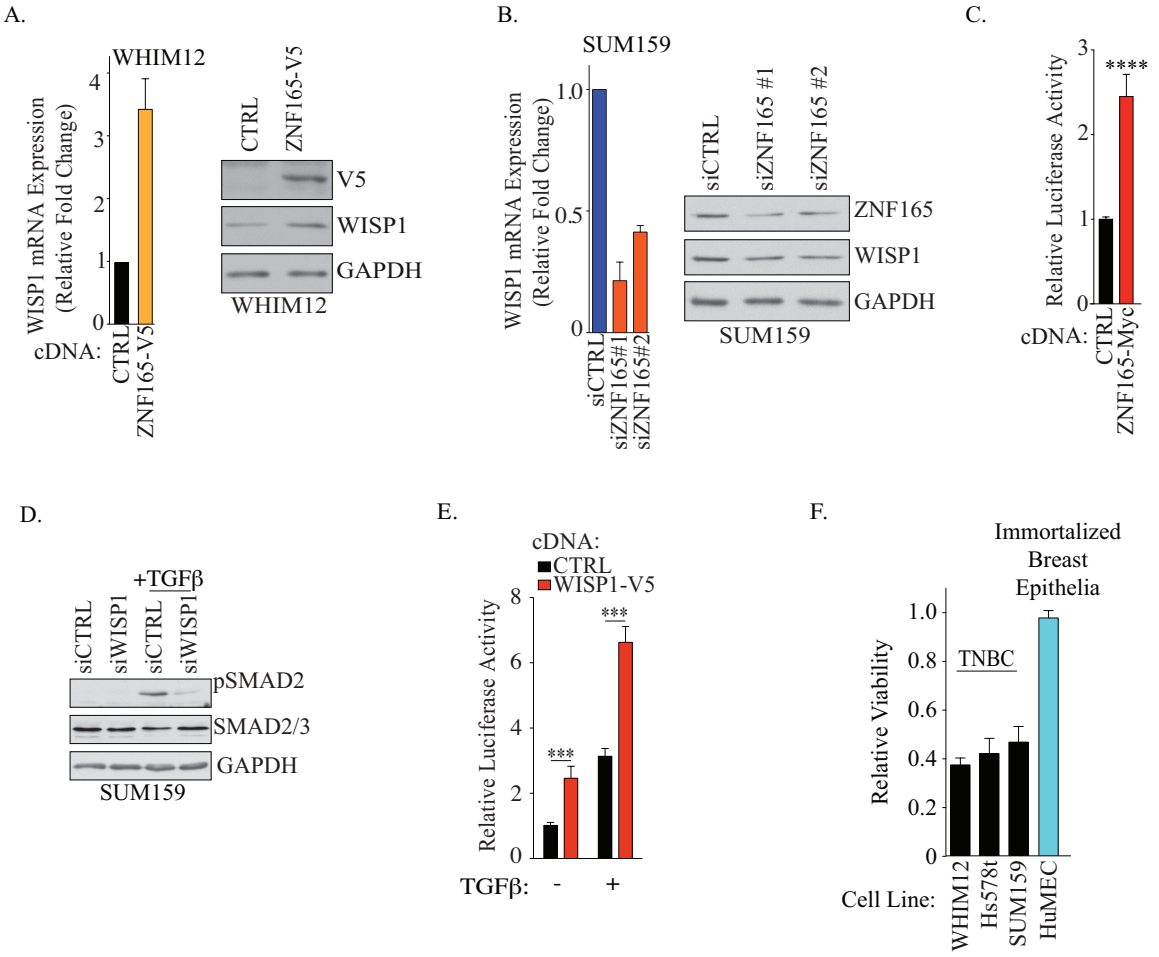
A.
WHIM12
WISP1 mRNA Expression (Relative Fold Change)
cDNA:
CTRL
ZNF165-V5
V5
WISP1
GAPDH
WHIM12
B.
SUM159
WISP1 mRNA Expression (Relative Fold Change)
siCTRL
siZNF165#1
siZNF165#2
ZNF165
WISP1
GAPDH
SUM159
C.
Relative Luciferase Activity
****
cDNA:
CTRL
ZNF165-Myc
D.
+TGFβ
siCTRL
siWISP1
pSMAD2
SMAD2/3
GAPDH
SUM159
E.
cDNA:
CTRL
WISP1-V5
Relative Luciferase Activity
***
TGFβ:
F.
Immortalized Breast Epithelia
TNBC
Relative Viability
Cell Line:
WHIM12
Hs578t
SUM159
HuMEC

Figure 14. WISP1 is a TGFβ and ZNF165-modulated gene that promotes TGFβ signaling and is required for TNBC viability. A. Left: Total RNA was isolated from WHIM12-ZNF165-V5 and vector control cells and qPCR was used to quantitate relative expression of WISP1 mRNA. Bars represent mean (n = 2) ± range. Right: Parallel WCLs were immunoblotted with indicated antibodies. B. Left: SUM159 cells were transfected with indicated siRNAs for 48 hours, total RNA was collected and qPCR was used to quantitate relative expression of WISP1 mRNA. Bars represent mean (n = 2) ± range. Right: Parallel WCLs were immunoblotted with indicated antibodies. C. HEK293T cells co-transfected with ZNF165-Myc and WISP1 (-1KB) promoter luciferase reporter were measured for luciferase activity 48 hours post transfection. Bars represent mean (n = 16) ± S.E.M. D. WCLs from SUM159 cells transfected with indicated siRNAs and exposed for 30 minutes to either vehicle or 10 ng/mL TGFβ 60 hours post transfection were immunoblotted for indicated antibodies. E. Indicated cDNAs were co-transfected with the SMAD Binding Element (SBE) luciferase reporter into HEK293T cells. Following 24 hours of 10 ng/mL TGFβ stimulation, luciferase activity was measured. F. Indicated TNBC cell lines were transfected with indicated siRNAs and cell viability was measured 120 hours post transfection (CTG). Values represent viability relative to siCTRL (n=3) ± S.D.

Discussion

Our pan-genomic siRNA screening approach identified ZNF165 as a vulnerability and collaborator with paclitaxel in TNBC. Through leveraging multiple screening platforms, we found that upon reactivation in TNBC, ZNF165 enhances TGFβ signaling through dual mechanisms. First, ZNF165 directly represses negative feedback regulators of TGFβ signaling, SMURF2 and SMAD7. This promotes a pro-tumorigenic TGFβ transcriptional network and in turn promotes feed forward amplification of TGFβ signaling and survival through expression of the oncogene, WISP1. The pro-tumorigenic features of TGFβ in late stage disease have made it a high value intervention target, particularly in TNBC (252, 253); however, TGFβ is a pleiotropic cytokine with important roles in normal physiology, thereby limiting the efficacy of direct inhibition (254). Given our results here, we hypothesize that re-expression of ZNF165 represents a mechanism by which tumors harness the tumor promoting capabilities of TGFβ signaling and may represent a mechanism to inhibit TGFβ signaling in a tumor cell-specific fashion (Figure 16). This work further highlights how re-expression of gametogenic genes in a somatic cell can wreak havoc on normal homeostatic regulatory mechanisms. There are ≥ 250 cancer testes antigens, few of which have annotated function. Our study suggests elaborating CTA functions can reveal cryptic aspects of the tumor cell regulatory environment that may lead to new intervention targets.

We further show that ZNF165 directly binds and represses negative regulators of TGFβ signaling to enhance protumorigenic TGFβ transcriptional response, suggesting that ZNF165 is a transcriptional repressor. Large-scale proteomic studies implicated

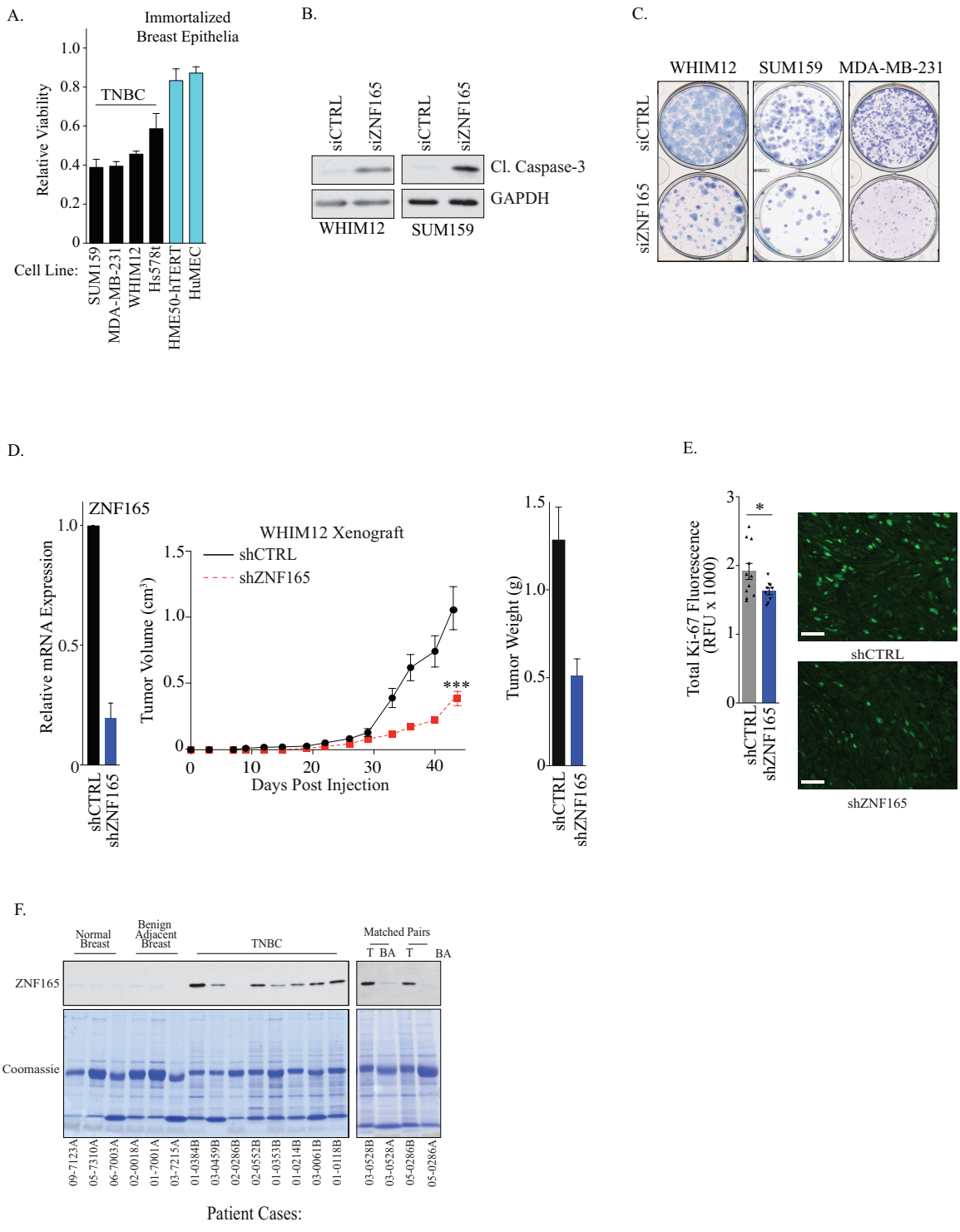
A.
Immortalized Breast Epithelia
TNBC
Relative Viability
1.0
0.8
0.6
0.4
0.2
0
Cell Line:
SUM159
MDA-MB-231
WHIM12
Hs578t
HME50-hTERT
HuMEC
B.
siCTRL
siZNF165
siCTRL
siZNF165
Cl. Caspase-3
GAPDH
WHIM12
SUM159
C.
WHIM12
SUM159
MDA-MB-231
siCTRL
siZNF165
D.
ZNF165
Relative mRNA Expression
1.0
0.5
0
shCTRL
shZNF165
WHIM12 Xenograft
shCTRL
shZNF165
Tumor Volume (cm³)
1.5
1.0
0.5
0
***
0
10
20
30
40
Days Post Injection
Tumor Weight (g)
1.5
1.0
0.5
0
shCTRL
shZNF165
E.
Total Ki-67 Fluorescence (RFU x 1000)
3
2
1
0
*
shCTRL
shZNF165
shCTRL
shZNF165
F.
Normal Breast
Benign Adjacent Breast
TNBC
Matched Pairs
T
BA
T
BA
ZNF165
Coomassie
09-7123A
05-7310A
06-7003A
02-0018A
01-7001A
03-7215A
01-0384B
03-0459B
02-0286B
02-0552B
01-0353B
01-0214B
03-0061B
01-0118B
03-0528B
03-0528A
05-0286B
05-0286A
Patient Cases:

Figure 15. ZNF165 is Required for TNBC Tumor Cell Survival In Vitro and In Vivo and is Upregulated in TNBC Patients Samples. A. Indicated TNBC cell lines were transfected with siCTRL or siZNF165 and cell viability was measured (CTG) 96 hours post transfection. Values represent viability relative to siCTRL (n=3) ± S.D. B. WCLs of SUM159 and WHIM12 cells transfected with indicated siRNAs were immunoblotted with indicated antibodies 72 and 48 hours post transfection, respectively. C. Indicated TNBC cell lines transfected with siZNF165 were re-plated at limiting dilution 48 hours post transfection. D. Left: Tumor growth curves for WHIM12 cells harboring shCTRL (n=11) or shZNF165 (n=9) ± S.E.M. Middle: Weight of WHIM12 xenograft tumors at time of harvesting. Right: Total RNA from WHIM12 cells expressing shCTRL or shZNF165 was isolated and qPCR was used to quantitate relative expression of ZNF165 mRNA prior to tumor implantation. E. Left: Tumors from D were stained for Ki-67. Bars represent mean total fluorescence across three randomly chosen fields corrected for background staining ± S.E.M (left). Right: Representative Ki-67 images. Scale bars represent 50 μm. F. WCLs from TNBC patient samples obtained from UNC Lineberger Tissue Procurement Center were immunoblotted for indicated antibodies. T: Tumor, BA: Benign-Adjacent.

several Krueppel-associated box (KRAB)-domain containing zinc finger proteins as direct binding partners to ZNF165 through their SCAN oligomerization domains, specifically ZNF446, ZNF250 and ZKSCAN8 (Figure 12A&C) (146, 195). KRAB domains are canonically transcriptionally repressive domains and function by recruiting methyltransferases to the DNA to transcriptionally silence (255). Given this, ZNF165 may interact with KRAB-domain containing proteins to repress downstream transcription. Furthermore, our ChIP-Seq analysis revealed the ZNF165 binding sites to be in the proximal regulatory regions of SMURF2 and SMAD7, which are over 100 kilobases away from the transcription start site. Enhancer regions are short DNA motifs located up to 1 megabase either upstream or downstream from the transcription start site that is essential for transcriptional modulation. Combinations of transcriptional coactivators and corepressors bound to the enhancer regions determine its effect on downstream transcriptional activity. Enhancer activity is associated with certain chromatin marks, such as Histone 3 Lysine 27 acetylation (H3K27ac) or Histone 3 Lysine 4 monomethylation (H3K4me1) (256, 257). Enhancer regions can also be silenced by KRAB domain-dependent methylation marks such as Histone 3 Lysine 9 trimethylation (257). Taken together, we hypothesize that ZNF165 interacts with KRAB-domain containing proteins and bind to enhancer regions to repress downstream transcription (Figure 16).

Our mechanistic analysis here focused on two negative regulators of the TGFβ pathway, SMURF2 and SMAD7. However, our ChIP-seq and expression profiling analysis revealed many direct and indirect targets of ZNF165 that have implicated

tumorigenic functions. For example, ZNF165 both directly binds to chromatin associated with and suppresses mRNA expression of the WNT signaling negative regulators and phosphatases of MAPK growth signaling, which would in turn release the pro-oncogenic WNT signaling and promote pro-proliferative MAPK signaling. This suggests that ZNF165 may also corrupt multiple signaling modules in addition to enhancing pro-tumorigenic TGFβ to promote tumorigenesis. Further mechanistic elaboration of additional signaling pathways affected by ZNF165 in TNBC may lead to additional ZNF165-mediated therapeutic exploits.

Our pan genomic screen identified a collaboration between loss of ZNF165 and the 1st line anti-mitotic chemotherapeutic, paclitaxel. One of the main characteristics of protumorigenic TGFβ signaling is conferring chemoresistance by promoting a TIC-like mesenchymal phenotype. Furthermore, treatment with first line chemotherapeutic agents like paclitaxel can induce TGFβ autocrine loops that drive the acquisition of stem-like features effectively producing chemoresistant tumors that lead to patient relapse (43, 252). Of our four TNBC screening cell lines, ZNF165 was identified as an outlier in the two TNBC claudin-low lines in comparison to the two basal-like cell lines. Of the two molecular subtypes that encompass TNBC, the claudin-low subtype is characterized as the more mesenchymal and chemoresistant. Activation of TGFβ signaling can also drive the claudin-low phenotype and TGFβ inhibition in claudin-low tumors causes loss of some of their stem-like features (42, 258, 259). Given this, we hypothesize that the ZNF165 might be essential for promoting pro-tumorigenic TGFβ signaling in the claudin-low phenotype and could be therapeutically leveraged as a

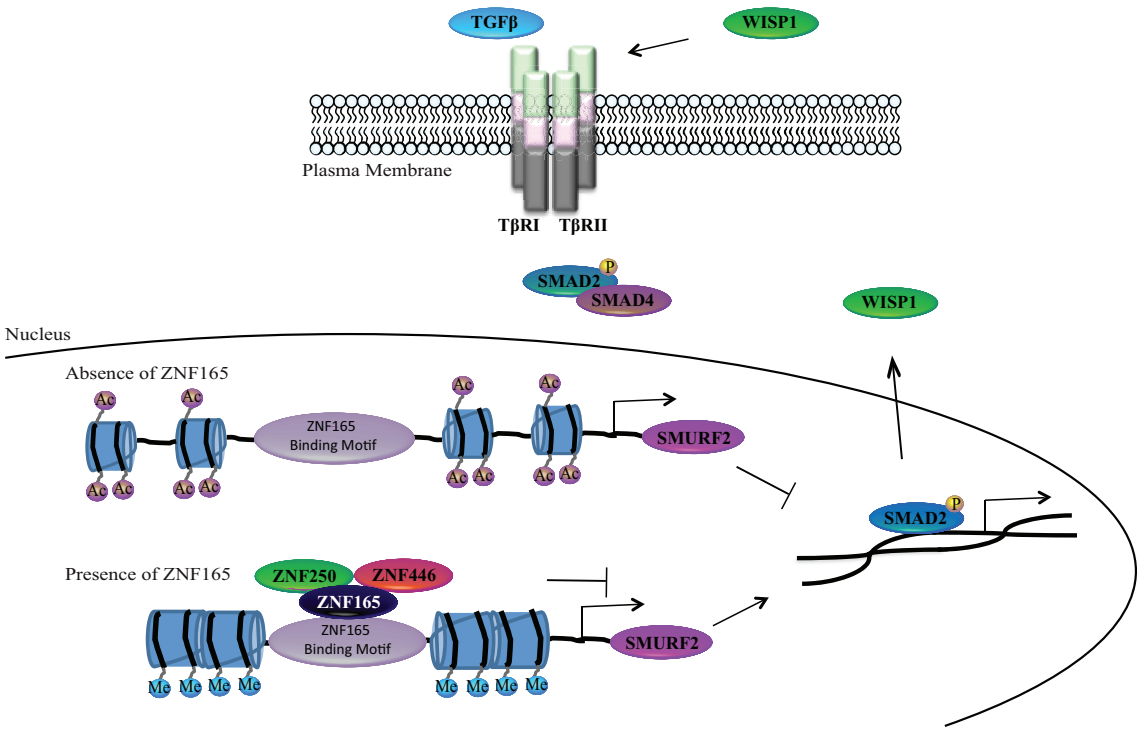

Figure 16. Model of ZNF165 Enhancing TGFβ Signaling to Support Expression of Pro-survival Oncogenes. ZNF165 binds to the enhancer regions of SMURF2 and SMAD7 to repress expression and enhance pro-oncogenic TGFβ in part through up regulation of WISP1.

biomarker for predicting a synergistic relationship between TGFβ inhibition and paclitaxel in claudin-low tumors.

Material and Methods

Cell lines and reagents - Cell lines were obtained from ATCC or John Minna (UT-Southwestern) with the following exceptions: SUM159, SUM149 and HuMEC (gift from Charles Perou, UNC Lineberger Cancer Center), HCC1806 (gift from Gray Pearson, UT Southwestern), WHIM12 (gift from Matthew Ellis, Baylor College of Medicine), HME50-hTERT (gift from Jerry Shay, UT Southwestern). All cell lines were cultured in provider's recommended medium. Antibodies were obtained from Santa Cruz (GAPDH), Novus Biologicals (ZNF165), Abcam (WISP1, SMURF2), Millipore (total SMAD2/3), Calbiochem (Phospho-specific Serine 465/467 SMAD2), Life Technologies (V5), Sigma (β-tubulin), and Cell Signaling Technologies (Cleaved Caspase-3). Transforming Growth Factor-β (TGFβ) was obtained from Cell Signaling. siRNAs were obtained from GE Healthcare (siGENOME siRNA) or Sigma (Mission® siRNA). CTRL siRNAs either were non-targeting control (GE Healthcare). Unless otherwise noted cDNAs were in pLX302 or pLX304 which contains a C-terminal V5 tag and was used for transient transfection. Full length ZNF165 was cloned into pCMV-myc (Clontech). WISP1 (-1kb) promoter luciferase construct was in pLightSwitch (Switchgear Genomics). For TGFβ reporter assays used stable expression of pSBE; (gift from Ben Major, University of North Carolina at Chapel Hill) (260). For TGFβ transient assays, pTL-Luc.SMAD construct and pRL-CMV (gift from Deborah Chapman, University of Pittsburgh) were used. For ZNF165 shRNA: ZNF165-TRIPz™-TetO-shRNA clones V3THS_366604 and

V3THS_366599 (Dharmacon), and TRIPZz™-Non-Silencing Control were used.

Whole genome expression analysis - Triplicate microarray analysis of SUM159 and WHIM12 cells depleted of ZNF165 was performed at the Functional Genomics Core (University of North Carolina at Chapel Hill) on Human GeneChip® 1.0 ST Arrays version 1.1 (Affymetrix). Microarray analysis was performed on 250 ng of RNA isolated and terminally labeled with the WT Expression Kit (Ambion® Life Technologies). Raw data was normalized using robust multi-array average (RMA) and significant analysis of microarrays (SAM) analysis identified significantly modulated genes. Datasets were deposited at the NCBI Gene Expression Omnibus (http://www.ncbi.nlm.nih.gov/geo/), accession number GSE63986.

Generation of stable cell lines - Stable cell lines were generated through either lentiviral or retroviral-mediated transduction of expression constructs. For ZNF165 stable cell lines, WHIM12 cells were transduced with pLX302-ZNF165 using lentiviral infection. Following infection, stable populations were selected using appropriate antibiotics.

Luciferase assay - For signaling assays, HEK293T cells were reverse transfected with 100 ng of luciferase reporter constructs and 2 ng pRL-CMV, and 100 ng indicated cDNAs using Fugene6® (Promega). Forty-eight hours post transfection, luciferase activity was measured using the Dual-Glo® Luciferase Assay System (Promega) following indicated exposures to TGFβ. Immunofluorescence for transfected cDNA was performed in parallel to verify transfection efficiency. For WISP1 promoter luciferase

assay, HEK293T were reverse transfected as stated above with 100 ng pLightSwitch-WISP1(-1kb) promoter (Switchgear Genomics) and indicated cDNAs. Forty-eight hours post transfection, luciferase activity was quantitated with *Renilla* Luciferase Assay system (Promega). Luciferase values were normalized to cell number quantitated using CTG.

Colony formation assay - Cells were reverse transfected with 10 pmoles of siRNA using RNAiMax® (Life Technologies). Forty-eight post transfection, cells were replated at limiting dilution in 6-well format. Cells were fed twice weekly until controls reached confluency at which point colonies were fixed in 3.7 % formaldehyde and stained with Geimsa (Sigma).

Gene expression - Total RNA was isolated using TRIzol® (Invitrogen) or an RNA isolation kit (Sigma) and reverse transcribed using the High-Capacity cDNA Reverse Transfection Kit (Life Technologies) according to manufacturer's instructions. An Applied Biosystems Real-Time PCR system and either Solaris™, SYBR® Green, or TaqMan® Real-Time PCR gene expression assays were used. Gene expression assays were multiplexed with RPL27, GAPDH or Actin as control assays. Relative expression values were calculated using the comparative Ct method.

Immunoblotting - Whole cell lysates were prepared in 2x Laemmli sample buffer and resolved using SDS-PAGE. Gels were transferred to Immobilon® PVDF (Millipore) or nitrocellulose (Bio-rad) membranes, blocked in tris-buffered saline containing 0.1 %

Tween20 (TBST) and either 5 % non-fat dry milk or bovine serum albumin (BSA), or Odyssey® blocking buffer and incubated with indicated primary antibodies for 1 hour or overnight. After washes in TBST, appropriate HRP-coupled secondary antibodies (Jackson Immunoresearch) or IRDye® antibodies (LI-COR) were used for chemiluminescence or fluorescence detection (LI-COR Odyssey®), respectively.

Immunofluorescence - Cells plated on glass coverslips were fixed with 3.7 % formaldehyde and permeabilized with 0.05 % Triton X-100 for ten minutes. Cells were blocked and washed in 1 % BSA, 0.1 % Tween-20 in 1X PBS (PBTA). Cells were incubated with primary antibodies for 1 hour followed by three washes in PBTA. Coverslips were then incubated with Alexa Fluor®-conjugated secondary antibodies (Invitrogen) for 30 minutes followed by 3 washes in PBTA and a wash in H_2O. Prolong® Gold Antifade reagent with DAPI (Life Technologies) was used to mount slips on glass slides and images were acquired on either a Leica DM55000 B upright microscope or a Leica TCS SP5 Confocal Microscope.

Chromatin Immunoprecipitation (ChIP) and ChIP-Seq - WHIM12-ZNF165-V5 cells were grown to 75 % confluency and cross-linked with 1 % formaldehyde for 10 minutes at room temperature. Cross-linking was quenched with 0.125M glycine for 5 minutes at room temperature. Nuclei were isolated by dounce homogenization in hypotonic buffer (20 mM HEPES pH 7.9, 10 mM KCl, 1 mM EDTA, 10 % glycerol, 1μg/mL pepstatin, 2 μg/mL leupeptin, 2 μg/mL aprotinin and 50 μM bestatin) followed by centrifugation at 600g for 5 minutes and then lysed in RIPA buffer (10 mM Tris-HCl, 150 mM NaCl, 1 %

NP-40, 1 % Deoxycholate, 0.1 % SDS, 1 mM EDTA, 1 μg/mL pepstatin, 2 μg/mL leupeptin, 2 μg/mL aprotinin and 50 μM bestatin). DNA was sheared using Diagenode Bioruptor® to a range of 300-500 bp fragments. Chromatin was immunoprecipitated using 2 μg of ChIP-Grade anti-V5 (Abcam) over night at 4 °C followed by a 2-hour incubation with Protein A/G beads. ChIPed DNA was recovered by reverse crosslinking with an overnight incubation at 65 °C. Excess RNA and protein were removed with 100 μg RNAse and 10 μg Proteinase K, respectively and the remaining DNA was purified using the Zymogen Zymo-Spin™ ChIP-Grade DNA Clean-Up Kit. 5 ng of ChIP-ed DNA underwent library preparation using the KAPA HTP Library Preparation Kit. Briefly, DNA is end repaired, 3' end adenylated and barcoded with multiplex adaptors. Ampure XP beads are used to purify DNA. Library size is then assessed using the Agilent 2100 Bioanalyzer. The Invitrogen Qubit® Fluorometer was then used to quantify samples prior to normalizing and pooling. Sequencing was performed on the Illumina® HiSeq 2500 using 50SR V3 reagents. Following sequencing, HOMER findPEAKS module was used to identify significantly enriched peaks using an FDR cutoff of 0.001, a cumulative Poisson p-value and required a 4-fold enrichment or normalized sequence reads in the experimental sample over control sample(261). Genomic Regions Enrichment of Annotation Tool (GREAT) was used to assign peak regions to genes and evaluate pathway enrichment(262). Datasets were deposited at the NCBI Gene Expression Omnibus (http://www.ncbi.nlm.nih.gov/geo/), accession number GSE63986. Homer package v4.2 findmotifsGenome.pl module with settings: –size150 –S 10-bits(261) was used for de novo motif analysis. Motif analysis was restricted to 150 base pairs surrounding peak summit. Homer module identified significantly enriched motifs in peak

region over the Homer-generated random background sequences.

ChIP-qPCR analysis was conducted using custom SYBR® Green assays designed to ChIP-Seq peaks (See Supplementary Data 7). The ACRBP open reading frame (ORF) lacked enrichment in the WHIM12-ZNF165-V5 ChIP-Seq and was used as a negative control for ZNF165-V5 binding. ZNF165-V5 occupancy was evaluated with immunoprecipitation efficiency using percent of total input DNA of WHIM12-CTRL and WHIM12-ZNF165-V5 cells.

Xenograft Injections - WHIM12 stably expressing ZNF165-TRIPz™-TetO-shRNA or a Non-Targeting control hairpin (200 µL) were injected in the right flank of NOD.cg-PRKDC^{SCID}Il2rg^{tm1Wjl}/SzJ (NSG) mice. Twenty-four hours prior to injection, cells were treated with 1 µg/mL doxycycline and mice were started on water containing 2 mg/mL doxycycline and 1 % sucrose. Tumors were measured twice weekly using a digital caliper and volume was calculated using: V = (Longest side) (perpendicular to longest side) ^{2}/ (π/6). According to IACUC guidelines, mice bearing tumors greater than 2000 mm^3 or exhibiting significantly diminished health were sacrificed. Tumors were surgically removed, weighed, formalin fixed for 48 hours, sectioned (5 µm) and stained with Ki-67. All studies were conducted in accordance with a UTSW IACUC approved protocol.

Human Breast Tissue Procurement - All human breast tissue was obtained from the UNC Lineberger Tissue Procurement center in compliance with all the laws and guidelines approved by the UNC IRB committee. Snap frozen human breast tissue samples were homogenized using mortar and pestle in lysis buffer (1 % Triton X-100, 50 mM HEPES pH 7.6, 150 mM NaCl, 1.5 mM $MgCl_2$, 1 mM EGTA, 25 mM β-glycerol phosphate, 10 % Glycerol, 1mM EGTA, 1 µg/mL pepstatin, 2 µg/mL leupeptin, 2 µg/mL

aprotinin and 50 μM bestatin, 1 mM $NaVO_4$). Samples were sonicated 3X for 5 seconds followed by 1 hour incubation on a rotator at 4 °C. Samples were then spun down at 14,000 rpm for 20 minutes at 4 °C and protein concentrations quantitated using Bio-Rad™ Protein Assay Dye Reagent. Samples were diluted to 1 mg/mL in 4X Laemmli sample buffer and immunoblotted as described. Coomassie stain (Genlantis) was incubated with SDS-PAGE gels for 30 minutes followed by destain for 4 hours.

CHAPTER VI: Conclusions and Future Directions

Thesis Summary

Triple negative breast cancer is the most aggressive form of breast cancer that is defined by the lack of the estrogen and progesterone receptor and is not HER2 amplified. This translates into heterogeneous group of tumors that display a wide variety of oncogenic aberrations, chemoresponse profiles and molecular subtypes. Despite efforts to develop TNBC targeted therapies, the standard of care for TNBC patients remains cytotoxic chemotherapeutic regimen, of which the anti-mitotic, paclitaxel, is the backbone. However, the vast heterogeneity found in the TNBC patient population results in unpredictable drug response, which limits the efficacy of these paclitaxel-based therapies. Without additional targeted therapies, TNBC patients who do not respond to paclitaxel combination therapies have no other therapeutic options and, therefore, present with poor clinical prognosis. We decided to employ a RNAi screening approach to uncover new cell autonomous tumor cell vulnerabilities that could be translated into additional therapeutic options for TNBC patients.

In Chapter II, we designed and executed an unbiased pan-genomic loss of function screening platform to uncover novel tumor cell vulnerabilities in TNBC that may translate into new therapeutic strategies. To model the heterogeneous patient

population, we screened four TNBC tumor-derived cell lines that display a variety of paclitaxel sensitivity, mutations and molecular subtypes. Across all four genomic-wide screens, we identified 2000 genes that were required for tumor cell viability and paclitaxel-induced cellular stress. We focused our follow-up efforts on the TNBC intervention targets, CXCR3, SIK2 and ZNF165, to highlight the strength of our screening approach to uncover new biological concepts and nominate new therapeutic strategies that may offer TNBC patients additional therapeutic options.

In Chapter III, we found that CXCR3/ CXCL9 signaling supports mitotic fidelity that is required for tumor cell viability specifically in the Basal-Like molecular subtype. Loss of CXCR3 signaling attenuated chromosomal alignment at the mitotic spindle, which initiated the spindle assembly checkpoint and induced apoptosis (Figure 6). These results suggest a new cell autonomous role of CXCR3/ CXCL9 signaling as supporting tumor cell survival. Given there were not expression differences between claudin-low and basal-like tumor cells, these findings also suggest fundamental differences between basal-like and claudin-low abilities to withstand mitotic stress.

In Chapter IV, we discovered SIK2 as a vulnerability in a subset of TNBC by acting as an autophagic break, possibly due to supporting the autophagic-inhibitory signaling of AKT (Figure 10). These results suggest that there are differential dependencies on autophagy in TNBC tumors and nominates SIK2 as a novel obligate component of the AKT/ mTOR nutrient-signaling pathway. Furthermore, small molecule inhibition of SIK2 recapitulated our screen findings warranting further investigation of

SIK2 as a therapeutic target in TNBC.

In Chapter V, we elucidated the role of the cancer testis antigen, ZNF165, supporting TNBC survival and TGFβ signaling. ZNF165 directly binds and represses negative regulators of TGFβ signaling that leads to global modulation of TGFβ transcription and promotes the expression pro-tumorigenic genes. One in particular, the poorly characterized oncogene, WISP1, provides additional feed-forward amplification of TGFβ signaling and is required for TNBC viability. These results suggest that reactivation of ZNF165 promotes unrestrained TGFβ activation to promote the tumorigenic phenotype (Figure 16). Given its testis specific expression profile, ZNF165 offers an extraordinarily wide therapeutic window for targeting oncogenic TGFβ signaling.

For the remainder of this chapter, I will explore the broader impacts of the work presented. Our mechanistic elaboration of each of our screen hits revealed new aspects of TNBC biology that could be therapeutically leveraged, suggesting that exploration of the TNBC functional landscape will reveal new therapeutic strategies and biomarkers for sensitive subsets of the TNBC patients population. The subsequent paragraphs will focus on discussion of the novel therapeutic strategies revealed here. When taken together, this work reinforces the current movement away from treating all TNBC patients as clinically equivalent and emphasizes the need for increasing our fundamental knowledge of TNBC biology to lead us to more informed and precise delivery of chemotherapeutic regimens. Our work here also highlights the strength of unbiased discovery-based screening

approaches to globally dissect and explore biological concepts and therapeutic strategies.

Future Directions

Paclitaxel-Based Therapies in Basal-Like Breast Cancer - TNBC is primarily comprised of two molecular subtypes, claudin-low and basal-like, based on cDNA microarray (32). These distinct gene expression profiles translate into strikingly differently tumors. Basal-Like tumors are characterized as epithelial in nature with the canonical epithelial cobblestone morphology and expression of E-cadherin and cytokeratin. Claudin-low tumors are stem-like with TIC features with more mesenchymal morphology and expression pattern including high expression of EMT markers like TWIST and SNAIL (33). These two subtypes also have strikingly differential pCR responses to the TNBC first line anti-mitotic chemotherapeutic agents. Patients with basal-like tumors are twice as likely to achieve pCR than patients with claudin-low tumors (33). Identification of CXCR3 in our screen nominates CXCR3 as a new therapeutic intervention target in TNBC. We found that basal-like tumors had an increased sensitivity to CXCR3 inhibition, suggesting that leveraging CXCR3 therapeutically maybe more beneficial for patients with basal-like tumors. An important future direction for CXCR3 is to examine the basal-like molecular subtypes as a selection criterion for CXCR3 inhibition. With the basal-like subtypes as an enrollment biomarker, CXCR3-based therapies may improve treatment options for basal-like patients without subjecting claudin-low patients to unnecessary side effects.

Therapeutic Splicing for CXCR3-Sensitive Tumors – CXCR3 exists in two main

isoforms (151). The CXCR3-A isoform is the slightly shorter isoform and promotes proliferation, survival and motility through coupling with Gαi and ROCK to modulate the actin cytoskeleton. CXCR3-B isoform is anti-proliferative and is implicated to signal through Gαs, elevating cAMP levels (134, 151, 152, 157, 263). Studies of CXCR3 in cancer have identified CXCR3 signaling to alter the actin cytoskeleton and promote metastatic potential (152, 153, 158-160, 264), suggesting CXCR3-A is the predominate isoform in the tumorigenic setting. Furthermore, increased cytoplasmic detection of CXCR3-A is associated with more aggressive tumors, suggesting differences in receptor trafficking (42, 152, 159). Given that CXCR3 protein can be detected in all tumor-derived cell lines regardless of sensitivity, an important future direction is an in-depth analysis of CXCR3 isoform composition, localization or signaling kinetics between basal-like and claudin-low tumors. This analysis may shed light on the mechanism behind CXCR3 selectivity. Furthermore, this analysis may lay the groundwork for a splicing-based therapy. A single splicing event is responsible for the differences in the CXCR3-A and CXCR3–B isoforms (151). Deregulation of splicing events is known to be critical during tumor evolution (265). Currently, new therapeutics are being developed to alter MYC-induced splicing in lymphomagenesis (266). Another future direction is to explore therapeutically leveraging the opposing tumorigenic functions of the two isoforms by targeting CXCR3 sensitive tumors with therapeutics to bias splicing machinery. Therapeutic splice switching oligonucleotides are currently in clinical trials for Duchenne muscular dystrophy (DMD) and therefore could be explored in TNBC basal-like breast cancer (267).

Targeting Autophagy-Dependent Tumors – Our screen revealed SIK2 as a TNBC vulnerability in a subset of TNBC tumors. Our tumor-derived cell line panel displayed a range of sensitivities to SIK2 depletion. During tumor evolution, autophagy has dual effects. Autophagy was originally thought to be solely tumor-suppressive by inducing cell death in metabolically deregulated neoplastic cells (268, 269). Loss of function mutations in the essential autophagy inducer, Beclin 1, are found in more than 40 % of breast, ovarian and prostate cancers (270), suggesting autophagy counteracts early tumorigenesis. However, once a tumor is established, autophagy can support tumor cell survival by increasing nutrient availability in large, poorly vascularized tumors (269, 271). Given this, autophagy inhibition was investigated as a therapeutic and, by both genetic and pharmacological means, can lead to tumor cell death in multiple preclinical models (272-274). Furthermore, autophagy inhibitors paired with first line chemotherapeutic agents are currently in clinical trials for prostate, glioma, and lung (ClinicalTrials.gov - NCT00933803, NCT02432417, NCT02421575). However, the understanding the context specific tumor biology that guides autophagy-dependency is important for precise application of these therapeutic regimens. We hypothesize that SIK2 becomes a vulnerability in tumors needing to harness autophagy to support oncogenesis without leading to loss of tumor cell viability. Metastatic tumors are thought to be particularly dependent on autophagy following detachment-induced metabolic stress and anoikis (207). An important future direction will be to focus on exploring the determinants of SIK2 sensitivity. Circulating tumors cells are often a prognostic indicator of metastatic disease (275, 276) and therefore, tumor cell burden in the blood stream could be explored as predictors of sensitivity to SIK2 inhibition. Most cancer deaths

occur from metastatic burden and TNBC tumors are often more aggressive and metastatic (35, 277). Therefore, further study of SIK2 in metastatic disease may yield a therapeutic alternative to TNBC patients with metastatic disease and improve their overall prognosis.

Leveraging TGFβ as a Therapeutic - TGFβ is a pleiotropic cytokine that drives a diverse and seemingly opposing set of developmental programs including differentiation, morphogenesis, tissue homeostasis as well as cell regeneration and self-renewal (227, 254). Under normal physiology, TGFβ is secreted as a pro-peptide by immune cells, like activated macrophages. Upon binding to the serine/threonine TGFβ Receptors RI and RII, it induces oligomerization and phosphorylation of SMAD2/3. Following this activation, phosphorylated SMAD2/3 associates with SMAD4 and translocates to the nucleus where it associates with additional transcriptional coactivators to drive transcription (254). How a single cytokine can induce both cell differentiation in one cell context and promote stemness and self-renewal in another is poorly understood but evidence is accumulating for differences in SMAD-associated transcriptional coactivators, chromatin structure and signaling pathway crosstalk (227). TGFβ's dual action is also seen during tumor evolution. In early tumorigenesis, TGFβ acts as a tumor suppressor by inducing anti-proliferative and differentiation genes like p21. Consistent with this, many tumors exhibit loss of function mutations in components of the canonical TGFβ pathway components like the TGFβRI and RII and SMAD4 (226). However, later stage tumors, TGFβ drives a more aggressive, proangiogenic, immune-evading and chemoresistant phenotype and best known as the master regulator of EMT that is required for metastatic potential (254). Here, our identification of ZNF165 in two orthogonal

datasets as required for TNBC survival and TGFβ signaling, suggests reactivation of this gametogenic gene may promote pro-tumorigenic TGFβ signaling. TGFβ inhibitors are currently in clinical trials for treatment of metastatic disease however, given its critical role in development, clinical implication of TGFβ inhibitors remains unsuccessful (253). An important future direction for ZNF165 is to explore ZNF165 expression as a biomarker for engagement of pro-oncogenic TGFβ signaling. Therefore, ZNF165 tumorigenic expression could predict sensitivity of TGFβ inhibition in the clinic. Furthermore, TGFβ signaling is particularly active in claudin-low tumors (42, 259) and our data suggests that ZNF165 supports TGFβ and supports claudin-Low TNBC viability, suggesting that claudin-low patients may be ideal candidates for TGFβ inhibition. Given that ZNF165 is selectively expressed the testis, implication of ZNF165 in the treatment of breast cancer may provide a therapeutic window for targeting TGFβ signaling in TNBC.

Precision Chemotherapy

All three therapeutic intervention points elaborated here were identified in our screen as potently collaborating with paclitaxel in different TNBC contexts. Paclitaxel is a backbone for the chemotherapeutic regimens used in TNBC and approximately 26 % - 45 % of TNBC patients initially respond to paclitaxel-based therapies (33). However, significant toxicity and innate drug resistance limits the efficacy of paclitaxel in the clinic (69, 73, 278, 279). Our data nominates potential new paclitaxel combination therapies. First, basal-like breast tumors may selectively require CXCR3 for survival. Therefore, the basal-like subtype might be able to be used as a biomarker to predict sensitivity to a

CXCR3 inhibitor, AMG487/ paclitaxel combination therapy. For SIK2, we hypothesize that SIK2 dependency is driven by autophagy-dependency. Autophagy is associated with anoikis prevention in disseminating metastatic tumor cells (207), therefore ARN3236/ paclitaxel based therapies may be effective in aggressive metastatic disease. For ZNF165, we found that ZNF165 expression is reactivated in some TNBC tumors and enhances pro-tumorigenic TGFβ signaling. Given that synergy between TGFβ inhibition and paclitaxel has been demonstrated in TNBC tumor-derived cell lines (252), we hypothesize that ZNF165 expression could be used as a biomarker for those tumors employing the pro-tumorigenic aspects of TGFβ and thus will be sensitive to TGFβ inhibitor/ paclitaxel-based chemotherapeutic regimens. Each of these stories offers a new piece of TNBC tumor biology that may allow for more informed and precise application of paclitaxel-based therapies. Deconstructing the 'one size fits all' approach to TNBC treatment will offer subsets of TNBC patients more therapeutic options and translate into improved patient prognosis. Small molecule inhibitors against SIK2 are in pre-clinical trials and CXCR3 inhibitors and TGFβ inhibitors are currently in clinical trials, allowing for evaluation of these precision chemotherapeutic approaches in the patient population.

Leveraging Discovery-Based Strategies to Uncover Biological Concepts

My work highlights the strength of siRNA screening approaches to identify new vulnerabilities. These screens allow for the generation of new hypotheses that lead to new mechanistic insight into tumor cell biology and nominates new therapeutic entry points. Since the first chemosensitizer screen in HeLa cells in 2005 (118), loss of function RNAi screens have been leveraged in discovery based biology in many different cellular

processes (108, 110, 111, 118, 125, 129). With the advent of new technologies like Clustered Regularly Interspaced Short Palindromic Repeat (CRISPR), sequencing technologies and generation of large natural product libraries (280, 281), single dimension RNAi screen are evolving into multi-dimensional functional genomic platforms (282). In cancer therapeutics, these platforms can correlate mechanistic and phenotypic responses with genetic information, followed by overlap with therapeutic responses across natural product libraries to facilitate simultaneous identification of new therapeutics and their cellular target. These strategies rapidly dissect tumor cell biology and identify new therapeutic strategies that will lead to continued improvement of therapeutic applications.

REFERENCES

1. Miller E, Lee HJ, Lulla A, Hernandez L, Gokare P, Lim B. Current treatment of early breast cancer: adjuvant and neoadjuvant therapy. F1000Research. 2014;3:198.

2. Lin SX, Chen J, Mazumdar M, Poirier D, Wang C, Azzi A, et al. Molecular therapy of breast cancer: progress and future directions. Nature reviews Endocrinology. 2010;6:485-93.

3. Benson JR, Jatoi I. The global breast cancer burden. Future oncology. 2012;8:697-702.

4. Polyak K. Heterogeneity in breast cancer. J Clin Invest. 2011;121:3786-8.

5. Polyak K. Breast cancer: origins and evolution. J Clin Invest. 2007;117:3155-63.

6. Jonat W, Pritchard KI, Sainsbury R, Klijn JG. Trends in endocrine therapy and chemotherapy for early breast cancer: a focus on the premenopausal patient. Journal of cancer research and clinical oncology. 2006;132:275-86.

7. Kulendran M, Salhab M, Mokbel K. Oestrogen-synthesising enzymes and breast cancer. Anticancer research. 2009;29:1095-109.

8. Osborne CK, Schiff R. Aromatase inhibitors: future directions. The Journal of steroid biochemistry and molecular biology. 2005;95:183-7.

9. Sledge GW, Mamounas EP, Hortobagyi GN, Burstein HJ, Goodwin PJ, Wolff AC. Past, present, and future challenges in breast cancer treatment. Journal of clinical oncology : official journal of the American Society of Clinical Oncology. 2014;32:1979-86.

10. Thomas C, Gustafsson JA. The different roles of ER subtypes in cancer biology and therapy. Nature reviews Cancer. 2011;11:597-608.

11. Labrie F. Intracrinology. Molecular and cellular endocrinology. 1991;78:C113-8.

12. Harada N. Aromatase and intracrinology of estrogen in hormone-dependent tumors. Oncology. 1999;57 Suppl 2:7-16.

13. Kiang DT, Kennedy BJ. Tamoxifen (antiestrogen) therapy in advanced breast cancer. Annals of internal medicine. 1977;87:687-90.

14. Osborne CK. Tamoxifen in the treatment of breast cancer. The New England journal of medicine. 1998;339:1609-18.

15. Paik S, Tang G, Shak S, Kim C, Baker J, Kim W, et al. Gene expression and

benefit of chemotherapy in women with node-negative, estrogen receptor-positive breast cancer. Journal of clinical oncology : official journal of the American Society of Clinical Oncology. 2006;24:3726-34.

16. Harries M, Smith I. The development and clinical use of trastuzumab (Herceptin). Endocrine-related cancer. 2002;9:75-85.

17. Jahanzeb M. Adjuvant trastuzumab therapy for HER2-positive breast cancer. Clinical breast cancer. 2008;8:324-33.

18. Vu T, Claret FX. Trastuzumab: updated mechanisms of action and resistance in breast cancer. Frontiers in oncology. 2012;2:62.

19. Moasser MM. The oncogene HER2: its signaling and transforming functions and its role in human cancer pathogenesis. Oncogene. 2007;26:6469-87.

20. Rubin I, Yarden Y. The basic biology of HER2. Annals of oncology : official journal of the European Society for Medical Oncology / ESMO. 2001;12 Suppl 1:S3-8.

21. Fink MY, Chipuk JE. Survival of HER2-Positive Breast Cancer Cells: Receptor Signaling to Apoptotic Control Centers. Genes & cancer. 2013;4:187-95.

22. Ross JS, Fletcher JA. The HER-2/neu Oncogene in Breast Cancer: Prognostic Factor, Predictive Factor, and Target for Therapy. The oncologist. 1998;3:237-52.

23. Shih C, Padhy LC, Murray M, Weinberg RA. Transforming genes of carcinomas and neuroblastomas introduced into mouse fibroblasts. Nature. 1981;290:261-4.

24. Schechter AL, Stern DF, Vaidyanathan L, Decker SJ, Drebin JA, Greene MI, et al. The neu oncogene: an erb-B-related gene encoding a 185,000-Mr tumour antigen. Nature. 1984;312:513-6.

25. Coussens L, Yang-Feng TL, Liao YC, Chen E, Gray A, McGrath J, et al. Tyrosine kinase receptor with extensive homology to EGF receptor shares chromosomal location with neu oncogene. Science. 1985;230:1132-9.

26. Semba K, Kamata N, Toyoshima K, Yamamoto T. A v-erbB-related protooncogene, c-erbB-2, is distinct from the c-erbB-1/epidermal growth factor-receptor gene and is amplified in a human salivary gland adenocarcinoma. Proc Natl Acad Sci U S A. 1985;82:6497-501.

27. Slamon DJ, Clark GM, Wong SG, Levin WJ, Ullrich A, McGuire WL. Human breast cancer: correlation of relapse and survival with amplification of the HER-2/neu oncogene. Science. 1987;235:177-82.

28. Barnes DM, Bartkova J, Camplejohn RS, Gullick WJ, Smith PJ, Millis RR. Overexpression of the c-erbB-2 oncoprotein: why does this occur more frequently in ductal carcinoma in situ than in invasive mammary carcinoma and is this of prognostic

significance? European journal of cancer. 1992;28:644-8.

29. Pauletti G, Godolphin W, Press MF, Slamon DJ. Detection and quantitation of HER-2/neu gene amplification in human breast cancer archival material using fluorescence in situ hybridization. Oncogene. 1996;13:63-72.

30. Liedtke C, Mazouni C, Hess KR, Andre F, Tordai A, Mejia JA, et al. Response to neoadjuvant therapy and long-term survival in patients with triple-negative breast cancer. Journal of clinical oncology : official journal of the American Society of Clinical Oncology. 2008;26:1275-81.

31. Shah SP, Roth A, Goya R, Oloumi A, Ha G, Zhao Y, et al. The clonal and mutational evolution spectrum of primary triple-negative breast cancers. Nature. 2012;486:395-9.

32. Perou CM, Sorlie T, Eisen MB, van de Rijn M, Jeffrey SS, Rees CA, et al. Molecular portraits of human breast tumours. Nature. 2000;406:747-52.

33. Prat A, Parker JS, Karginova O, Fan C, Livasy C, Herschkowitz JI, et al. Phenotypic and molecular characterization of the claudin-low intrinsic subtype of breast cancer. Breast cancer research : BCR. 2010;12:R68.

34. Sotiriou C, Neo SY, McShane LM, Korn EL, Long PM, Jazaeri A, et al. Breast cancer classification and prognosis based on gene expression profiles from a population-based study. Proc Natl Acad Sci U S A. 2003;100:10393-8.

35. Perou CM. Molecular stratification of triple-negative breast cancers. The oncologist. 2011;16 Suppl 1:61-70.

36. Sorlie T, Perou CM, Tibshirani R, Aas T, Geisler S, Johnsen H, et al. Gene expression patterns of breast carcinomas distinguish tumor subclasses with clinical implications. Proc Natl Acad Sci U S A. 2001;98:10869-74.

37. Clarke R, Liu MC, Bouker KB, Gu Z, Lee RY, Zhu Y, et al. Antiestrogen resistance in breast cancer and the role of estrogen receptor signaling. Oncogene. 2003;22:7316-39.

38. Fisher B, Costantino J, Redmond C, Poisson R, Bowman D, Couture J, et al. A randomized clinical trial evaluating tamoxifen in the treatment of patients with node-negative breast cancer who have estrogen-receptor-positive tumors. The New England journal of medicine. 1989;320:479-84.

39. Wolmark N, Redmond C, Fisher B. A comparison of two and three years of adjuvant tamoxifen. Hormone research. 1989;32 Suppl 1:166-8.

40. Leary A, Dowsett M. Combination therapy with aromatase inhibitors: the next era of breast cancer treatment? British journal of cancer. 2006;95:661-6.

41. Prat A, Karginova O, Parker JS, Fan C, He X, Bixby L, et al. Characterization of cell lines derived from breast cancers and normal mammary tissues for the study of the intrinsic molecular subtypes. Breast cancer research and treatment. 2013;142:237-55.

42. Walser TC, Rifat S, Ma X, Kundu N, Ward C, Goloubeva O, et al. Antagonism of CXCR3 inhibits lung metastasis in a murine model of metastatic breast cancer. Cancer Res. 2006;66:7701-7.

43. Creighton CJ, Li X, Landis M, Dixon JM, Neumeister VM, Sjolund A, et al. Residual breast cancers after conventional therapy display mesenchymal as well as tumor-initiating features. Proc Natl Acad Sci U S A. 2009;106:13820-5.

44. Harper MJ, Walpole AL. A new derivative of triphenylethylene: effect on implantation and mode of action in rats. Journal of reproduction and fertility. 1967;13:101-19.

45. Jordan VC. Tamoxifen: a most unlikely pioneering medicine. Nature reviews Drug discovery. 2003;2:205-13.

46. Livi L, Paiar F, Saieva C, Scoccianti S, Dicosmo D, Borghesi S, et al. Survival and breast relapse in 3834 patients with T1-T2 breast cancer after conserving surgery and adjuvant treatment. Radiotherapy and oncology : journal of the European Society for Therapeutic Radiology and Oncology. 2007;82:287-93.

47. Fisher B, Dignam J, Bryant J, Wolmark N. Five versus more than five years of tamoxifen for lymph node-negative breast cancer: updated findings from the National Surgical Adjuvant Breast and Bowel Project B-14 randomized trial. J Natl Cancer Inst. 2001;93:684-90.

48. Cummings SR, Eckert S, Krueger KA, Grady D, Powles TJ, Cauley JA, et al. The effect of raloxifene on risk of breast cancer in postmenopausal women: results from the MORE randomized trial. Multiple Outcomes of Raloxifene Evaluation. Jama. 1999;281:2189-97.

49. Baum M, Budzar AU, Cuzick J, Forbes J, Houghton JH, Klijn JG, et al. Anastrozole alone or in combination with tamoxifen versus tamoxifen alone for adjuvant treatment of postmenopausal women with early breast cancer: first results of the ATAC randomised trial. Lancet. 2002;359:2131-9.

50. Duggan C, Marriott K, Edwards R, Cuzick J. Inherited and acquired risk factors for venous thromboembolic disease among women taking tamoxifen to prevent breast cancer. Journal of clinical oncology : official journal of the American Society of Clinical Oncology. 2003;21:3588-93.

51. Marino M, Galluzzo P, Ascenzi P. Estrogen signaling multiple pathways to impact gene transcription. Current genomics. 2006;7:497-508.

52. Manni A. Clinical use of aromatase inhibitors in the treatment of breast cancers.

Journal of cellular biochemistry Supplement. 1993;17G:242-6.

53. Geisler J. Aromatase inhibitors: from bench to bedside and back. Breast cancer. 2008;15:17-26.

54. Geisler J, Helle H, Ekse D, Duong NK, Evans DB, Nordbo Y, et al. Letrozole is superior to anastrozole in suppressing breast cancer tissue and plasma estrogen levels. Clin Cancer Res. 2008;14:6330-5.

55. Breast International Group 1-98 Collaborative G, Thurlimann B, Keshaviah A, Coates AS, Mouridsen H, Mauriac L, et al. A comparison of letrozole and tamoxifen in postmenopausal women with early breast cancer. The New England journal of medicine. 2005;353:2747-57.

56. Klapper LN, Waterman H, Sela M, Yarden Y. Tumor-inhibitory antibodies to HER-2/ErbB-2 may act by recruiting c-Cbl and enhancing ubiquitination of HER-2. Cancer Res. 2000;60:3384-8.

57. Clynes RA, Towers TL, Presta LG, Ravetch JV. Inhibitory Fc receptors modulate in vivo cytotoxicity against tumor targets. Nature medicine. 2000;6:443-6.

58. Arnould L, Gelly M, Penault-Llorca F, Benoit L, Bonnetain F, Migeon C, et al. Trastuzumab-based treatment of HER2-positive breast cancer: an antibody-dependent cellular cytotoxicity mechanism? British journal of cancer. 2006;94:259-67.

59. Junttila TT, Akita RW, Parsons K, Fields C, Lewis Phillips GD, Friedman LS, et al. Ligand-independent HER2/HER3/PI3K complex is disrupted by trastuzumab and is effectively inhibited by the PI3K inhibitor GDC-0941. Cancer cell. 2009;15:429-40.

60. Nagata Y, Lan KH, Zhou X, Tan M, Esteva FJ, Sahin AA, et al. PTEN activation contributes to tumor inhibition by trastuzumab, and loss of PTEN predicts trastuzumab resistance in patients. Cancer cell. 2004;6:117-27.

61. Zhang S, Huang WC, Li P, Guo H, Poh SB, Brady SW, et al. Combating trastuzumab resistance by targeting SRC, a common node downstream of multiple resistance pathways. Nature medicine. 2011;17:461-9.

62. Fendly BM, Winget M, Hudziak RM, Lipari MT, Napier MA, Ullrich A. Characterization of murine monoclonal antibodies reactive to either the human epidermal growth factor receptor or HER2/neu gene product. Cancer Res. 1990;50:1550-8.

63. Hudziak RM, Lewis GD, Winget M, Fendly BM, Shepard HM, Ullrich A. p185HER2 monoclonal antibody has antiproliferative effects in vitro and sensitizes human breast tumor cells to tumor necrosis factor. Mol Cell Biol. 1989;9:1165-72.

64. Slamon DJ, Leyland-Jones B, Shak S, Fuchs H, Paton V, Bajamonde A, et al. Use of chemotherapy plus a monoclonal antibody against HER2 for metastatic breast cancer that overexpresses HER2. The New England journal of medicine. 2001;344:783-92.

65. Viale G. The current state of breast cancer classification. Annals of oncology : official journal of the European Society for Medical Oncology / ESMO. 2012;23 Suppl 10:x207-10.

66. Crown J, O'Shaughnessy J, Gullo G. Emerging targeted therapies in triple-negative breast cancer. Annals of oncology : official journal of the European Society for Medical Oncology / ESMO. 2012;23 Suppl 6:vi56-65.

67. von Minckwitz G, Martin M. Neoadjuvant treatments for triple-negative breast cancer (TNBC). Annals of oncology : official journal of the European Society for Medical Oncology / ESMO. 2012;23 Suppl 6:vi35-9.

68. Wani MC, Taylor HL, Wall ME, Coggon P, McPhail AT. Plant antitumor agents. VI. The isolation and structure of taxol, a novel antileukemic and antitumor agent from Taxus brevifolia. Journal of the American Chemical Society. 1971;93:2325-7.

69. McGuire WP, Rowinsky EK, Rosenshein NB, Grumbine FC, Ettinger DS, Armstrong DK, et al. Taxol: a unique antineoplastic agent with significant activity in advanced ovarian epithelial neoplasms. Annals of internal medicine. 1989;111:273-9.

70. Holmes FA, Walters RS, Theriault RL, Forman AD, Newton LK, Raber MN, et al. Phase II trial of taxol, an active drug in the treatment of metastatic breast cancer. J Natl Cancer Inst. 1991;83:1797-805.

71. Finkelstein DM, Ettinger DS, Ruckdeschel JC. Long-term survivors in metastatic non-small-cell lung cancer: an Eastern Cooperative Oncology Group Study. Journal of clinical oncology : official journal of the American Society of Clinical Oncology. 1986;4:702-9.

72. Rowinsky EK, Donehower RC. Paclitaxel (taxol). The New England journal of medicine. 1995;332:1004-14.

73. Jordan MA, Wilson L. Microtubules as a target for anticancer drugs. Nature reviews Cancer. 2004;4:253-65.

74. Gascoigne KE, Taylor SS. How do anti-mitotic drugs kill cancer cells? Journal of cell science. 2009;122:2579-85.

75. Andre F, Zielinski CC. Optimal strategies for the treatment of metastatic triple-negative breast cancer with currently approved agents. Annals of oncology : official journal of the European Society for Medical Oncology / ESMO. 2012;23 Suppl 6:vi46-51.

76. Zhu M, Settele F, Kotak S, Sanchez-Pulido L, Ehret L, Ponting CP, et al. MISP is a novel Plk1 substrate required for proper spindle orientation and mitotic progression. J Cell Biol. 2013;200:773-87.

77. Isakoff SJ. Triple-negative breast cancer: role of specific chemotherapy agents.

Cancer journal. 2010;16:53-61.

78. Gudmundsdottir K, Ashworth A. The roles of BRCA1 and BRCA2 and associated proteins in the maintenance of genomic stability. Oncogene. 2006;25:5864-74.

79. Fong PC, Boss DS, Yap TA, Tutt A, Wu P, Mergui-Roelvink M, et al. Inhibition of poly(ADP-ribose) polymerase in tumors from BRCA mutation carriers. The New England journal of medicine. 2009;361:123-34.

80. Dantzer F, de La Rubia G, Menissier-De Murcia J, Hostomsky Z, de Murcia G, Schreiber V. Base excision repair is impaired in mammalian cells lacking Poly(ADP-ribose) polymerase-1. Biochemistry. 2000;39:7559-69.

81. Tutt A, Robson M, Garber JE, Domchek SM, Audeh MW, Weitzel JN, et al. Oral poly(ADP-ribose) polymerase inhibitor olaparib in patients with BRCA1 or BRCA2 mutations and advanced breast cancer: a proof-of-concept trial. Lancet. 2010;376:235-44.

82. Yap TA, Sandhu SK, Carden CP, de Bono JS. Poly(ADP-ribose) polymerase (PARP) inhibitors: Exploiting a synthetic lethal strategy in the clinic. CA: a cancer journal for clinicians. 2011;61:31-49.

83. Nielsen TO, Hsu FD, Jensen K, Cheang M, Karaca G, Hu Z, et al. Immunohistochemical and clinical characterization of the basal-like subtype of invasive breast carcinoma. Clin Cancer Res. 2004;10:5367-74.

84. Bethune G, Bethune D, Ridgway N, Xu Z. Epidermal growth factor receptor (EGFR) in lung cancer: an overview and update. Journal of thoracic disease. 2010;2:48-51.

85. Lynch TJ, Bell DW, Sordella R, Gurubhagavatula S, Okimoto RA, Brannigan BW, et al. Activating mutations in the epidermal growth factor receptor underlying responsiveness of non-small-cell lung cancer to gefitinib. The New England journal of medicine. 2004;350:2129-39.

86. Corkery B, Crown J, Clynes M, O'Donovan N. Epidermal growth factor receptor as a potential therapeutic target in triple-negative breast cancer. Annals of oncology : official journal of the European Society for Medical Oncology / ESMO. 2009;20:862-7.

87. Baselga J, Gomez P, Greil R, Braga S, Climent MA, Wardley AM, et al. Randomized phase II study of the anti-epidermal growth factor receptor monoclonal antibody cetuximab with cisplatin versus cisplatin alone in patients with metastatic triple-negative breast cancer. Journal of clinical oncology : official journal of the American Society of Clinical Oncology. 2013;31:2586-92.

88. Jain RK. Normalizing tumor vasculature with anti-angiogenic therapy: a new paradigm for combination therapy. Nature medicine. 2001;7:987-9.

89. McMahon G. VEGF receptor signaling in tumor angiogenesis. The oncologist.

2000;5 Suppl 1:3-10.

90. Ferrara N, Hillan KJ, Gerber HP, Novotny W. Discovery and development of bevacizumab, an anti-VEGF antibody for treating cancer. Nature reviews Drug discovery. 2004;3:391-400.

91. Spigel DR, Hainsworth JD, Burris HA, 3rd, Molthrop DC, Peacock N, Kommor M, et al. A pilot study of adjuvant doxorubicin and cyclophosphamide followed by paclitaxel and sorafenib in women with node-positive or high-risk early-stage breast cancer. Clinical advances in hematology & oncology : H&O. 2011;9:280-6.

92. Bergh J, Bondarenko IM, Lichinitser MR, Liljegren A, Greil R, Voytko NL, et al. First-line treatment of advanced breast cancer with sunitinib in combination with docetaxel versus docetaxel alone: results of a prospective, randomized phase III study. Journal of clinical oncology : official journal of the American Society of Clinical Oncology. 2012;30:921-9.

93. Curigliano G, Pivot X, Cortes J, Elias A, Cesari R, Khosravan R, et al. Randomized phase II study of sunitinib versus standard of care for patients with previously treated advanced triple-negative breast cancer. Breast. 2013;22:650-6.

94. Laplante M, Sabatini DM. mTOR signaling in growth control and disease. Cell. 2012;149:274-93.

95. Gordon V, Banerji S. Molecular pathways: PI3K pathway targets in triple-negative breast cancers. Clin Cancer Res. 2013;19:3738-44.

96. Morrow PK, Wulf GM, Ensor J, Booser DJ, Moore JA, Flores PR, et al. Phase I/II study of trastuzumab in combination with everolimus (RAD001) in patients with HER2-overexpressing metastatic breast cancer who progressed on trastuzumab-based therapy. Journal of clinical oncology : official journal of the American Society of Clinical Oncology. 2011;29:3126-32.

97. Ellard SL, Clemons M, Gelmon KA, Norris B, Kennecke H, Chia S, et al. Randomized phase II study comparing two schedules of everolimus in patients with recurrent/metastatic breast cancer: NCIC Clinical Trials Group IND.163. Journal of clinical oncology : official journal of the American Society of Clinical Oncology. 2009;27:4536-41.

98. Finn RS, Dering J, Ginther C, Wilson CA, Glaspy P, Tchekmedyian N, et al. Dasatinib, an orally active small molecule inhibitor of both the src and abl kinases, selectively inhibits growth of basal-type/"triple-negative" breast cancer cell lines growing in vitro. Breast cancer research and treatment. 2007;105:319-26.

99. Fornier MN, Morris PG, Abbruzzi A, D'Andrea G, Gilewski T, Bromberg J, et al. A phase I study of dasatinib and weekly paclitaxel for metastatic breast cancer. Annals of oncology : official journal of the European Society for Medical Oncology / ESMO. 2011;22:2575-81.

100. Marotta LL, Almendro V, Marusyk A, Shipitsin M, Schemme J, Walker SR, et al. The JAK2/STAT3 signaling pathway is required for growth of CD44(+)CD24(-) stem cell-like breast cancer cells in human tumors. J Clin Invest. 2011;121:2723-35.

101. Caldas-Lopes E, Cerchietti L, Ahn JH, Clement CC, Robles AI, Rodina A, et al. Hsp90 inhibitor PU-H71, a multimodal inhibitor of malignancy, induces complete responses in triple-negative breast cancer models. Proc Natl Acad Sci U S A. 2009;106:8368-73.

102. Proia DA, Zhang C, Sequeira M, Jimenez JP, He S, Spector N, et al. Preclinical activity profile and therapeutic efficacy of the HSP90 inhibitor ganetespib in triple-negative breast cancer. Clin Cancer Res. 2014;20:413-24.

103. Wilson RC, Doudna JA. Molecular mechanisms of RNA interference. Annual review of biophysics. 2013;42:217-39.

104. Carthew RW, Sontheimer EJ. Origins and Mechanisms of miRNAs and siRNAs. Cell. 2009;136:642-55.

105. Napoli C, Lemieux C, Jorgensen R. Introduction of a Chimeric Chalcone Synthase Gene into Petunia Results in Reversible Co-Suppression of Homologous Genes in trans. The Plant cell. 1990;2:279-89.

106. Mello CC, Conte D, Jr. Revealing the world of RNA interference. Nature. 2004;431:338-42.

107. Fire A, Xu S, Montgomery MK, Kostas SA, Driver SE, Mello CC. Potent and specific genetic interference by double-stranded RNA in Caenorhabditis elegans. Nature. 1998;391:806-11.

108. Mohr SE, Smith JA, Shamu CE, Neumuller RA, Perrimon N. RNAi screening comes of age: improved techniques and complementary approaches. Nature reviews Molecular cell biology. 2014;15:591-600.

109. Padmanabhan S, Mukhopadhyay A, Narasimhan SD, Tesz G, Czech MP, Tissenbaum HA. A PP2A regulatory subunit regulates C. elegans insulin/IGF-1 signaling by modulating AKT-1 phosphorylation. Cell. 2009;136:939-51.

110. Krishnan MN, Ng A, Sukumaran B, Gilfoy FD, Uchil PD, Sultana H, et al. RNA interference screen for human genes associated with West Nile virus infection. Nature. 2008;455:242-5.

111. Schramek D, Sendoel A, Segal JP, Beronja S, Heller E, Oristian D, et al. Direct in vivo RNAi screen unveils myosin IIa as a tumor suppressor of squamous cell carcinomas. Science. 2014;343:309-13.

112. Gumireddy K, Li A, Gimotty PA, Klein-Szanto AJ, Showe LC, Katsaros D, et al. KLF17 is a negative regulator of epithelial-mesenchymal transition and metastasis in

breast cancer. Nature cell biology. 2009;11:1297-304.

113. Toledo CM, Herman JA, Olsen JB, Ding Y, Corrin P, Girard EJ, et al. BuGZ is required for Bub3 stability, Bub1 kinetochore function, and chromosome alignment. Developmental cell. 2014;28:282-94.

114. Schmidt EE, Pelz O, Buhlmann S, Kerr G, Horn T, Boutros M. GenomeRNAi: a database for cell-based and in vivo RNAi phenotypes, 2013 update. Nucleic acids research. 2013;41:D1021-6.

115. Chen N, Harris TW, Antoshechkin I, Bastiani C, Bieri T, Blasiar D, et al. WormBase: a comprehensive data resource for Caenorhabditis biology and genomics. Nucleic acids research. 2005;33:D383-9.

116. Flockhart IT, Booker M, Hu Y, McElvany B, Gilly Q, Mathey-Prevot B, et al. FlyRNAi.org--the database of the Drosophila RNAi screening center: 2012 update. Nucleic acids research. 2012;40:D715-9.

117. Bernards R, Brummelkamp TR, Beijersbergen RL. shRNA libraries and their use in cancer genetics. Nat Methods. 2006;3:701-6.

118. MacKeigan JP, Murphy LO, Blenis J. Sensitized RNAi screen of human kinases and phosphatases identifies new regulators of apoptosis and chemoresistance. Nature cell biology. 2005;7:591-600.

119. Niemi NM, Lanning NJ, Klomp JA, Tait SW, Xu Y, Dykema KJ, et al. MK-STYX, a catalytically inactive phosphatase regulating mitochondrially dependent apoptosis. Mol Cell Biol. 2011;31:1357-68.

120. Giroux V, Iovanna J, Dagorn JC. Probing the human kinome for kinases involved in pancreatic cancer cell survival and gemcitabine resistance. FASEB journal : official publication of the Federation of American Societies for Experimental Biology. 2006;20:1982-91.

121. Bartz SR, Zhang Z, Burchard J, Imakura M, Martin M, Palmieri A, et al. Small interfering RNA screens reveal enhanced cisplatin cytotoxicity in tumor cells having both BRCA network and TP53 disruptions. Mol Cell Biol. 2006;26:9377-86.

122. Whitehurst AW, Bodemann BO, Cardenas J, Ferguson D, Girard L, Peyton M, et al. Synthetic lethal screen identification of chemosensitizer loci in cancer cells. Nature. 2007;446:815-9.

123. Swanton C, Marani M, Pardo O, Warne PH, Kelly G, Sahai E, et al. Regulators of mitotic arrest and ceramide metabolism are determinants of sensitivity to paclitaxel and other chemotherapeutic drugs. Cancer cell. 2007;11:498-512.

124. Berns K, Horlings HM, Hennessy BT, Madiredjo M, Hijmans EM, Beelen K, et al. A functional genetic approach identifies the PI3K pathway as a major determinant of

trastuzumab resistance in breast cancer. Cancer cell. 2007;12:395-402.

125. Iorns E, Turner NC, Elliott R, Syed N, Garrone O, Gasco M, et al. Identification of CDK10 as an important determinant of resistance to endocrine therapy for breast cancer. Cancer cell. 2008;13:91-104.

126. Cappell KM, Larson B, Sciaky N, Whitehurst AW. Symplekin specifies mitotic fidelity by supporting microtubule dynamics. Mol Cell Biol. 2010;30:5135-44.

127. Fotheringham S, Epping MT, Stimson L, Khan O, Wood V, Pezzella F, et al. Genome-wide loss-of-function screen reveals an important role for the proteasome in HDAC inhibitor-induced apoptosis. Cancer cell. 2009;15:57-66.

128. Khan O, Fotheringham S, Wood V, Stimson L, Zhang C, Pezzella F, et al. HR23B is a biomarker for tumor sensitivity to HDAC inhibitor-based therapy. Proc Natl Acad Sci U S A. 2010;107:6532-7.

129. Luo J, Emanuele MJ, Li D, Creighton CJ, Schlabach MR, Westbrook TF, et al. A genome-wide RNAi screen identifies multiple synthetic lethal interactions with the Ras oncogene. Cell. 2009;137:835-48.

130. Birmingham A, Selfors LM, Forster T, Wrobel D, Kennedy CJ, Shanks E, et al. Statistical methods for analysis of high-throughput RNA interference screens. Nat Methods. 2009;6:569-75.

131. Woitach JT, Zhang M, Niu CH, Thorgeirsson SS. A retinoblastoma-binding protein that affects cell-cycle control and confers transforming ability. Nature genetics. 1998;19:371-4.

132. Cappell KM, Sinnott R, Taus P, Maxfield K, Scarbrough M, Whitehurst AW. Multiple cancer testis antigens function to support tumor cell mitotic fidelity. Mol Cell Biol. 2012;32:4131-40.

133. Sinnott R, Winters L, Larson B, Mytsa D, Taus P, Cappell KM, et al. Mechanisms promoting escape from mitotic stress-induced tumor cell death. Cancer Res. 2014;74:3857-69.

134. Ma B, Khazali A, Wells A. CXCR3 in carcinoma progression. Histology and histopathology. 2015:11594.

135. Liu L, Callahan MK, Huang D, Ransohoff RM. Chemokine receptor CXCR3: an unexpected enigma. Current topics in developmental biology. 2005;68:149-81.

136. Groom JR, Luster AD. CXCR3 ligands: redundant, collaborative and antagonistic functions. Immunology and cell biology. 2011;89:207-15.

137. Loetscher M, Gerber B, Loetscher P, Jones SA, Piali L, Clark-Lewis I, et al. Chemokine receptor specific for IP10 and mig: structure, function, and expression in

activated T-lymphocytes. The Journal of experimental medicine. 1996;184:963-9.

138. Yates CC, Whaley D, A YC, Kulesekaran P, Hebda PA, Wells A. ELR-negative CXC chemokine CXCL11 (IP-9/I-TAC) facilitates dermal and epidermal maturation during wound repair. The American journal of pathology. 2008;173:643-52.

139. Huen AC, Wells A. The Beginning of the End: CXCR3 Signaling in Late-Stage Wound Healing. Advances in wound care. 2012;1:244-8.

140. Bodnar RJ, Yates CC, Rodgers ME, Du X, Wells A. IP-10 induces dissociation of newly formed blood vessels. Journal of cell science. 2009;122:2064-77.

141. Ahmed AA, Lu Z, Jennings NB, Etemadmoghadam D, Capalbo L, Jacamo RO, et al. SIK2 is a centrosome kinase required for bipolar mitotic spindle formation that provides a potential target for therapy in ovarian cancer. Cancer cell. 2010;18:109-21.

142. Wang Z, Takemori H, Halder SK, Nonaka Y, Okamoto M. Cloning of a novel kinase (SIK) of the SNF1/AMPK family from high salt diet-treated rat adrenal. FEBS Lett. 1999;453:135-9.

143. Tirosvoutis KN, Divane A, Jones M, Affara NA. Characterization of a novel zinc finger gene (ZNF165) mapping to 6p21 that is expressed specifically in testis. Genomics. 1995;28:485-90.

144. Dong XY, Yang XA, Wang YD, Chen WF. Zinc-finger protein ZNF165 is a novel cancer-testis antigen capable of eliciting antibody response in hepatocellular carcinoma patients. British journal of cancer. 2004;91:1566-70.

145. Wu H, Yang WP, Barbas CF, 3rd. Building zinc fingers by selection: toward a therapeutic application. Proceedings of the National Academy of Sciences of the United States of America. 1995;92:344-8.

146. Williams AJ, Blacklow SC, Collins T. The zinc finger-associated SCAN box is a conserved oligomerization domain. Mol Cell Biol. 1999;19:8526-35.

147. Cappell KM, Sinnott R, Taus P, Maxfield K, Scarbrough M, Whitehurst AW. Multiple cancer testes antigens function to support tumor cell mitotic fidelity. Molecular and cellular biology. 2012;32:4131-40.

148. Horuk R. Chemokine receptor antagonists: overcoming developmental hurdles. Nature reviews Drug discovery. 2009;8:23-33.

149. Brouard S, Soulillou JP. Pre-transplant serum level of CXCL9 as a biomarker of acute rejection and graft failure risk in kidney transplantation. Transplant international : official journal of the European Society for Organ Transplantation. 2010;23:461-2.

150. Roedder S, Vitalone M, Khatri P, Sarwal MM. Biomarkers in solid organ transplantation: establishing personalized transplantation medicine. Genome medicine.

2011;3:37.

151. Lasagni L, Francalanci M, Annunziato F, Lazzeri E, Giannini S, Cosmi L, et al. An alternatively spliced variant of CXCR3 mediates the inhibition of endothelial cell growth induced by IP-10, Mig, and I-TAC, and acts as functional receptor for platelet factor 4. The Journal of experimental medicine. 2003;197:1537-49.

152. Wu Q, Dhir R, Wells A. Altered CXCR3 isoform expression regulates prostate cancer cell migration and invasion. Molecular cancer. 2012;11:3.

153. Thompson BD, Jin Y, Wu KH, Colvin RA, Luster AD, Birnbaumer L, et al. Inhibition of G alpha i2 activation by G alpha i3 in CXCR3-mediated signaling. J Biol Chem. 2007;282:9547-55.

154. Smit MJ, Verdijk P, van der Raaij-Helmer EM, Navis M, Hensbergen PJ, Leurs R, et al. CXCR3-mediated chemotaxis of human T cells is regulated by a Gi- and phospholipase C-dependent pathway and not via activation of MEK/p44/p42 MAPK nor Akt/PI-3 kinase. Blood. 2003;102:1959-65.

155. Kouroumalis A, Nibbs RJ, Aptel H, Wright KL, Kolios G, Ward SG. The chemokines CXCL9, CXCL10, and CXCL11 differentially stimulate G alpha i-independent signaling and actin responses in human intestinal myofibroblasts. J Immunol. 2005;175:5403-11.

156. Bonacchi A, Romagnani P, Romanelli RG, Efsen E, Annunziato F, Lasagni L, et al. Signal transduction by the chemokine receptor CXCR3: activation of Ras/ERK, Src, and phosphatidylinositol 3-kinase/Akt controls cell migration and proliferation in human vascular pericytes. J Biol Chem. 2001;276:9945-54.

157. Ehlert JE, Addison CA, Burdick MD, Kunkel SL, Strieter RM. Identification and partial characterization of a variant of human CXCR3 generated by posttranscriptional exon skipping. J Immunol. 2004;173:6234-40.

158. Ma X, Norsworthy K, Kundu N, Rodgers WH, Gimotty PA, Goloubeva O, et al. CXCR3 expression is associated with poor survival in breast cancer and promotes metastasis in a murine model. Mol Cancer Ther. 2009;8:490-8.

159. Datta D, Flaxenburg JA, Laxmanan S, Geehan C, Grimm M, Waaga-Gasser AM, et al. Ras-induced modulation of CXCL10 and its receptor splice variant CXCR3-B in MDA-MB-435 and MCF-7 cells: relevance for the development of human breast cancer. Cancer Res. 2006;66:9509-18.

160. Lo BK, Yu M, Zloty D, Cowan B, Shapiro J, McElwee KJ. CXCR3/ligands are significantly involved in the tumorigenesis of basal cell carcinomas. The American journal of pathology. 2010;176:2435-46.

161. Fulton AM. The chemokine receptors CXCR4 and CXCR3 in cancer. Current oncology reports. 2009;11:125-31.

162. Carreno S, Kouranti I, Glusman ES, Fuller MT, Echard A, Payre F. Moesin and its activating kinase Slik are required for cortical stability and microtubule organization in mitotic cells. J Cell Biol. 2008;180:739-46.

163. Nigg EA. Mitotic kinases as regulators of cell division and its checkpoints. Nature reviews Molecular cell biology. 2001;2:21-32.

164. Castedo M, Perfettini JL, Roumier T, Andreau K, Medema R, Kroemer G. Cell death by mitotic catastrophe: a molecular definition. Oncogene. 2004;23:2825-37.

165. Ritchey L, Chakrabarti R. Aurora A kinase modulates actin cytoskeleton through phosphorylation of Cofilin: Implication in the mitotic process. Biochimica et biophysica acta. 2014;1843:2719-29.

166. Cole KE, Strick CA, Paradis TJ, Ogborne KT, Loetscher M, Gladue RP, et al. Interferon-inducible T cell alpha chemoattractant (I-TAC): a novel non-ELR CXC chemokine with potent activity on activated T cells through selective high affinity binding to CXCR3. The Journal of experimental medicine. 1998;187:2009-21.

167. Shin SY, Nam JS, Lim Y, Lee YH. TNFalpha-exposed bone marrow-derived mesenchymal stem cells promote locomotion of MDA-MB-231 breast cancer cells through transcriptional activation of CXCR3 ligand chemokines. J Biol Chem. 2010;285:30731-40.

168. Thery M, Racine V, Pepin A, Piel M, Chen Y, Sibarita JB, et al. The extracellular matrix guides the orientation of the cell division axis. Nature cell biology. 2005;7:947-53.

169. Fink J, Carpi N, Betz T, Betard A, Chebah M, Azioune A, et al. External forces control mitotic spindle positioning. Nature cell biology. 2011;13:771-8.

170. Solinet S, Mahmud K, Stewman SF, Ben El Kadhi K, Decelle B, Talje L, et al. The actin-binding ERM protein Moesin binds to and stabilizes microtubules at the cell cortex. J Cell Biol. 2013;202:251-60.

171. Roubinet C, Decelle B, Chicanne G, Dorn JF, Payrastre B, Payre F, et al. Molecular networks linked by Moesin drive remodeling of the cell cortex during mitosis. J Cell Biol. 2011;195:99-112.

172. Kunda P, Pelling AE, Liu T, Baum B. Moesin controls cortical rigidity, cell rounding, and spindle morphogenesis during mitosis. Current biology : CB. 2008;18:91-101.

173. Maier B, Kirsch M, Anderhub S, Zentgraf H, Kramer A. The novel actin/focal adhesion-associated protein MISP is involved in mitotic spindle positioning in human cells. Cell cycle. 2013;12:1457-71.

174. Zheng Z, Wan Q, Liu J, Zhu H, Chu X, Du Q. Evidence for dynein and astral microtubule-mediated cortical release and transport of Galphai/LGN/NuMA complex in

mitotic cells. Mol Biol Cell. 2013;24:901-13.

175. Kaji N, Muramoto A, Mizuno K. LIM kinase-mediated cofilin phosphorylation during mitosis is required for precise spindle positioning. J Biol Chem. 2008;283:4983-92.

176. Mihaylova MM, Shaw RJ. The AMPK signalling pathway coordinates cell growth, autophagy and metabolism. Nature cell biology. 2011;13:1016-23.

177. Lizcano JM, Goransson O, Toth R, Deak M, Morrice NA, Boudeau J, et al. LKB1 is a master kinase that activates 13 kinases of the AMPK subfamily, including MARK/PAR-1. EMBO J. 2004;23:833-43.

178. Katoh Y, Takemori H, Horike N, Doi J, Muraoka M, Min L, et al. Salt-inducible kinase (SIK) isoforms: their involvement in steroidogenesis and adipogenesis. Molecular and cellular endocrinology. 2004;217:109-12.

179. Itoh Y, Sanosaka M, Fuchino H, Yahara Y, Kumagai A, Takemoto D, et al. Salt Inducible Kinase 3 Signaling Is Important for the Gluconeogenic Programs in Mouse Hepatocytes. J Biol Chem. 2015.

180. Dentin R, Liu Y, Koo SH, Hedrick S, Vargas T, Heredia J, et al. Insulin modulates gluconeogenesis by inhibition of the coactivator TORC2. Nature. 2007;449:366-9.

181. Koo SH, Flechner L, Qi L, Zhang X, Screaton RA, Jeffries S, et al. The CREB coactivator TORC2 is a key regulator of fasting glucose metabolism. Nature. 2005;437:1109-11.

182. Henriksson E, Sall J, Gormand A, Wasserstrom S, Morrice NA, Fritzen AM, et al. SIK2 regulates CRTCs, HDAC4 and glucose uptake in adipocytes. Journal of cell science. 2015;128:472-86.

183. Walkinshaw DR, Weist R, Kim GW, You L, Xiao L, Nie J, et al. The tumor suppressor kinase LKB1 activates the downstream kinases SIK2 and SIK3 to stimulate nuclear export of class IIa histone deacetylases. J Biol Chem. 2013;288:9345-62.

184. Sakamaki J, Fu A, Reeks C, Baird S, Depatie C, Al Azzabi M, et al. Role of the SIK2-p35-PJA2 complex in pancreatic beta-cell functional compensation. Nature cell biology. 2014;16:234-44.

185. Henriksson E, Jones HA, Patel K, Peggie M, Morrice N, Sakamoto K, et al. The AMPK-related kinase SIK2 is regulated by cAMP via phosphorylation at Ser358 in adipocytes. Biochem J. 2012;444:503-14.

186. Kim J, Kundu M, Viollet B, Guan KL. AMPK and mTOR regulate autophagy through direct phosphorylation of Ulk1. Nature cell biology. 2011;13:132-41.

187. Kim DH, Sarbassov DD, Ali SM, King JE, Latek RR, Erdjument-Bromage H, et al. mTOR interacts with raptor to form a nutrient-sensitive complex that signals to the cell growth machinery. Cell. 2002;110:163-75.

188. Nazio F, Strappazzon F, Antonioli M, Bielli P, Cianfanelli V, Bordi M, et al. mTOR inhibits autophagy by controlling ULK1 ubiquitylation, self-association and function through AMBRA1 and TRAF6. Nature cell biology. 2013;15:406-16.

189. Chan EY. mTORC1 phosphorylates the ULK1-mAtg13-FIP200 autophagy regulatory complex. Science signaling. 2009;2:pe51.

190. Funderburk SF, Wang QJ, Yue Z. The Beclin 1-VPS34 complex--at the crossroads of autophagy and beyond. Trends in cell biology. 2010;20:355-62.

191. Manning BD, Cantley LC. AKT/PKB signaling: navigating downstream. Cell. 2007;129:1261-74.

192. Inoki K, Li Y, Zhu T, Wu J, Guan KL. TSC2 is phosphorylated and inhibited by Akt and suppresses mTOR signalling. Nature cell biology. 2002;4:648-57.

193. Degtyarev M, De Maziere A, Orr C, Lin J, Lee BB, Tien JY, et al. Akt inhibition promotes autophagy and sensitizes PTEN-null tumors to lysosomotropic agents. J Cell Biol. 2008;183:101-16.

194. Wang RC, Wei Y, An Z, Zou Z, Xiao G, Bhagat G, et al. Akt-mediated regulation of autophagy and tumorigenesis through Beclin 1 phosphorylation. Science. 2012;338:956-9.

195. Rual J-F, Venkatesan K, Hao T, Hirozane-Kishikawa T, Dricot A, Li N, et al. Towards a proteome-scale map of the human protein-protein interaction network. Nature. 2005;437:1173-8.

196. Bon H, Wadhwa K, Schreiner A, Osborne M, Carroll T, Ramos-Montoya A, et al. Salt-inducible kinase 2 regulates mitotic progression and transcription in prostate cancer. Molecular cancer research : MCR. 2015;13:620-35.

197. Li YN, Cao YQ, Wu X, Han GS, Wang LX, Zhang YH, et al. The association between Salt-inducible kinase 2 (SIK2) and gamma isoform of the regulatory subunit B55 of PP2A (B55gamma) contributes to the survival of glioma cells under glucose depletion through inhibiting the phosphorylation of S6K. Cancer cell international. 2015;15:21.

198. Klionsky DJ, Abdalla FC, Abeliovich H, Abraham RT, Acevedo-Arozena A, Adeli K, et al. Guidelines for the use and interpretation of assays for monitoring autophagy. Autophagy. 2012;8:445-544.

199. Glaumann H, Ahlberg J. Comparison of different autophagic vacuoles with regard to ultrastructure, enzymatic composition, and degradation capacity--formation of

crinosomes. Experimental and molecular pathology. 1987;47:346-62.

200. Bach M, Larance M, James DE, Ramm G. The serine/threonine kinase ULK1 is a target of multiple phosphorylation events. Biochem J. 2011;440:283-91.

201. Mizushima N, Noda T, Yoshimori T, Tanaka Y, Ishii T, George MD, et al. A protein conjugation system essential for autophagy. Nature. 1998;395:395-8.

202. Mizushima N, Sugita H, Yoshimori T, Ohsumi Y. A new protein conjugation system in human. The counterpart of the yeast Apg12p conjugation system essential for autophagy. J Biol Chem. 1998;273:33889-92.

203. Hresko RC, Mueckler M. mTOR.RICTOR is the Ser473 kinase for Akt/protein kinase B in 3T3-L1 adipocytes. J Biol Chem. 2005;280:40406-16.

204. Levine B, Kroemer G. Autophagy in the pathogenesis of disease. Cell. 2008;132:27-42.

205. Choi AM, Ryter SW, Levine B. Autophagy in human health and disease. The New England journal of medicine. 2013;368:651-62.

206. Fung C, Lock R, Gao S, Salas E, Debnath J. Induction of autophagy during extracellular matrix detachment promotes cell survival. Mol Biol Cell. 2008;19:797-806.

207. Kenific CM, Thorburn A, Debnath J. Autophagy and metastasis: another double-edged sword. Current opinion in cell biology. 2010;22:241-5.

208. Makarevic J, Tawanaie N, Juengel E, Reiter M, Mani J, Tsaur I, et al. Cross-communication between histone H3 and H4 acetylation and Akt-mTOR signalling in prostate cancer cells. Journal of cellular and molecular medicine. 2014;18:1460-6.

209. Beagle BR, Nguyen DM, Mallya S, Tang SS, Lu M, Zeng Z, et al. mTOR kinase inhibitors synergize with histone deacetylase inhibitors to kill B-cell acute lymphoblastic leukemia cells. Oncotarget. 2015;6:2088-100.

210. Peng X, Gong F, Chen Y, Jiang Y, Liu J, Yu M, et al. Autophagy promotes paclitaxel resistance of cervical cancer cells: involvement of Warburg effect activated hypoxia-induced factor 1-alpha-mediated signaling. Cell death & disease. 2014;5:e1367.

211. Veldhoen RA, Banman SL, Hemmerling DR, Odsen R, Simmen T, Simmonds AJ, et al. The chemotherapeutic agent paclitaxel inhibits autophagy through two distinct mechanisms that regulate apoptosis. Oncogene. 2013;32:736-46.

212. Furuya T, Kim M, Lipinski M, Li J, Kim D, Lu T, et al. Negative regulation of Vps34 by Cdk mediated phosphorylation. Molecular cell. 2010;38:500-11.

213. Van den Eynde B, Hainaut P, Herin M, Knuth A, Lemoine C, Weynants P, et al. Presence on a human melanoma of multiple antigens recognized by autologous CTL.

International journal of cancer Journal international du cancer. 1989;44:634-40.

214. van der Bruggen P, Traversari C, Chomez P, Lurquin C, De Plaen E, Van den Eynde B, et al. A gene encoding an antigen recognized by cytolytic T lymphocytes on a human melanoma. Science. 1991;254:1643-7.

215. Almeida LG, Sakabe NJ, deOliveira AR, Silva MC, Mundstein AS, Cohen T, et al. CTdatabase: a knowledge-base of high-throughput and curated data on cancer-testis antigens. Nucleic acids research. 2009;37:D816-9.

216. Zhao S, Zhu W, Xue S, Han D. Testicular defense systems: immune privilege and innate immunity. Cellular & molecular immunology. 2014;11:428-37.

217. Coulie PG, Van den Eynde BJ, van der Bruggen P, Boon T. Tumour antigens recognized by T lymphocytes: at the core of cancer immunotherapy. Nature reviews Cancer. 2014;14:135-46.

218. Old LJ. Cancer/testis (CT) antigens - a new link between gametogenesis and cancer. Cancer immunity. 2001;1:1.

219. Simpson AJ, Caballero OL, Jungbluth A, Chen YT, Old LJ. Cancer/testis antigens, gametogenesis and cancer. Nature reviews Cancer. 2005;5:615-25.

220. Robbins PF, Morgan RA, Feldman SA, Yang JC, Sherry RM, Dudley ME, et al. Tumor regression in patients with metastatic synovial cell sarcoma and melanoma using genetically engineered lymphocytes reactive with NY-ESO-1. Journal of clinical oncology : official journal of the American Society of Clinical Oncology. 2011;29:917-24.

221. Dhodapkar MV, Sznol M, Zhao B, Wang D, Carvajal RD, Keohan ML, et al. Induction of antigen-specific immunity with a vaccine targeting NY-ESO-1 to the dendritic cell receptor DEC-205. Science translational medicine. 2014;6:232ra51.

222. Whitehurst AW. Cause and consequence of cancer/testis antigen activation in cancer. Annual review of pharmacology and toxicology. 2014;54:251-72.

223. Doyle JM, Gao J, Wang J, Yang M, Potts PR. MAGE-RING protein complexes comprise a family of E3 ubiquitin ligases. Molecular cell. 2010;39:963-74.

224. May WA, Lessnick SL, Braun BS, Klemsz M, Lewis BC, Lunsford LB, et al. The Ewing's sarcoma EWS/FLI-1 fusion gene encodes a more potent transcriptional activator and is a more powerful transforming gene than FLI-1. Mol Cell Biol. 1993;13:7393-8.

225. Epping MT, Wang L, Edel MJ, Carlee L, Hernandez M, Bernards R. The human tumor antigen PRAME is a dominant repressor of retinoic acid receptor signaling. Cell. 2005;122:835-47.

226. Massague J. TGFbeta in Cancer. Cell. 2008;134:215-30.

227. Massague J. TGFbeta signalling in context. Nature reviews Molecular cell biology. 2012;13:616-30.

228. Pavletich NP, Pabo CO. Zinc finger-DNA recognition: crystal structure of a Zif268-DNA complex at 2.1 A. Science. 1991;252:809-17.

229. Lee PL, Gelbart T, West C, Adams M, Blackstone R, Beutler E. Three genes encoding zinc finger proteins on human chromosome 6p21.3: members of a new subclass of the Kruppel gene family containing the conserved SCAN box domain. Genomics. 1997;43:191-201.

230. Rual JF, Venkatesan K, Hao T, Hirozane-Kishikawa T, Dricot A, Li N, et al. Towards a proteome-scale map of the human protein-protein interaction network. Nature. 2005;437:1173-8.

231. Lin X, Liang M, Feng XH. Smurf2 is a ubiquitin E3 ligase mediating proteasome-dependent degradation of Smad2 in transforming growth factor-beta signaling. J Biol Chem. 2000;275:36818-22.

232. Kavsak P, Rasmussen RK, Causing CG, Bonni S, Zhu H, Thomsen GH, et al. Smad7 binds to Smurf2 to form an E3 ubiquitin ligase that targets the TGF beta receptor for degradation. Molecular cell. 2000;6:1365-75.

233. Lonn P, Vanlandewijck M, Raja E, Kowanetz M, Watanabe Y, Kowanetz K, et al. Transcriptional induction of salt-inducible kinase 1 by transforming growth factor beta leads to negative regulation of type I receptor signaling in cooperation with the Smurf2 ubiquitin ligase. J Biol Chem. 2012;287:12867-78.

234. Zhang Y, Chang C, Gehling DJ, Hemmati-Brivanlou A, Derynck R. Regulation of Smad degradation and activity by Smurf2, an E3 ubiquitin ligase. Proc Natl Acad Sci U S A. 2001;98:974-9.

235. Kennedy BA, Deatherage DE, Gu F, Tang B, Chan MW, Nephew KP, et al. ChIP-seq defined genome-wide map of TGFbeta/SMAD4 targets: implications with clinical outcome of ovarian cancer. PloS one. 2011;6:e22606.

236. Ranganathan P, Agrawal A, Bhushan R, Chavalmane AK, Kalathur RK, Takahashi T, et al. Expression profiling of genes regulated by TGF-beta: differential regulation in normal and tumour cells. BMC genomics. 2007;8:98.

237. Anderson KD, Pan L, Yang XM, Hughes VC, Walls JR, Dominguez MG, et al. Angiogenic sprouting into neural tissue requires Gpr124, an orphan G protein-coupled receptor. Proc Natl Acad Sci U S A. 2011;108:2807-12.

238. Cross NA, Chandrasekharan S, Jokonya N, Fowles A, Hamdy FC, Buttle DJ, et al. The expression and regulation of ADAMTS-1, -4, -5, -9, and -15, and TIMP-3 by TGFbeta1 in prostate cells: relevance to the accumulation of versican. The Prostate. 2005;63:269-75.

239. Xu L, Corcoran RB, Welsh JW, Pennica D, Levine AJ. WISP-1 is a Wnt-1- and beta-catenin-responsive oncogene. Genes Dev. 2000;14:585-95.

240. Kawahara T, Hotta N, Ozawa Y, Kato S, Kano K, Yokoyama Y, et al. Quantitative proteomic profiling identifies DPYSL3 as pancreatic ductal adenocarcinoma-associated molecule that regulates cell adhesion and migration by stabilization of focal adhesion complex. PloS one. 2013;8:e79654.

241. Benassi B, Flavin R, Marchionni L, Zanata S, Pan Y, Chowdhury D, et al. MYC is activated by USP2a-mediated modulation of microRNAs in prostate cancer. Cancer discovery. 2012;2:236-47.

242. Shan J, Zhao W, Gu W. Suppression of cancer cell growth by promoting cyclin D1 degradation. Molecular cell. 2009;36:469-76.

243. Graner E, Tang D, Rossi S, Baron A, Migita T, Weinstein LJ, et al. The isopeptidase USP2a regulates the stability of fatty acid synthase in prostate cancer. Cancer cell. 2004;5:253-61.

244. Chen Z, Ruan Q, Han S, Xi L, Jiang W, Jiang H, et al. Discovery of structure-based small molecular inhibitor of alphaB-crystallin against basal-like/triple-negative breast cancer development in vitro and in vivo. Breast cancer research and treatment. 2014;145:45-59.

245. Hartzell C, Ksionda O, Lemmens E, Coakley K, Yang M, Dail M, et al. Dysregulated RasGRP1 responds to cytokine receptor input in T cell leukemogenesis. Science signaling. 2013;6:ra21.

246. Luke CT, Oki-Idouchi CE, Cline JM, Lorenzo PS. RasGRP1 overexpression in the epidermis of transgenic mice contributes to tumor progression during multistage skin carcinogenesis. Cancer Res. 2007;67:10190-7.

247. Pennica D, Swanson TA, Welsh JW, Roy MA, Lawrence DA, Lee J, et al. WISP genes are members of the connective tissue growth factor family that are up-regulated in wnt-1-transformed cells and aberrantly expressed in human colon tumors. Proc Natl Acad Sci U S A. 1998;95:14717-22.

248. Su F, Overholtzer M, Besser D, Levine AJ. WISP-1 attenuates p53-mediated apoptosis in response to DNA damage through activation of the Akt kinase. Genes Dev. 2002;16:46-57.

249. Xie D, Nakachi K, Wang H, Elashoff R, Koeffler HP. Elevated levels of connective tissue growth factor, WISP-1, and CYR61 in primary breast cancers associated with more advanced features. Cancer Res. 2001;61:8917-23.

250. Saxena N, Banerjee S, Sengupta K, Zoubine MN, Banerjee SK. Differential expression of WISP-1 and WISP-2 genes in normal and transformed human breast cell lines. Molecular and cellular biochemistry. 2001;228:99-104.

251. Inkson CA, Ono M, Kuznetsov SA, Fisher LW, Robey PG, Young MF. TGF-beta1 and WISP-1/CCN-4 can regulate each other's activity to cooperatively control osteoblast function. Journal of cellular biochemistry. 2008;104:1865-78.

252. Bhola NE, Balko JM, Dugger TC, Kuba MG, Sánchez V, Sanders M, et al. TGF-β inhibition enhances chemotherapy action against triple-negative breast cancer. J Clin Invest. 2013;123:1348-58.

253. Buijs JT, Stayrook KR, Guise TA. The role of TGF-beta in bone metastasis: novel therapeutic perspectives. BoneKEy reports. 2012;1:96.

254. Principe DR, Doll JA, Bauer J, Jung B, Munshi HG, Bartholin L, et al. TGF-β: duality of function between tumor prevention and carcinogenesis. J Natl Cancer Inst. 2014;106:djt369.

255. Witzgall R, O'Leary E, Leaf A, Onaldi D, Bonventre JV. The Kruppel-associated box-A (KRAB-A) domain of zinc finger proteins mediates transcriptional repression. Proc Natl Acad Sci U S A. 1994;91:4514-8.

256. Creyghton MP, Cheng AW, Welstead GG, Kooistra T, Carey BW, Steine EJ, et al. Histone H3K27ac separates active from poised enhancers and predicts developmental state. Proc Natl Acad Sci U S A. 2010;107:21931-6.

257. Shlyueva D, Stampfel G, Stark A. Transcriptional enhancers: from properties to genome-wide predictions. Nature reviews Genetics. 2014;15:272-86.

258. Asiedu MK, Ingle JN, Behrens MD, Radisky DC, Knutson KL. TGFbeta/TNF(alpha)-mediated epithelial-mesenchymal transition generates breast cancer stem cells with a claudin-low phenotype. Cancer Res. 2011;71:4707-19.

259. Taube JH, Herschkowitz JI, Komurov K, Zhou AY, Gupta S, Yang J, et al. Core epithelial-to-mesenchymal transition interactome gene-expression signature is associated with claudin-low and metaplastic breast cancer subtypes. Proc Natl Acad Sci U S A. 2010;107:15449-54.

260. Biechele TL, Moon RT. Assaying beta-catenin/TCF transcription with beta-catenin/TCF transcription-based reporter constructs. Methods in molecular biology. 2008;468:99-110.

261. Heinz S, Benner C, Spann N, Bertolino E, Lin YC, Laslo P, et al. Simple combinations of lineage-determining transcription factors prime cis-regulatory elements required for macrophage and B cell identities. Molecular cell. 2010;38:576-89.

262. McLean CY, Bristor D, Hiller M, Clarke SL, Schaar BT, Lowe CB, et al. GREAT improves functional interpretation of cis-regulatory regions. Nature biotechnology. 2010;28:495-501.

263. Balan M, Pal S. A novel CXCR3-B chemokine receptor-induced growth-

inhibitory signal in cancer cells is mediated through the regulation of Bach-1 protein and Nrf2 protein nuclear translocation. J Biol Chem. 2014;289:3126-37.

264. Kawada K, Sonoshita M, Sakashita H, Takabayashi A, Yamaoka Y, Manabe T, et al. Pivotal role of CXCR3 in melanoma cell metastasis to lymph nodes. Cancer Res. 2004;64:4010-7.

265. Oltean S, Bates DO. Hallmarks of alternative splicing in cancer. Oncogene. 2014;33:5311-8.

266. Koh CM, Bezzi M, Low DH, Ang WX, Teo SX, Gay FP, et al. MYC regulates the core pre-mRNA splicing machinery as an essential step in lymphomagenesis. Nature. 2015.

267. Disterer P, Kryczka A, Liu Y, Badi YE, Wong JJ, Owen JS, et al. Development of therapeutic splice-switching oligonucleotides. Human gene therapy. 2014;25:587-98.

268. Karantza-Wadsworth V, Patel S, Kravchuk O, Chen G, Mathew R, Jin S, et al. Autophagy mitigates metabolic stress and genome damage in mammary tumorigenesis. Genes & development. 2007;21:1621-35.

269. Degenhardt K, Mathew R, Beaudoin B, Bray K, Anderson D, Chen G, et al. Autophagy promotes tumor cell survival and restricts necrosis, inflammation, and tumorigenesis. Cancer cell. 2006;10:51-64.

270. Qu X, Yu J, Bhagat G, Furuya N, Hibshoosh H, Troxel A, et al. Promotion of tumorigenesis by heterozygous disruption of the beclin 1 autophagy gene. J Clin Invest. 2003;112:1809-20.

271. White E. Deconvoluting the context-dependent role for autophagy in cancer. Nature reviews Cancer. 2012;12:401-10.

272. Wei H, Wei S, Gan B, Peng X, Zou W, Guan JL. Suppression of autophagy by FIP200 deletion inhibits mammary tumorigenesis. Genes Dev. 2011;25:1510-27.

273. Amaravadi RK, Yu D, Lum JJ, Bui T, Christophorou MA, Evan GI, et al. Autophagy inhibition enhances therapy-induced apoptosis in a Myc-induced model of lymphoma. J Clin Invest. 2007;117:326-36.

274. Ding WX, Ni HM, Gao W, Chen X, Kang JH, Stolz DB, et al. Oncogenic transformation confers a selective susceptibility to the combined suppression of the proteasome and autophagy. Mol Cancer Ther. 2009;8:2036-45.

275. Aceto N, Bardia A, Miyamoto DT, Donaldson MC, Wittner BS, Spencer JA, et al. Circulating tumor cell clusters are oligoclonal precursors of breast cancer metastasis. Cell. 2014;158:1110-22.

276. Baccelli I, Schneeweiss A, Riethdorf S, Stenzinger A, Schillert A, Vogel V, et al.

Identification of a population of blood circulating tumor cells from breast cancer patients that initiates metastasis in a xenograft assay. Nature biotechnology. 2013;31:539-44.

277. Weigelt B, Peterse JL, van 't Veer LJ. Breast cancer metastasis: markers and models. Nature reviews Cancer. 2005;5:591-602.

278. Orr GA, Verdier-Pinard P, McDaid H, Horwitz SB. Mechanisms of Taxol resistance related to microtubules. Oncogene. 2003;22:7280-95.

279. Mielke S, Sparreboom A, Mross K. Peripheral neuropathy: a persisting challenge in paclitaxel-based regimes. European journal of cancer. 2006;42:24-30.

280. Sander JD, Joung JK. CRISPR-Cas systems for editing, regulating and targeting genomes. Nature biotechnology. 2014;32:347-55.

281. Harvey AL. Natural products in drug discovery. Drug discovery today. 2008;13:894-901.

282. Potts MB, Kim HS, Fisher KW, Hu Y, Carrasco YP, Bulut GB, et al. Using functional signature ontology (FUSION) to identify mechanisms of action for natural products. Science signaling. 2013;6:ra90.